A STUDY OF PROPERTIES AND APPLICATIONS OF CONTROL CHARTS FOR HIGH YIELD PROCESSES

PRIYA RANJAN SHARMA

(*B. Eng.*, REC, Jalandhar, India)

A THESIS SUBMITTED

FOR THE DEGREE OF DOCTOR OF PHILOSOPHY

DEPARTMENT OF INDUSTRIAL & SYSTEMS ENGINEERING

THE NATIONAL UNIVERSITY OF SINGAPORE

2003

ACKNOWLEDGEMENT

Any project owes it success to two kinds of people, one who execute the project and take the credit and others who lend their invaluable support and guidance, and remain unknown. The successful completion of this dissertation, also, was made possible only with the support and guidance of many others. I would like to take this opportunity to thank all those concerned.

First, I would like to thank my supervisors, Professor Goh Thong Ngee and Associate Professor Xie Min for their invaluable guidance, support and patience throughout the whole course of my stay at NUS. They were always willing to clear any doubts I had which made my task a lot easier.

I also wish to thank the National University of Singapore for offering me a Research Scholarship and President's Graduate Fellowship, and the Department of Industrial and Systems Engineering for the use of its facilities. I would like to thank all my colleagues in Computing Lab who extended their support whenever I needed it and thus made my stay in NUS a pleasant memory. Lastly I would like to thank my wife and our parents for their moral support and encouragement.

Priya Ranjan Sharma

TABLE OF CONTENTS

Acknowledgement ..... **i**

Table of Contents ..... **ii**

List of Figures ..... **vi**

List of Tables ..... **ix**

Summary ..... **xiv**

1. Introduction **1**

1.1 Properties of a control chart **4**

1.2 The Shewhart charts for attributes **5**

1.3 The Statistical property of the Shewhart charts for attributes **7**

1.4 CUSUM and EWMA charts **8**

1.5 Problem Statement **11**

1.6 Scope of Research **14**

2. Literature Review **16**

2.1 The use of exact probability limits for Shewhart charts **17**

2.2 The Q chart **18**

2.3 Goh's pattern recognition approach **19**

2.4 Control charts based on cumulative count of conforming items **20**

2.5 Cumulative Quantity Control (CQC) chart **22**

2.5.1 The decision rule for the CQC chart **23**

2.6 The Cumulative Probability Control chart **24**

2.7 Application issues in the CCC charting procedure **25**

2.7.1 Resetting the initial count when applying the CCC chart **25**

2.7.2 Inspection errors **27**

2.8 Extension of the CCC and CQC charting techniques **28**

2.8.1 Control charting by fixing the number of nonconforming units, the CCC-*r* chart **28**

2.8.2 Serial correlation **31**

2.8.3 Transforming the geometric and exponential random variable **34**

2.8.4 Control charts for near zero-defect processes **34**

2.8.5 Economic design of run length control charts **35**

2.8.6 The CCC and exponential CUSUM Charts **36**

3. Monitoring Counted Data **40**

3.1 Monitoring defect rate in a Poisson process **41**

3.2 Monitoring quantity between *r* defects **43**

3.2.1 The distribution of Q_r **43**

3.2.2 Control limits of CQC_r chart **44**

3.3 Using the CQC_r charts for reliability monitoring **51**

3.4 An illustrative example **53**

3.5 Some statistical properties of CQC_r chart **58**

3.6 Comparison of CQC_r chart and c chart **64**

3.6.1 Average Item Run Length of the c chart **64**

3.6.2 An Example **68**

4. Control Charts for Monitoring the Inter-arrival Times **72**

4.1 Overview of Exponential CUSUM Charts **73**

4.2 Numerical comparison based on ARL and ATS performance **75**

4.2.1 Case I: Process Deterioration **76**

4.2.2 Case II: Process Improvement **78**

4.3 Implementing the charts **81**

4.4 An Example **82**

4.5 Detecting the shift when the underlying distribution changes **85**

4.5.1 Case I: Weibull distribution **85**
4.5.2 Case II: lognormal distribution **89**

5. Optimal Control Limits for the run length type control charts 96

5.1 The ARL behavior of the run length type charts 97

5.2 The optimizing procedure for maximizing the ARL 99

5.3 The inspection error and modification of CCC chart 103
5.3.1 The control limits and ARL in the presence of inspection errors **104**
5.3.2 The behavior of ARL in the CCC chart **109**
5.3.3 Implementation procedure **112**
5.3.4 An application example **116**
5.3.5 Statistical comparison of chart performance **117**

5.4 Attaining the desired false alarm Probability 120

6. Process Monitoring with estimated parameters 125

6.1 The effect of inaccurate control limits 126

6.2 Estimated control limits and their effect on chart properties 130
6.2.1 Estimation of λ **130**
6.2.2 Properties of the CQC chart with estimated parameter **131**
6.2.3 Zero defect samples **132**
6.2.4 The case when samples contain at least one defect **134**
6.2.5 The effect of estimated parameter on the run length **135**

6.3 The optimal limits for the CQC chart with estimated parameters 138

7. Monitoring quality characteristics following Weibull distribution 142

7.1 Weibull distribution and the t chart 143
7.1.1 Control limits for Weibull time-between-event chart **145**
7.1.2 An example **147**

7.2 The chart properties 150
7.2.1 Case 1: Change in the scale parameter **151**

7.2.2 Case 2: Change in the shape parameter **153**

7.2.3 Case 3: Change in both the shape and the scale parameter **154**

7.2.4 Comparison with Weibull CUSUM chart **155**

7.3 Individual chart with Weibull distribution **157**

7.4 Maximizing ARL for fixed in-control state **160**

7.5 The effect of estimated parameters on the Weibull t chart **162**

8. Combined decision schemes for CQC chart **169**

8.1 The need **170**

8.2 The Combined Scheme **171**

8.3 Average Run Length of the combined scheme **178**

8.4 Average Time to Signal of the combined scheme **187**

8.5 An example to illustrate the charting procedure **190**

9. Conclusion and Recommendation **193**

Declaration **202**

Bibliography **203**

LIST OF FIGURES

Figure 2.1 Selecting the suitable charting procedure

Figure 3.1 The traditional u chart for the monitoring of number of failures per unit time

Figure 3.2 The decision rule for the CQC_r chart

Figure 3.3 The CQC chart for the data in Table 3.5 and no alarm is raised

Figure 3.4 The CQC_3 chart for the data in Table 3.6

Figure 3.5 Some AIRL curves of CQC_r charts with $\lambda_o = 0.001$ and $\alpha = 0.0027$

Figure 3.6 Some AIRL curves of CQC_r charts (with only a lower control limit) with $\lambda_o = 0.001$ and $\alpha = 0.00135$

Figure 3.7 The CQC_3 chart for the data in Table 3.12

Figure 3.8 The c chart for the data in Table 3.13

Figure 4.1 The CQC chart for data in Table 4.6

Figure 4.2 The CUSUM chart for data in Table 4.6

Figure 4.3 The CQC_3 chart data in Table 4.7

Figure 4.4 The Type II error probability of CQC chart (top view)

Figure 4.5 The Type II error probability of the CQC chart (side view)

Figure 5.1 The behavior of the average run length in the CQC_r chart ($\alpha = 0.0027$)

Figure 5.2 The effect of r on the ARL of CQC_r charts for process deterioration (α = 0.0027)

Figure 5.3 ARL curves after adjusting the limits ($\alpha = 0.0027$)

Figure 5.4 Some ARL Curves with p = 50 ppm, $\psi = 0.2, \theta = 0.0001$

Figure 5.5 ARL curves with p = 50 ppm, $\alpha = 0.0027$ for different values of inspection errors.

Figure 5.6 Implementation Procedure

Figure 5.7 The CCC chart for the data set in Table 5.6

Figure 5.8 ARL curves with p = 50 ppm, $\psi = 0.2, \theta = 0.0001$ with maximum ARL at p = 50 ppm (for the proposed method)

Figure 5.9 ARL curves with p = 50 ppm, $\alpha = 0.0027$ for different values of inspection errors with maximum ARL value p = 50 ppm

Figure 5.10 The effect of the maximizing procedure on the anticipated false alarm

Figure 5.11 The ARL curves for the three methods

Figure 6.1 A CQC chart with actual (continuous) and estimated (dotted) control limits

Figure 6.2 Decision path for an out of control situation

Figure 7.1 t chart for shift from $\theta = 10$ to $\theta = 20$ (with $\beta = 1.3$)

Figure 7.2 Weibull t chart for shift from $\beta = 1.3$ to $\beta = 2$

Figure 7.3 Some ARL curves with the in-control $\theta_0 = 10$

Figure 7.4 OC curves when the shape parameter increases

Figure 7.5 The ARL curves when both the parameters change with in-control $\theta_0 = 10$, $\beta_0 = 1.5$

Figure 7.6 I chart for shift from $\theta = 10$ to $\theta = 20$

Figure 7.7 EWMA chart for shift from $\theta = 10$ to $\theta = 20$

Figure 7.8 Some ARL curves with adjusted control limits and the in-control $\theta_0 = 10$

Figure 8.1 Decision Rule for CQC_1 chart

Figure 8.2 Decision Rule for the combined procedure

Figure 8.3 OC Curves of CQC_{1+1} and CQC_1 charts for small process deteriorations

Figure 8.4 OC Curves of CQC_{1+2} and CQC_1 charts for small process deteriorations

Figure 8.5 OC Curves of CQC_{1+3} and CQC_1 charts for small process deteriorations

Figure 8.6 OC Curves of CQC_{1+4} and CQC_1 charts for small process deteriorations

Figure 8.7 The CQC_{1+1} chart

LIST OF TABLES

Table 1.1 Comparison of the CCC and CQC charts

Table 3.1 Some control limits of CQC_r charts with $\alpha = 0.0027$

Table 3.1 Some control limits of CQC_1 and CQC_2 charts with $\alpha = 0.0027$

Table 3.2 Some control limits of CQC_3 and CQC_4 charts with $\alpha = 0.0027$

Table 3.3 Some control limits of CQC_5 and CQC_6 charts with $\alpha = 0.0027$

Table 3.4 Some Control Limits of CQC_r charts with $\lambda_0 = 0.001$

Table 3.5 Failure time data of the components

Table 3.6 Cumulative Failure Time between every three failures

Table 3.7 Some ARL values of CQC_r charts ($\alpha = 0.0027$)

Table 3.8 Some AIRL values for CQC_r chart with $\lambda_0 = 0.001$ and $\alpha = 0.0027$

Table 3.9 The AIRL values of the CQC_r chart

Table 3.10 The AIRL values of the c chart

Table 3.11 Quantity inspected to observe one defect

Table 3.12 Quantity inspected till the occurrence of 3 defects

Table 3.13 Number of defects observed per sample

Table 4.1 ARL values when the process deteriorates from $\lambda_0 = 1$

Table 4.2 ATS values when the process deteriorates from $\lambda_0 = 1$

Table 4.3 ARL values when the process improves from $\lambda_0 = 1$

Table 4.4 ATS values when the process improves from $\lambda_0 = 1$

Table 4.5 Implementation Issues

Table 4.6 Time between events data (read across for consecutive values)

Table 4.7 Cumulative time between every three events

Table 4.8 ARL values when the shape parameter increases

Table 4.9 ATS values when the shape parameter increases

Table 4.10 ARLs when the shape parameter decreases

Table 4.11 ATS when the shape parameter decreases

Table 4.12 ARL of CQC chart when the distribution changes to lognormal

Table 4.13 ATS of CQC chart when the distribution changes to lognormal

Table 4.14 ARL of CQC_2 chart when the distribution changes to lognormal

Table 4.15 ATS of CQC_2 chart when the distribution changes to lognormal

Table 5.1 Values of Adjustment Factors for different values of false alarm probabilities

Table 5.2 Some numerical value of the ARL for different values of observed fraction nonconforming and desired false alarm rate.

Table 5.3 Some numerical value of the ARL for different values of observed fraction nonconforming and inspection errors

Table 5.4 Some values of the fraction nonconforming at which the maximum ARL is reached for different values of false alarm rate.

Table 5.5 Some values of the fraction nonconforming at which the maximum ARL is reached for different values of inspection errors.

Table 5.6 Values of the adjustment factor for a process with average fraction nonconforming = 50 ppm, $\psi = 0.2$ and $\theta = 0.0002$

Table 5.7 Number of conforming items observed before observing a nonconforming item (for p = 500 ppm, $\alpha = 0.1$, $\theta = 0.0002$ and $\psi = 0.1$)

Table 5.8 A comparison of current and proposed methods for given process average, $\alpha = 0.0027$, $\psi = 0.2$ and $\theta = 0.0001$

Table 5.9 Some ARL values of the adjustment method and existing methods (α = 0.0027)

Table 5.10 Some values of desired and specified false alarm probabilities

Table 6.1 Probability of obtaining zero defect in a sample

Table 6.2 Values of FAR with Estimated Control Limits, $\alpha = 0.0027$

Table 6.3 Values of AR with Estimated Control Limits: $\alpha = 0.0027$, λ_0=0.0002

Table 6.4 Values of ARL (upper entry) and SDRL (lower entry) with Estimated Control Limits, $\lambda_0 = 0.0002$

Table 6.5 Values of FAR with estimated adjusted control limits, $\alpha = 0.0027$

Table 6.6 Values of AR with estimated adjusted control limits: $\alpha = 0.0027$, $\lambda_0 = 0.0002$

Table 6.7 Values of ARL (upper entry) and SDRL (lower entry) with Estimated (and adjusted) Control Limits, $\lambda_0 = 0.0002$

Table 7.1 Control Limits of a control chart based on two-parameter Weibull distribution with $\theta = 10$ and $\alpha = 0.0027$

Table 7.2 Time between failures

Table 7.3 ARLs of the lower Weibull CUSUM for $\theta = 1$

Table 7.4 The MLEs and the estimated control limits for different sample sizes ($\alpha = 0.0027$, $\beta_0 = 1.5$, $\theta_0 = 10$)

Table 7.5 The MLEs and the estimated control limits for different sample sizes ($\alpha = 0.0027$, $\beta_0 = 0.5$, $\theta_0 = 10$)

Table 7.6 The corrected unbiased MLEs and the estimated control limits for different sample sizes ($\alpha = 0.0027$, $\beta_0 = 0.5$, $\theta_0 = 10$)

Table 7.7 The corrected unbiased MLEs and the estimated control limits for different sample sizes ($\alpha = 0.0027$, $\beta_0 = 1.5$, $\theta_0 = 10$)

Table 8.1 The ARL values of the CQC_{1+1} and CQC_1 charts

Table 8.2 The ARL values of the CQC_{1+2} and CQC_1 charts

Table 8.3 The ARL values of the CQC_{1+3} and CQC_1 charts

Table 8.4 The ARL values of the CQC_{1+4} and CQC_1 charts

Table 8.5 The ATS of CQC_{1+1} and CQC_2 charts

Table 8.6 The ATS of CQC_{1+2} and CQC_3 charts

Table 8.7 A Simulated data set

SUMMARY

The Shewhart type control charts such as the p chart or the c chart have proven their usefulness over time but are ineffective when the fraction nonconforming level reaches a low value. This dissertation is an attempt to look at the alternatives that can replace the Shewhart charts and to improve them to make them more efficient in today's ever changing environment. This dissertation also focuses on some new control charts that are not frequently used and tries to find out some instances where such control charts can be suitably applied. One such instance is to monitor the reliability of a component or a system. This is a comparatively new concept and desires attention.

Chapter 2 reviews some of the recent work in control charting techniques that are suitable or can be suitably applied for high quality processes. Apart from the other monitoring techniques, the cumulative count of conforming control (CCC) charting and cumulative quantity control (CQC) charting are explained in detail.

Chapter 3 extends the recent control scheme based on monitoring the cumulative quantity between observations of defects to monitor the quantity required to observe a fixed number of defects and is given the name CQC_r. The advantages of this scheme include the fact that the scheme does not require any subjective sample size, it can be used for both high and low quality items, it can detect process improvement even in a high-quality environment and that the decision regarding the statistical control of the process is not based on a single observation. An investigation of its use for reliability monitoring is

presented in this chapter and the scheme can be easily extended to monitor inter-failure times that follow other distributions such as the Weibull distribution.

The time between events control charts as an alternative to the traditional Shewhart charts for monitoring attribute type of quality characteristics have attracted increasing interest recently. In Chapter 4 the performance of three such charts, the CUSUM chart, the Cumulative Quantity Control (CQC) chart and the CQC_r chart, is compared. The performance is compared based on their average run length and average time to signal behavior. Two cases are concerned when the underlying distribution is exponential and when the underlying distribution changes to Weibull. The properties of the CQC_r chart are also studied when the underlying distribution changes to lognormal. The information acquired in this study can be used to select the proper charting procedure in manufacturing applications, and can as well be applied to study the time between accidents and in reliability studies.

In Chapter 5 the Average run length behavior of the run-length control charts, based on skewed distributions like erlang and negative binomial, is studied. Ideally, we would like the ARL to be large when the process is at the in-control state, and decrease when the process is changed. However, it is observed that the average time to alarm may increase at the beginning when the process deteriorates. Some researchers have suggested multiplying the control limits with an adjustment factor so that the average run length is maximized when the process is at the normal level. However their findings are limited for the case of exponential and geometric distribution, that are special cases of erlang and

negative binomial distribution respectively. This chapter presents a general solution for the problem and also highlights that other than adjusting the limit it is also essential to specify an appropriate false alarm probability in order to get the desired in-control run length and thus increase the chart's sensitivity to small process improvements. As an application example, the maximizing procedure is applied to the CCC chart in presence of inspection errors.

Chapter 6 studies the effect of incorrect estimation of the control limits and their effect on the chart properties. Like any other control chart the performance of the CQC chart depends upon the control limits, which are generally estimated. An accurate estimate of the control limits requires an accurate estimation of the parameter involved. Most of the studies on control charts assume that the process average is either known or an accurate estimate is available. In cases where the process parameter is unknown, a preliminary sample is usually taken and the process parameter is estimated. The question is how large the sample size should be, as a poor estimation can lead to false interpretations. Even when the parameters are accurately estimated, as pointed out before, the CQC chart has an undesirable property that the chance for alarm first decreases and then increases as the process deteriorates. So apart from highlighting the importance of accurate estimation of control limits, this chapter also suggests how to obtain an optimal performance out of those control limits, based on the findings in Chapter 5.

Chapter 7 proposes the control chart based on Weibull distribution to monitor quality characteristics following Weibull distribution. The CQC charts are no doubt a good

alternative to Shewhart charts for monitoring time or quantity between events. However, they are mostly based on the assumption of exponential distribution of time between events. A flexible alternative is to use Weibull distribution and it is especially useful for processes related to or affected by equipment failures. This chapter investigates time-between-events chart based on Weibull distribution, their application and chart performance. We study the cases when the Weibull scale parameter, shape parameter or both change. It is noted that the in-control average run length with probability limits is not optimized at the in-control parameter value and adjustment is proposed. The problems of estimation error and biasness of the likelihood estimators are discussed.

Chapter 8 proposes a combined decision scheme for the CQC charts to improve their sensitivity. No doubt CQC_r chart has many advantages compared to the CQC chart and the traditional Shewhart charts, like the c or the u charts. However, even this approach suffers form a major drawback; that the average time to plot a point increases with r. On the other hand in the case of CQC chart, the decision regarding the statistical control of the process is based on a single observation. A combined decision based on the advantages of the two schemes would be an ideal choice. The properties of the combined procedure is studied and compared with the current design of the CQC and CQC_r charts.

Chapter 1

Introduction

Quality and control charts

The meaning of the word quality as given in dictionaries is:

- Peculiar and essential character
- An inherent feature
- Degree of excellence
- Superiority in kind
- A distinguishing and intelligible feature by which a thing may be identified
- A general term applicable to any trait or characteristic whether individual or generic
- The totality of features & characteristics of a product or service that bear on its ability to satisfy stated or implied needs. Not to be mistaken for "degree of excellence" or "fitness for use" which meet only part of the definition.

The traditional definition of quality from a customer's point of view is given as "quality means fitness for use". With time this definition has found itself associated with the tag of conformance to specifications and has led to the widely held belief that the quality problems can be dealt with only in manufacturing. Another famous definition of Quality defines it as an ongoing process of building & sustaining relationship by assessing & anticipating & fulfilling stated & implied needs. The modern definition of quality defines it as "Quality is inversely proportional to variability" and so quality improvement, the root cause behind this dissertation, is defined as "the reduction of variability in processes and products".

The first quarter of the twentieth century can be aptly referred to as an era of renaissance in quality engineering. It was during this period that R. A. Fischer came out with the concept of design of experiments. The second notable milestone was the introduction of control chart by W.A. Shewhart, Shewhart (1926, 1931).

The huge impact of these two findings can be judged from the fact that even now, after three quarter of a century, they are still a topic of interest among the researchers. The methods may have been modified to suit the trends of changing times but the motivation remains same, Quality Improvement.

The control chart is considered as the formal beginning of the statistical quality control. Control chart is one of the seven (often referred to as the magnificent seven) tools of Statistical Process Control (SPC). Statistical process control (SPC) can be defined as a collection of tools, which track the statistical behavior of production processes, in order to maintain and improve product quality. The ideology behind SPC is similar to that of other quality philosophies like Total Quality Management (TQM) and Six Sigma. Therefore, SPC is regarded as an important component of Total Quality Management (see Cheng and Dawson (1998)) and other quality philosophies.

Of all the tools of Statistical Process Control, Control charts are, perhaps, most technically sophisticated. The basic idea behind any control chart is to monitor a process and to identify any unusual causes (also referred to as assignable causes) of variation from the chance causes of variation (inherent to the process).

This dissertation attempts to discuss the new concepts in control charting and to improve the performance of the existing methods. The motivation behind this study is the unsuitability of the Shewhart charts, especially for attributes, in today's automated and high quality environment. The term high quality, which will be used again and again during this study, defines a situation where the defects or defectives are very low, generally to the order of parts per million (ppm). In such a case the problems associated with the Shewhart charts makes it important to look for other alternatives.

1.1 Properties of a control chart

Any process suffers from two kinds of variations, chance causes and assignable causes. Chance causes are the causes that are inherently present in the process and thus have to be accepted. On the other hand assignable causes, as the name suggests are induced by the system, *i.e.* man, machine, material etc. The main objective of the control chart is to detect the presence of assignable causes and to inform the user by raising an alarm.

Usually the control chart has three lines, which are known as the upper control limit, the lower control limit, and the center line. The chart plots the sample statistic of some quality characteristic, which is to be monitored. The presence of an unusual source of variation results in a point plotting outside the control limits and warrants investigation and removal of such sources to bring the process back to its original state or if possible to improve it. A general formula to calculate the control limits is:

$$\begin{aligned} UCL &= \mu_x + k\sigma_x \\ CL &= \mu_x \\ LCL &= \mu_x - k\sigma_x \end{aligned} \tag{1.1}$$

where x is the plotted sample statistic that measures the quality characteristic and μ_x and σ_x are the mean and the standard deviation. k is the "distance" of the upper and lower control limits from the center line in terms of the standard deviation. k is often taken as 3, which means that the 99.73 % of all the observations will fall within the control limits under the normality assumption.

1.2 The Shewhart charts for attributes

Of the two types of Shewhart charts, variable charts are perhaps more widely used than attribute charts. Shewhart charts for variable data, *e.g.* $\overline{X}$ and R charts and individual charts are powerful tools for monitoring a process but their use is limited to only a few quality characteristics. One of their major limitations is that they can be used to monitor only those quality characteristics that can be measured and expressed in numbers, *i.e.* variable data. However, some quality characteristics can be observed only as attributes, *i.e.*, either the items confirm to the requirements or they do not confirm. Generally it is quite difficult to represent such quality characteristics in terms of measurements on a continuous scale.

An item is said to be defective (nonconforming) if it fails to confirm to the specifications in any characteristics. Each characteristic that does not meet the specifications is a defect

(nonconformity). An item is considered defective if it contains at least one defect. Sometimes it is possible that a product or an item is passed as conforming but still has some flaws, which do not affect its functioning but may affect the price of the product. *e.g.* the broken case of a calculator does not affect the functioning of a calculator but can affect its price. So we can say that in this case the calculator is conforming but it has one nonconformity. In such cases, sometimes it becomes important to monitor the nonconformities or defects in a process. The Shewhart charts for attribute monitor discrete measurements that can be generally modeled by the binomial or the Poisson distribution. The four attribute charts commonly used for this purpose are:

- p chart: Used for monitoring the fraction nonconforming in a sample
- np chart: Used for monitoring number of nonconforming items per sample, where the sample is generally constant
- u chart: Used for monitoring number of defects per unit
- c chart: Used for monitoring number of defects per inspection unit.

The p and the np chart are based on the binomial distribution, with probability density function (p.d.f.), mean and variance given as:

$$f(x) = \binom{n}{x} p^x (1-p)^{n-x}, \quad \mu = np, \ \sigma^2 = np(1-p) \tag{1.2}$$

While, the c and the u chart are based on the Poisson distribution, with p.d.f., mean and variance given as:

$$f(x) = \frac{e^{-\lambda}\lambda^{x}}{x!} \qquad \mu = \lambda \qquad \sigma = \sqrt{\lambda} \tag{1.3}$$

The control limits of the attribute charts are calculated under the assumption of normality approximation. However the approximation is not free of constraints. For example, in the case of binomial distribution and Poisson distribution, the approximation holds true only when the value of $n\bar{p}$ and λ is reasonably large.

1.3. The Statistical property of the Shewhart charts for attributes

Two important statistical properties of the control chart are the Type I and the Type II errors defined as:

Type I error (also referred to as false alarm rate): The probability that a plotted point falls outside the control limit when the process is in control

Type II error: The probability that a plotted point falls within the control limits when the process has actually shifted

Under ideal conditions we would want the control chart to raise less false alarms (to avoid unnecessarily interrupting the process) which in other words means a small Type I

error. While at the same time we would like it to detect the process shift as soon as possible, which means that the control chart should also have a small Type II error. If the control limits are widened, the Type I error decreases but the Type II error increases. Similarly, when the control limits are tightened, the opposite happens, *i.e.* the Type I error increases while Type II error decreases. Thus it is a question of compromise or trade off, and so 3 sigma limits were found out to be acceptable because they have a small Type I error when the process is in control and also have a small Type II error when the process is out of control.

The average run length (ARL) is a commonly used measure of chart performance; see Grant and Leavenworth (1988), Ryan (1989), Quesenberry (1997), and Montgomery (2001). It is defined as the average number of points that must be plotted on the control chart before a point fall outside the control limits. A good control chart should have a large average run length when the process is in control and small average run length when the process shifts away from the target. The general way to represent the ARL of a control chart is

$$ARL = \frac{1}{1 - Type\ II\ error} \tag{1.4}$$

1.4. CUSUM and EWMA charts

CUmulative **SUM** (CUSUM) control charts were first introduced by Page (1954). One of the limitations of the Shewhart charts is that. the decision whether the process is in

control is taken on the basis of last plotted point and it ignores the information contained in the previous points. Due to this reason the Shewhart charts are not able to detect small shifts, of the order of 1.5σ or less. The Cumulative Sum (CUSUM) charts and the Exponentially Weighted Moving Average Control (EWMA) charts are two such alternatives that are frequently used when the detection of small shifts is more important.

The CUSUM charts have been studied in detail by many researchers, Page (1961), Johnson (1961), Ewan (1963), Lucas (1976, 1982, 1989), Moustakides (1986), Gan (1991, 1993), Hawkins (1981), and Woodall and Adams (1993, 1985), Reynolds and Stoumbos (1999), Bourke (2001a,b). The CUSUM chart, unlike the Shewhart charts, makes use of the information contained in the previous plotted points. It plots the cumulative sum of the deviation of the observations from a target value. The CUSUM works by accumulating deviations from μ_0 that are above target with one statistic C^+ and accumulating deviations from μ_0 that are below target with another statistic C^-. The statistics C^+ and C^- are called one-sided upper and lower CUSUMs, respectively. They are computed as follows:

$$\begin{aligned} C_i^+ &= \max[0, X_i - (\mu_0 + K) + C_{i-1}^+] \\ C_i^- &= \max[0, (\mu_0 - K) - X_i + C_{i-1}^-] \end{aligned} \tag{1.5}$$

where the starting values are $C_0^+ = C_0^- = 0$.

In the above equations, K is the reference value, and is often chosen about halfway between the target μ_0 and the out-of-control value of the mean, μ_1, which we are interested in detecting quickly, that is,

$$K = \frac{|\mu_1 - \mu_0|}{2} = \frac{\delta}{2}\sigma \tag{1.6}$$

The statistic C_i^+ and C_i^- are plotted on the upper and lower CUSUM respectively. When either one of them becomes negative it is set to zero. There is another parameter of tabular CUSUM, H, which is called decision interval. That is to say, if either C_i^+ or C_i^- exceeds H, the process is considered to be out of control.

The EWMA chart was introduced by Roberts (1959). The EWMA chart plots the exponentially weighted statistic

$$z_i = \lambda x_i + (1-\lambda) z_{i-1} \tag{1.7}$$

where, $0 < \lambda \leq 1$ is the smoothing constant. The process average, μ_0, is usually taken as the starting value for the statistic, z_0. In case the process average is unknown, then an estimate of the average can be treated as the starting value.

Since the EWMA chart is insensitive to the normality assumption, see Borror *et al.* (1999), so the chart can have (L) sigma limits. The steady-state (L) sigma limits of the EWMA chart are given by.

$$\begin{aligned} UCL &= \mu_0 + L\sigma\sqrt{\frac{\lambda}{2-\lambda}} \\ CL &= \mu_0 \\ LCL &= \mu_0 - L\sigma\sqrt{\frac{\lambda}{2-\lambda}} \end{aligned} \tag{1.8}$$

The selection of λ and L depends upon the desired shift that needs to be detected. The user can decide on an in-control ARL and then select the appropriate values corresponding to the in-control ARL. The choice of λ and L have been studied in detail and ARL tables and graphs have been generated for different combinations of λ and L, Crowder (1987, 1989), Lucas and Saccucci (1990).

1.5. Problem Statement

Even though Shewhart charts for attributes are effective most of the time, they become inadequate when the nonconforming or nonconformity level becomes very small, i.e. in high yield processes. The Shewhart charts are based on the normal approximation theory and for this theory to hold true it is important that the value of np and c be reasonably large, where n is the sample size, p is the fraction nonconforming and c is the number of nonconformities per inspection unit. When this is not so the normal approximation is no

longer valid. Some of the concerns that must be addressed while applying Shewhart charts for attributes are listed below:

- The control limits will not be symmetrical about the central line, which means statistical foundation of the control chart is no longer valid.
- The lower control limit will be often set to zero. To obtain a positive lower control limit the sample size has to be quite large which is impractical. Such a control chart, with lower control limit set at zero will not be able to detect process improvement.
- A large sample size, for the sake of better approximation, would result in excessive number of nonconforming items when there is sudden change in the process.
- The rational sub grouping of items becomes difficult in an automated or 100% inspection environment.
- If the approximation is not true, the traditional three sigma upper control limit can be less than 1. This means that the only way the process can be kept in control is by continuously generating zero-defect samples, which is impossible to achieve. This also means that the control chart will be thrown out of control even if a single nonconforming item appears.

A good alternative, which is free from the above disadvantages, is to monitor the items or quantity between two successive defectives or defects. This approach is studied in detail by many researchers and is further discussed in Chapter 2. Another alternative is to

monitor the process with the aid of time between events charts. Some issues that need to be considered while using these charts are:

Decision regarding the statistical control of the process is based on a single point: Monitoring the defect occurrence process using the time between events control chart is straightforward. However, since the decision is based on only one observation, it may cause many false alarms or maybe insensitive to process shift if the control limits are wide (with small value of false alarm probability). As a result the chart becomes less sensitive to small changes in the process average.

Selecting the appropriate charting method for monitoring time between events: This is an important issue for the end user. The user needs to know and decide which control chart is best suited for his/her process requirements

The effect of skewness on the sensitivity of the chart: Often when we monitor the process based on a skewed distribution, say geometric or exponential, it becomes essential to study the effect of the skewness of the distribution on the chart properties, and therefore, on its sensitivity.

Control charting for Weibull distributed quality characteristics: Most of the studies assume that time-between event is exponentially distributed. An important assumption when exponential distribution is used is that the event occurrence rate is constant. This assumption is usually violated in reality. Due to wear and tear and other usage conditions,

items usually have an increasing defect rate. To be able to monitor processes for which the exponential assumption is violated, Weibull distribution is a good alternative and it is a simple generalization of the exponential distribution. Thus there is a need for a control chart which can monitor the quality characteristics following Weibull distribution.

Improving the sensitivity of the chart to small process deteriorations: An effective charting method is one which detects process changes faster and at the same time raises fewer false alarms when the process is in control. The time between events chart are often slow in detecting small process changes. This makes it important to look for options, other than increasing the sample size, to improve the sensitivity of the chart.

1.6. Scope of Research

This dissertation attempts to look at the alternatives to monitor the time (or quantity) between events type of data and to improve them to make them more efficient in today's ever changing environment. Some relatively new charting methods are studied and their application issues are discussed.

Chapter 2 is a review of some of the process monitoring techniques relevant to our study. Chapter 3 extends the recent control scheme based on monitoring the cumulative quantity between observations of defects to monitor the quantity required to observe a fixed number of defects. In Chapter 4 the performance of some of the time between events control charts are compared. In Chapter 5 the average run length behavior of the run-length control charts, based on skewed distributions like erlang and negative binomial, is

studied and a procedure is developed to optimize the performance of the chart. Chapter 6 studies the effect of incorrect estimation of the control limits and their effect on the properties of the cumulative quantity control chart. Chapter 7 proposes the control chart based on Weibull distribution to monitor quality characteristics following Weibull distribution. Chapter 8 proposes a combined decision scheme for the cumulative quantity charting procedure to improve their sensitivity.

Chapter 2

Literature Survey

2.1. The use of exact probability limits for Shewhart charts

As discussed earlier the conventional Shewhart charts for attributes suffer from limitations when the value of fraction nonconforming or the rate of occurrence of nonconformities is small. Due to this most of the time the lower control limit has to be fixed at zero. Xie and Goh (1993a), Wetherill and Brown (1991), and Montgomery (2001) advocate the use of exact probability limits in place of the usual three-sigma limits. In the case of Poisson distribution, which is not a symmetrical distribution, the upper and the lower 3-sigam limits do not correspond to equal probabilities of a point on the control chart falling outside the limits even though process is in control. Using the exact probability limits actually modifies the control chart in such a way that each point has an equal chance of falling above or below the upper and lower control limits respectively. For the case of c chart the probability limits are given as:

$$\sum_{x=0}^{UCL} \frac{e^{-c} c^{x}}{x!} = 1 - \frac{\alpha}{2}, \qquad \sum_{x=0}^{CL} \frac{e^{-c} c^{x}}{x!} = 0.5, \qquad \sum_{x=0}^{LCL} \frac{e^{-c} c^{x}}{x!} = \frac{\alpha}{2} \tag{2.1}$$

where, α is the acceptable false alarm probability.

Similarly for the case of np chart the probability limits are given as:

$$\sum_{k=0}^{UCL}\binom{n}{k}p^k(1-p)^{n-k} = 1-\frac{\alpha}{2}$$
$$\sum_{k=0}^{CL}\binom{n}{k}p^k(1-p)^{n-k} = 0.5 \qquad (2.2)$$
$$\sum_{k=0}^{LCL}\binom{n}{k}p^k(1-p)^{n-k} = \frac{\alpha}{2}$$

Using the exact probability limits we can enhance the performance of the control chart but it cannot be treated as a permanent solution. When the fraction nonconforming level or the rate of occurrence of nonconformities is substantially low, the lower control limit would still be zero.

2.2. The Q chart

Quesenberry (1995) proposed a transformation procedure, named as the geometric *Q* chart. The geometric *Q* chart is a form of standardized *G* chart. By using the transformation, the problem of detecting changes in the geometric distribution is transformed into one of monitoring a normally distributed variable so that other well developed techniques such as supplementary run rules, and CUSUM and EWMA control schemes can be used.

The method utilizes the probability integral transformation to transform geometrically distributed data. Using ϕ^{-1} to denote the inverse function of the standard normal distribution, the Q_i statistic can be calculated as

$$Q_i = -\Phi^{-1}(u_i) \tag{2.3}$$

where, $u_i = F(x_i; p) = 1-(1-p)^{x_i}$. For i = 1, 2, ……, Q_i will approximately follow standard normal distribution.

The accuracy of the chart improves as p approaches zero, thus making it suitable for monitoring high yield proceses.

2.3. Goh's pattern recognition approach

Goh (1987a, 1991) suggested an approach which studies the occurring patterns of samples containing defectives or defects which can be applied to both np as well as c charts. A similar idea was also proposed by Rowlands (1992).

Goh's approach defines a nonconforming sample as one that contains a nonconforming item and a nonconforming item as one containing nonconformities. The approach is based on exact Poisson and binomial distribution with a pre-defined Type I error, α.

Since, the defect rate or the fraction nonconforming is quite small for high quality process, an out of control signal will be raised whenever a sample containing more than one defect or defective is observed or when there are more than a specified number of

nonconforming samples within another specified number of consecutively collected samples.

2.4. Control charts based on cumulative count of conforming items

Calvin (1983) proposed that instead of concentrating on nonconforming items, the other alternative is to concentrate on conforming items, especially when p is low. Goh (1987b) further expanded this idea into the Cumulative Count of Conforming (CCC) chart. The CCC chart monitors the number of items inspected to observe a nonconforming item. This count is then plotted against the ordinal number of nonconforming item on the chart. If an item is nonconforming with probability p, then the number of items inspected to observe a nonconforming item, Y, follows geometric distribution. So, the probability that the n^{th} item being inspected is defective is given by

$$g(n) = (1-p)^{n-1} p, \quad n = 1,2,3..... \tag{2.4}$$

The mean and variance of the geometric distribution are given as

$$\mu = \frac{1}{p} \text{ and } \sigma^2 = \frac{(1-p)}{p^2} \tag{2.5}$$

respectively. The cumulative distribution function of the geometric distribution is given by:

$$F(Y=n)=\sum_{i=1}^{n}(1-p)^{i-1}p=1-(1-p)^{n} \tag{2.6}$$

Instead of using the 3σ limits the CCC chart employs the exact probability limits, see Xie and Goh (1997). Assuming that the acceptable false alarm risk level is α, the upper control limit (*UCL*), the centre line (*CL*)and the lower control limit (*LCL*) for the CCC chart are obtained as the solutions of

$$\begin{aligned} F(Y=UCL)&=1-(1-p)^{UCL}=1-\alpha/2\\ F(Y=CL)&=1-(1-p)^{CL}=1/2\\ F(Y=LCL)&=1-(1-p)^{LCL}=\alpha/2 \end{aligned} \tag{2.7}$$

On further solving the control limits can be written as:

$$\begin{aligned} UCL&=\ln(\alpha/2)/\ln(1-p)\\ CL&=\ln(1/2)/\ln(1-p)\\ LCL&=\ln(1-\alpha/2)/\ln(1-p) \end{aligned} \tag{2.8}$$

The implementation involves maintaining a count, n', of cumulative count of conforming items and every conforming item is added to that count. The moment a nonconforming item is found out, n' (including the nonconforming item) is plotted on the chart and then the counter is set back to zero. The decision rule is similar to that of cumulative charting technique, discussed in detail in the next section.

Some other related work on the monitoring of high quality processes can be found in Kaminsky *et al.* (1992), Lawson and Hathway (1990), Glushkovsky (1994), Goh (1991, 1993), Goh and Xie (1994, 1995), McCool and Joyner (1998), Nelson (1994), and Pesotchinsky (1987) Xie *et al.* (1995a).

2.5. Cumulative Quantity Control (CQC) chart

The Cumulative Quantity Control chart or the CQC chart was proposed by Chan *et al.* (2000). The chart is based on the fact that if defects (per unit quantity of product) occurring in a process follow Poisson distribution then the number of units inspected (Q) before exactly one defect is observed will be an exponential random variable. If the defects have a mean rate of occurrence λ, then Q can be described with

Probability Density Function: $$f(Q) = \lambda e^{-\lambda Q} \tag{2.9}$$

Cumulative Distribution Function: $$F(Q) = 1 - e^{-\lambda Q} \tag{2.10}$$

Mean: $$E(Q) = \frac{1}{\lambda} \tag{2.11}$$

If the false alarm probability is set as α, then the probability limits of the CQC chart are calculated by equating Equation (2.10) to the respective probabilities (as in Equation (2.7)), and are given as

$$
\begin{aligned}
Q_U &= -\frac{\ln(\alpha/2)}{\lambda} \\
Q_c &= -\frac{\ln(0.5)}{\lambda} \approx \frac{0.6931}{\lambda} \\
Q_L &= -\frac{\ln(1-\alpha/2)}{\lambda}
\end{aligned}
\tag{2.12}
$$

As it is evident from the above formulae that the functioning of the CQC chart is not affected by the choice of the sample size, which is a major advantage.

2.5.1. The decision rule for the CQC chart

The plotting procedure and decision rule for the CQC charts is as follows:

- The horizontal axis is the sample number and the vertical axis is the logarithm of the quantity Q (for the CQC chart).
- Initially Q is taken as zero.
- An item is inspected from a sample. If the item does not contain any defects the value of Q is increased by 1. Then next item is taken and if it is also defect free Q is again increased by 1. After inspecting all the items in the sample if we do not find any defect then the value of Q, which will then be equal to the sample size, is plotted on the chart and next sample is taken and the process continues. So if after second sample (say of size N) we do not find any defect then the value of Q will be $2N$ and this will plotted against the sample number 2.

- The moment a defect is encountered the value of Q is plotted on the chart and is then reset to zero and the counting process starts again.
- If the plotted point lies within the upper and lower control limits then the process is said to be in control.
- If a point lies below the lower control limit, it may mean that the process average has shifted (or the defect rate has increased, *i.e.* the process has deteriorated) and action should be taken to identify any assignable causes responsible for this shift. If an assignable cause can be found then it should be removed to bring the process back to its original state. If no assignable causes are found then the out of limit point can be treated as a false alarm and plotting process will continue.
- If a point lies above the upper control limit, then it may mean that the process average has improved (the defect rate has decreased, *i.e.* the process has improved). In such a case the process should be stopped and the reason for this improvement should be identified and a new chart should be implemented with the new defect rate.

2.6. The Cumulative Probability Control chart

Chan *et al.* (2002) proposed a statistical process control chart called the cumulative probability control chart (CPC chart). The CPC chart is motivated from two existing statistical control charts, the cumulative count control chart (CCC chart) and the cumulative quantity control chart (CQC chart). The CCC and CQC charts are effective in monitoring production processes when the defect rate is low and the traditional p and c charts do not perform well. In a CPC chart, the cumulative probability of the geometric or

exponential random variable is plotted against the sample number, and hence the actual cumulative probability is indicated on the chart.

Apart from maintaining all the favorable features of the CCC and CQC charts, the CPC chart is more flexible and it can resolve the technical plotting inconvenience of the CCC and CQC charts.

Criteria	**CCC chart**	**CQC chart**
Underlying Distribution	Geometric Distribution	Exponential distribution
Substitutes	p, np chart	c, u chart
Monitored statistic	Number of items inspected to observe one nonconforming item	Number of items inspected (need not be an integer) to observe exactly one nonconformity
Advantages	• Improved sensitivity to process improvements especially in a high quality process • No approximation assumptions required	
Parameter	Process fraction nonconforming (p), false alarm probability (α)	Process defect rate (λ), false alarm probability (α)
Disadvantages	Not accurate in detecting small deteriorations in the process	

Table 1.1 Comparison of the CCC and CQC charts

2.7. Application issues in the CCC charting procedure

2.7.1. Resetting the initial count when applying the CCC chart

The charting procedure proposed by Goh (1987b) was very effective but there is an area of concern. The charting procedure suggests that the moment a nonconforming item is discovered, the value of counter should be set back to zero, which means any past

information till this point is ignored. Xie and Goh (1992) addressed this issue. They pointed out two problems in this approach.

The first is that in the traditional Shewhart control charts the α is fixed while in the CCC control charts it is not because the value of p is low and the decision whether the process is in control has to be based on the current value of p. They developed a decision graph to judge the statistical control of the process by the p- α relationship. Probability that no nonconforming item has been observed in n items inspected is

$$(1-p)^n \tag{2.13}$$

This probability is treated as the certainty with which the process is judged to be out of control when a nonconforming item is observed. Denoting the certainty by s, the above equation can be written as

$$s = (1-p)^n \tag{2.14}$$

Taking log and rearranging, the relationship can be represented as

$$n = \frac{\ln s}{\ln(1-p)} \tag{2.15}$$

Using different values of p, s and n, a decision graph is plotted. The user can then find out where his control chart is operating and then accordingly take decision whether the process is in control.

The second problem is related to setting the counter back to zero whenever a nonconforming item is observed. Setting it back to zero, especially when the process is judged to be in control, does not make any sense as one would like to make use of all the information about the process. Xie and Goh proposed that when the process is judged to be in control then the counter be set at some another value n_o. The relationship between n_c and n_0 is given as

$$n_0 = n_c(n_c - 1)\frac{p}{2} \tag{2.16}$$

where, n_c is the number of items inspected before a nonconforming item is encountered.

2.7.2. Inspection errors

Lu *et al.* (2000) studied the effect of inspection errors on the properties of the run length control charts. In the presence of inspection errors, the control limits can be modified based on the errors. The relationship between p_t, the true probability of nonconforming and p_0, the observed fraction nonconforming can be represented as (see Burke *et al.* (1995)):

$$p_t = (p_o - \theta)/(1 - \theta - \psi) \tag{2.17}$$

where, θ = the probability of classifying a conforming item as nonconforming and ψ = the probability of classifying a nonconforming item as conforming are the classification error probabilities. It can be shown that the adjusted control limits of the CCC chart in the presence of inspection errors can be derived as follows:

$$\begin{aligned} LCL_c &= \ln\{1 - \frac{0.5\alpha_{desired}\, p_t}{p_o}\} / \ln[1 - p_o] \\ CL_c &= \ln(0.5) / \ln[1 - p_o] \\ UCL_c &= \ln\{\frac{0.5\alpha_{desired}\, p_t}{p_o}\} / \ln[1 - p_o] \end{aligned} \tag{2.18}$$

In the above formulae $\alpha_{desired}$ is the desired false alarm probability when the process is in control. It should be noted that generally $\alpha_{desired}$ is taken as 0.0027, which is equivalent to the standard 3-sigma control limits.

2.8. Extension of the CCC and CQC charting techniques

2.8.1. Control charting by fixing the number of nonconforming units, the CCC-*r* chart

Xie *et al.* (1998b, 1999) proposed a control charting procedure to monitor cumulative count of items produced until a fixed number of nonconforming items (*r*) is observed.

Such a chart was given the name of CCC-*r* chart. The chart is particularly suitable for one-by-one inspection process and so no subjective sample size is needed. The CCC-*r* charting technique was also studied by Lu *et al.* (1998, 1999). Chan *et al.* (1997) proposed the CCC-2 control chart which is just a special case of the more general CCC-*r* charts. Some other related discussion can also be found in Wu *et al.* (2000).

Let *Y* be the cumulative count of items inspected until *r* nonconforming items have been observed. If the probability of an item to be nonconforming is *p,* then *Y* follows a negative binomial distribution given by

$$P(Y=n)=\binom{n-1}{r-1}p^{r}(1-p)^{n-r} \qquad n=r,r+1,..... \tag{2.19}$$

The cumulative distribution function of count *Y* is

$$F(n,r,p)=\sum_{i=r}^{n}P(Y=i)=\sum_{i=r}^{n}\binom{i-1}{r-1}p^{r}(1-p)^{i-r} \tag{2.20}$$

The use of exact probability limits in case of CCC-*r* chart can be explained due to the fact that in case of negative binomial distribution there is a poor normal approximation in the tails of the distribution. If the acceptable false alarm probability is α, then the upper control limit, the lower control limit and the centre line, UCL_r, LCL_r, and CL_r

respectively, of the CCC-*r* chart can be obtained as the solution of the following equations:

$$\begin{aligned} F(UCL_r, r, p) &= \sum_{i=r}^{UCL_r} \binom{i-1}{r-1} p^r (1-p)^{i-r} = 1-\alpha/2 \\ F(CL_r, r, p) &= \sum_{i=r}^{CL_r} \binom{i-1}{r-1} p^r (1-p)^{i-r} = 0.5 \\ F(LCL_r, r, p) &= \sum_{i=r}^{LCL_r} \binom{i-1}{r-1} p^r (1-p)^{i-r} = \alpha/2 \end{aligned} \tag{2.21}$$

The term ARL has little meaning in case of CCC-*r* chart as the number of points plotted does not signify the number of samples taken but rather denote the number of nonconforming items (= $r \times$ ARL) observed until an alarm signal. So the term Average Item Run Length (AIRL) is used in the case of CCC-*r* charts. Bourke (1991) in his paper has also called it the Average Number Inspected (ANI). Let the probability for count *Y* not falling within the control limits be β_r , then

$$\beta_r = \sum_{i=LCL_r}^{UCL_r} \binom{i-1}{r-1} p^r (1-p)^{i-r} \tag{2.22}$$

Using the type II error probability calculated in Equation (2.22) the AIRL of the CCC-*r* charts, $AIRL_r$, can be written as:

$$AIRL_r = \frac{r}{(1-\beta_r)\,p} \tag{2.23}$$

The selection of *r* can be treated as a subjective issue, if cost involved is not a consideration. Some facts, which should be kept in mind while choosing *r*, are

- As *p* approaches zero the central line, which indicates the average number of items inspected until a point is plotted, is very large so it is not appropriate to use CCC-*r* charts with large *r* values for small values of *p*
- The control limits of CCC-*r* chart are much larger for charts with large *r* than those with small *r* for the same value of *p.*

Thus as the value of *r* increases the sensitivity of the chart increases, however, the user needs to wait too long to plot a point. So it becomes a question of trade off. Ohta *et al.* (2001) addressed this issue from an economic design perspective and proposed a simplified design method to select a suitable value of *r* based on the economic design method for control charts that monitor discrete quality characteristics. Other related work can be found in Wu *et al.* (2001) where the authors studied the design of CCC-*r* charts for a random shift model.

2.8.2. Serial correlation

The control charts make an important assumption regarding the independence of observations from a production process. However, this is generally not the case in most of the manufacturing processes. The correlated observations are especially common in automated manufacturing processes where the sample size is one and sampling interval is

very small and due to this small interval the observations will be serially correlated over time.

Broadbent (1958) proposed the use of a Markov Serial dependence model to capture the correlation between the items produced in a manufacturing environment. This model assumes that the state of the current item depends only on that of the previous one. For a two-state Markov chain model, two probabilities are considered,

a = probability of obtaining a nonconforming item if the preceding one is conforming.
b = probability of obtaining a conforming item if the preceding one is nonconforming.

Some related work on Markov serially dependent processes can be found in Bhat & Lal (1990), Bhat *et al.* (1990) and Lai *et al.* (1998). Bhat and Lal (1990) show that the long run fraction defective is $p = a / (a + b)$ while the serial correlation coefficient is $d = 1 - (a + b)$.

Suppose that the user is interested in the cumulative count of items inspected until observing two nonconforming items (CCC-2 chart). Hence, for a specific count Y, an automated manufacturing process can be represented by sequences of $(Y+1)$ items, in which the zeroth and Y^{th} item are always nonconforming with a third nonconforming item in between them, while the remaining items are all conforming.

Based on this finding Lai *et al.* (2000) generalized the probability distribution function and the cumulative probability function of *Y* as:

$$P(Y=n)=\begin{cases}(1-b)^2, n=2\\ 2ab(1-b), n=3\\ 2ab(1-b)(1-a)^{n-3}+a^2b^2(n-3)(1-a)^{n-4}, n\geq 4\end{cases} \tag{2.24}$$

$$F(n)=\begin{cases}(1-b)^2, n=2\\ (1-b)^2+2ab(1-b), n=3\\ (1-b)^2+2ab(1-b)+2(1-b)bc(1-c^{n-3})+b^2[1-(n-2)c^{n-3}+(n-3)c^{n-2}], n\geq 4\end{cases} \tag{2.25}$$

where, $c = (1\text{-}a)$. Putting $d = 0$ (independent observations), the above two equations will reduce to the respective equations of negative binomial distribution with parameters (2, *p*).

If the conventional control limits are used for a Markov serially dependent process (i.e. if there exists a serial correlation between the items produced) then the false alarm probability of the CCC-*r* chart deviates from the desired false alarm probability (generally taken as 0.0027). The conventional CCC-2 chart gives fewer alarms when the serial correlation is negative while more alarms when it is positive. As for the AIRL, it decreases when correlation coefficient *d* increases. This means that the conventional CCC-*r* chart, which does not take into account the serial correlation existing between the

items produced, will give more alarms if d is positive and will give few alarms if d is negative.

The decision making procedure for CCC-r charts for automated manufacturing process having serial correlation is same as before except for the fact that the control limits should be calculated as explained above. Other related work on data correlation can be found in Berthouex *et al.* (1978), and Montgomery and Freidman (1991).

2.8.3. Transforming the geometric and exponential random variable

The power transformation by Box and Cox (1964) is very suitable for transforming the geometric random variable to normal so that Shewhart control chart for variable data and other process monitoring techniques like CUSUM and EWMA can be applied on the transformed data. Xie *et al.* (2000b) compared three methods, namely Quesenberry's Q-transformation, the log transformation and the double square root transformation. They found that the double square root is the simplest and most suitable technique to transform the geometrically distributed quality characteristic. This finding is also supported by Kittlitz (1999) who proposed the double square root transformation for transforming exponentially distributed data. Some general discussion regarding transformation can also be found in Chou (1998).

2.8.4. Control charts for near zero-defect processes

In the so called near zero-defect manufacturing environments, when the number of defects or nonconformities is considered, usually a large number of zero-count values

along with some non-zero values are observed. Many researchers have studied the monitoring of near zero defect processes; see Bohning (1998), Bohning *et al*. (1999), Chang and Gan (1999), He and Goh (2002), Lambert (1992), and Vieira *et al*. (2000). It is now well established that the common pure Poisson distribution cannot adequately describe the data pattern, and a generalized Poisson distribution is preferred instead, which is usually canned zero-inflated Poisson (ZIP) distribution. The probability mass function of the zero-inflated Poisson distribution is given by:

$$\begin{cases} P(k=0) = (1-p) + pe^{-\lambda} \\ P(k=d) = p\dfrac{\lambda^d e^{-\lambda}}{d!} \quad d = 1,2,... \end{cases} \tag{2.26}$$

where p is the probability of the occurrence of random shock, and d denotes the number of nonconformities and λ is the expected number of nonconformities found in a sample when the random shock occurs. The CCC chart and the c chart can then be used to monitor p and λ respectively. The details regarding the use of CCC chart in monitoring a near zero-defect process can be found in Xie and Goh (1993b), Xie *et al*. (1995b), and Xie *et al.* (2001b).

2.8.5. Economic design of run length control Charts

Cost consideration is always a concern in industry and any quality related activities should be put into the context of cost saving to improve profitability. In using control chart in practice, economic factors should be taken into account for designing control

chart. Xie *et al.* (1997), Tang *et al.* (2000) and Xie *et al.* (2001a) studied the economic deign of the CCC chart based on the flexible cost model proposed by Lorenzen and Vance (1986). In Xie *et al.* (1997) a general loss function and a design process was proposed based on an optimizing procedure to calculate the design parameters of the CCC charts. For a more detailed study of CCC chart and its properties the users can refer to Xie *et al.* (2002a).

2.8.6 The CCC and exponential CUSUM Charts

An alternative to monitor time between events data is to use a CUSUM chart. The CUSUM chart has proved to be very useful in detecting small shifts in the process. The time-between-events CUSUM has been studied by many authors, see Gan (1992, 1994), Lorden and Eisenberger (1973), Lucas (1985), Vardeman and Ray (1985), and Woodall (1983). The CUSUM scheme has also been developed for quality characteristics following geometric distribution and thus can be readily applied to cumulative count of conforming data. Related discussion can be found in Bourke (1991, 2001a) and Xie *et al.* (1998a).

The CUSUM charts are known to be quite sensitive to small shifts in a process. Many researchers have studied the properties and charting procedures of the time-between-events CUSUM, see Lucas (1985) and Gan (1992). If X_1, X_2,… be the inter-arrival times then the time-between-events CUSUM for detecting an increase or decrease in the inter-arrival times can be respectively defined as

$$S_i^+ = \max\{S_{i-1}^+ + (X_i - k)\}$$
$$S_i^- = \min\{S_{i-1}^- + (X_i - k)\}$$

where, k is the pre-chosen parameter.

The control limits are denoted by h and the decision on the statistical control of the process is taken depending on whether $S_t^- \leq -h$ or $S_t^+ \geq h$. Most of the research on the time-between-events CUSUM assumes that the inter-arrival times follow exponential distribution.

The average run length calculation for a CUSUM scheme is comparatively more difficult than that for a Shewhart chart. Vardeman and Ray (1985) obtained the exact expressions for the ARLs of CUSUM schemes when the inter-arrival times follow exponential distribution. Gan (1992) obtained the probability function of the run length, the ARLs, the standard deviation of the run length (SDRL) and the run length percentiles of exponential CUSUM schemes by solving the integral equations. Reynolds (1975) derived an expression for the ARLs by Brownian motion approximation. Lucas (1985) computed average run length of the CUSUM scheme by the Markov chain approach proposed by Brook and Evans (1972), which gives approximate but quite accurate results. Some other related discussions on ARL of CUSUM charts can be found in Gardiner (1987), Fellener (1990), Hawkins (1992), and Woodall (1983).

With so many monitoring options available, it becomes important for the users to correctly identify the monitoring method that is simple and easy to use and satisfies their requirements. Figure 2.1 shows the flow chart that helps the user in selecting an appropriate charting procedure for monitoring time between events type of data. First, when the distribution of the data is unknown, the plotting techniques can be employed to establish the underlying distribution as well as to calculate the relevant parameters. Then a judgment regarding the normality of the data has to be made.. If the data are normally distributed, we can either use the Shewhart control charts, EWMA, or CUSUM charts to monitor the process.

For exponentially distributed data, we can use CQC chart, as well as exponential EWMA and CUSUM chart. Another option is to transform the data to normal. Once the data has been transformed to normal, either the Shewhart, or the EWMA or the CUSUM charts can be used for monitoring purposes.

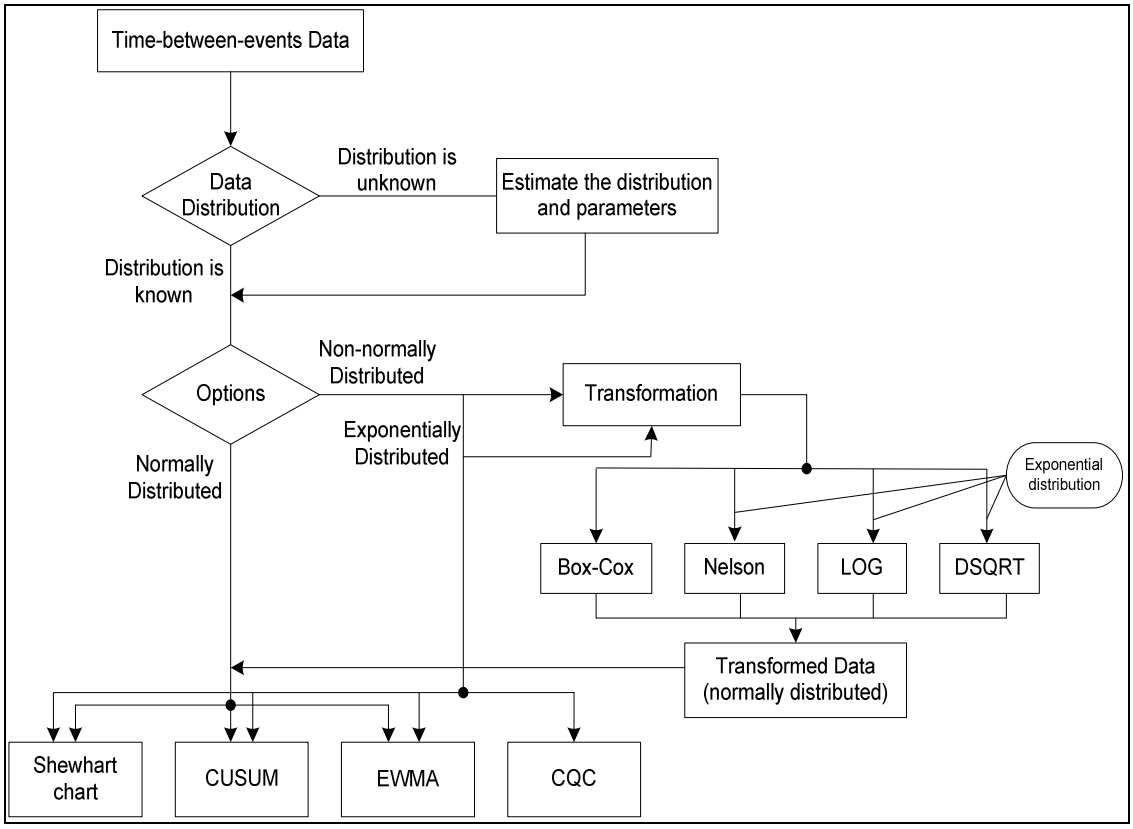

Figure 2.1 Selecting the suitable charting procedure

Chapter 3

Monitoring counted data

3.1. Monitoring defect rate in a Poisson process

Standard c chart or u chart, which is for the monitoring of the number of defects in a sample, are extensively used in the industry for monitoring counted data. However, they require a large number of defects and are not appropriate for application to a process with low count levels. Figure 3.1 is a typical example of periodic defect reports monitored with a c chart. When there are an excessive number of defects, the chart will signal an out-of-control situation. Although the anticipated false alarm probability is 0.27% by a traditional chart, it could be much higher because when the number of failures is Poisson distributed, normal distribution, which is used, is not a good approximation when the average number of defects is small. Moreover, the lower control limit is usually set at zero, which is not useful because then process improvement cannot be detected.

Chan *et al.* (2000) recently proposed a procedure based on the monitoring of cumulative production quantity between the observations of two defects in a manufacturing process. This approach has shown to have a number of advantages: it does not involve the choice of a subjective sample size; it raises fewer false alarms; it can be used in any environment irrespective of whether the process is of high quality; and it can detect further process improvement.

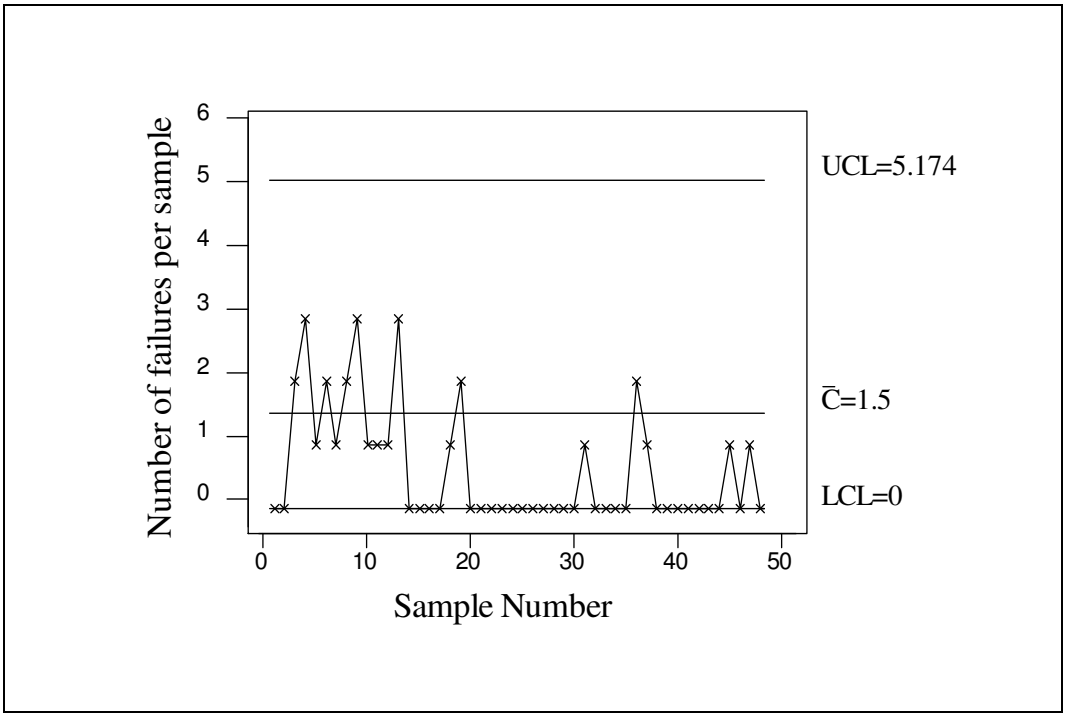

Figure 3.1 The traditional u chart for the monitoring of number of failures per unit time.

For a process in normal operation, defects are random event caused by, for example, sudden increase of stress and human error. The defect occurrence process can usually be modeled by a homogeneous Poisson process with certain intensity. Hence, our aim here is to monitor the defect process and detect any change of the intensity parameter. The procedure in Chan *et al*. (2000) is based on the monitoring of the cumulative production quantity between observing two defects in a manufacturing process. This cumulative production quantity is an exponential random variable that describes the length till the occurrence of next defect in a Poisson process.

The use of cumulative quality is a different and new approach. We further extend the procedure to the case when cumulative quantity to the r^{th} defect is used to monitor the

defect process. The implementation and interpretations are provided and numerical examples are used to illustrate the application procedure. We also investigate some basic properties of the proposed scheme.

3.2. Monitoring quantity between *r* defects

Monitoring the defect occurrence process using the CQC chart is straightforward. However, since the decision is based on only one observation, it may cause many false alarms or it is insensitive to process shift if the control limits are wide (with small value of α). To deal with this problem, we can consider using the quantity between *r* defects. Denote the quantity to observe the r^{th} defect by Q_r, a CQC$_r$ chart is proposed and studied here.

3.2.1 The distribution of Q_r

To monitor the process based on the quantity between the occurrences of *r* defects, we need a distribution to model the cumulative quantity till the r^{th} failure, Q_r. It is well known that the sum of *r* exponentially distributed random variables is the Erlang distribution. An Erlang random variable is defined as the length till the occurrence of *r* defects (failures) in a Poisson process. Then the probability density function of Q_r, is given as:

$$f(Q_r, r, \lambda) = \frac{\lambda^r Q_r^{\,r-1}}{(r-1)!} \exp\{-\lambda Q_r\} \tag{3.1}$$

The cumulative Erlang distribution is

$$F(Q_r, r, \lambda) = 1 - \sum_{k=0}^{r-1} \frac{(\lambda Q_r)^k}{k!} \exp\{-\lambda Q_r\} \tag{3.2}$$

Q_r can then be used to model the quantity to the r^{th} defect in a Poisson process. We propose another chart; henceforth know as the CQC_r chart, to monitor Q_r.

It should be noted that for r =1, the Gamma distribution reduces to the exponential distribution. Hence, the CQC_1 chart is same as the CQC chart proposed by Chan *et al.* (2000) chart.

3.2.2 Control limits of CQC_r- chart

To calculate the control limits of the CQC_r chart, the exact probability limits will be used. If α is the accepted false alarm risk then the upper control limit, UCL_r, the center line, CL_r, and the lower control limit, LCL_r, can be easily calculated by using Equation (3.2) in the following manner:

$$\begin{aligned} F(LCL_r, r, \lambda) &= 1 - \sum_{k=0}^{r-1} e^{-\lambda LCL_r} \frac{(\lambda LCL_r)^k}{k!} = \alpha/2 \\ F(CL_r, r, \lambda) &= 1 - \sum_{k=0}^{r-1} e^{-\lambda CL_r} \frac{(\lambda CL_r)^k}{k!} = 0.5 \\ F(UCL_r, r, \lambda) &= 1 - \sum_{k=0}^{r-1} e^{-\lambda UCL_r} \frac{(\lambda UCL_r)^k}{k!} = 1 - \alpha/2 \end{aligned} \tag{3.3}$$

The control limits can be easily calculated using some mathematical or statistical software such as MATHEMATICA. Tables 3.1-3.3 show the computed control limits for some CQC_r charts with the false alarm risk, $\alpha = 0.0027$. It should be noted that UCL_r and LCL_r appear in Equation (3.3) in product with λ, which means that the control limits are inversely proportional to the λ. That is, when λ is increased by a factor, the limits will decrease by the same factor.

Table 3.4 shows the control limits of some CQC_r charts for different values of false alarm risk with the assumed in control defect rate of 0.001.As expected the lower control limits and the upper control limit, respectively, increase and decrease as the false alarm probability increases. The center line for the charts has not been computed as it only depends on the in control parameter and is not influenced by changes in false alarm probability. The center line for all the charts shown in Table 3.4 is thus - ln(0.5)/0.001 = 693.147.

The decision-making procedure for the CQC_r chart remains same as the CQC chart and is shown in Figure 3.2.

λ_0	CQC_1			CQC_2		
	UCL	CL	LCL	UCL	CL	LCL
0.000001	6.61E+06	693147	1350.91	8.90E+06	1.68E+06	52883.6
0.000002	3.30E+06	346574	675.46	4.45E+06	839173.5	26441.8
0.000003	2.20E+06	231049	450.3	2.97E+06	559449	17627.9
0.000004	1.65E+06	173287	337.73	2.23E+06	419586.75	13220.9
0.000005	1.32E+06	138629	270.18	1.78E+06	335669.4	10576.7
0.000006	1.10E+06	115525	225.15	1.48E+06	279724.5	8813.93
0.000007	943950.1	99021	192.99	1.27E+06	239763.86	7554.79
0.000008	825956.34	86643.4	168.86	1.11E+06	209793.37	6610.44
0.000009	734183.41	77016.4	150.1	988911.8	186483	5875.95
0.000015	440510.05	46209.8	90.06	593347.1	111889.8	3525.57
0.000016	412978.17	43321.7	84.43	556262.9	104896.69	3305.22
0.000017	388685.33	40773.4	79.47	523541.6	98726.29	3110.8
0.000018	367091.7	38508.2	75.05	494455.9	93241.5	2937.98
0.000019	347771.09	36481.4	71.1	468431.9	88334.05	2783.35
0.00031	21315	2235.96	4.36	28710.34	5414.02	170.59
0.00032	20648.91	2166.08	4.22	27813.14	5244.83	165.26
0.00033	20023.18	2100.45	4.09	26970.32	5085.9	160.25
0.00034	19434.27	2038.67	3.97	26177.08	4936.31	155.54
0.00035	18879	1980.42	3.86	25429.16	4795.28	151.1
0.00036	18354.59	1925.41	3.75	24722.8	4662.07	146.9
0.00037	17858.52	1873.37	3.65	24054.61	4536.07	142.93
0.00038	17388.55	1824.07	3.56	23421.6	4416.7	139.17
0.00039	16942.69	1777.3	3.46	22821.04	4303.45	135.6
0.0041	1611.62	169.06	0.33	2170.78	409.35	12.9
0.0042	1573.25	165.04	0.32	2119.1	399.61	12.59
0.0043	1536.66	161.2	0.31	2069.82	390.31	12.3
0.0044	1501.74	157.53	0.31	2022.77	381.44	12.02
0.0045	1468.37	154.03	0.3	1977.82	372.97	11.75
0.0046	1436.45	150.68	0.29	1934.83	364.86	11.5
0.0047	1405.88	147.48	0.29	1893.66	357.1	11.25
0.0048	1376.59	144.41	0.28	1854.21	349.66	11.02
0.0049	1348.5	141.46	0.28	1816.37	342.52	10.79
0.055	120.14	12.6	0.02	161.82	30.52	0.96
0.1	66.08	6.93	0.01	89	16.78	0.53

Table 3.1 Some control limits of CQC_1 and CQC_2 charts with $\alpha = 0.0027$

λ_0	CQC_3			CQC_4		
	UCL	CL	LCL	UCL	CL	LCL
0.000001	1.09E+07	2.67E+06	211684	1.27E+07	3.67E+06	465296
0.000002	5.43E+06	1.34E+06	105842	6.34E+06	1.84E+06	232648
0.000003	3.62E+06	891353.4	70561.4	4.23E+06	1.22E+06	155099
0.000004	2.72E+06	668515.1	52921.1	3.17E+06	918015	116324
0.000005	2.17E+06	534812.1	42336.9	2.54E+06	734412	93059.2
0.000006	1.81E+06	445676.7	35280.7	2.11E+06	612010	77549.4
0.000007	1.55E+06	382008.6	30240.6	1.81E+06	524580	66470.9
0.000008	1.36E+06	334257.5	26460.5	1.59E+06	459008	58162
0.000009	1.21E+06	297117.8	23520.5	1.41E+06	408007	51699.6
0.000015	724635	178270.7	14112.3	845365	244804	31019.8
0.000016	679345.3	167128.8	13230.3	792529	229504	29081
0.000017	639383.8	157297.7	12452	745910	216004	27370.4
0.000018	603862.5	148558.9	11760.2	704471	204003	25849.8
0.000019	572080.3	140740	11141.3	667393	193266	24489.3
0.00031	35062.98	8626	682.85	40904.7	11845.4	1500.96
0.00032	33967.26	8356.44	661.51	39626.5	11475.2	1454.05
0.00033	32937.95	8103.21	641.47	38425.7	11127.5	1409.99
0.00034	31969.19	7864.88	622.6	37295.5	10800.2	1368.52
0.00035	31055.78	7640.17	604.81	36229.9	10491.6	1329.42
0.00036	30193.12	7427.95	588.01	35223.5	10200.2	1292.49
0.00037	29377.09	7227.19	572.12	34271.5	9924.49	1257.56
0.00038	28604.01	7037	557.06	33369.7	9663.32	1224.46
0.00039	27870.58	6856.56	542.78	32514	9415.54	1193.07
0.0041	2651.1	652.21	51.63	3092.8	895.62	113.49
0.0042	2587.98	636.68	50.4	3019.16	874.3	110.78
0.0043	2527.8	621.87	49.23	2948.95	853.97	108.21
0.0044	2470.35	607.74	48.11	2881.92	834.56	105.75
0.0045	2415.45	594.24	47.04	2817.88	816.01	103.4
0.0046	2362.94	581.32	46.02	2756.62	798.27	101.15
0.0047	2312.66	568.95	45.04	2697.97	781.29	99
0.0048	2264.48	557.1	44.1	2641.76	765.01	96.94
0.0049	2218.27	545.73	43.2	2587.85	749.4	94.96
0.055	197.63	48.62	3.85	230.55	66.76	8.46
0.1	108.7	26.74	2.12	126.8	36.72	4.65

Table 3.2 Some control limits of CQC_3 and CQC_4 charts with $\alpha = 0.0027$

λ_0	CQC_5			CQC_6		
	UCL	CL	LCL	UCL	CL	LCL
0.000001	1.44E+07	4.67E+06	791874	1.60E+07	5.67E+06	1.17E+06
0.000002	7.20E+06	2.34E+06	395937	8.02E+06	2.84E+06	587486.1
0.000003	4.80E+06	1.56E+06	263958	5.34E+06	1.89E+06	391657.4
0.000004	3.60E+06	1.17E+06	197968	4.01E+06	1.42E+06	293743
0.000005	2.88E+06	934181.8	158375	3.21E+06	1.13E+06	234994.4
0.000006	2.40E+06	778484.8	131979	2.67E+06	945027	195828.7
0.000007	2.06E+06	667272.7	113125	2.29E+06	810023	167853.2
0.000008	1.80E+06	583863.6	98984.2	2.00E+06	708770	146871.5
0.000009	1.60E+06	518989.9	87986	1.78E+06	630018	130552.5
0.000015	959492.9	311393.9	52791.6	1.07E+06	378011	78331.48
0.000016	899524.6	291931.8	49492.1	1.00E+06	354385	73435.76
0.000017	846611.3	274759.4	46580.8	943222	333539	69116.01
0.000018	799577.4	259494.9	43993	890821	315009	65276.23
0.000019	757494.4	245837.3	41677.6	843935	298430	61840.64
0.00031	46427.07	15067.45	2554.43	51725.1	18290.8	3790.23
0.00032	44976.23	14596.59	2474.61	50108.7	17719.3	3671.79
0.00033	43613.31	14154.27	2399.62	48590.2	17182.3	3560.52
0.00034	42330.57	13737.97	2329.04	47161.1	16676.9	3455.8
0.00035	41121.12	13345.45	2262.5	45813.6	16200.5	3357.06
0.00036	39978.87	12974.75	2199.65	44541	15750.5	3263.81
0.00037	38898.36	12624.08	2140.2	43337.2	15324.8	3175.6
0.00038	37874.72	12291.87	2083.88	42196.8	14921.5	3092.03
0.00039	36903.57	11976.69	2030.45	41114.8	14538.9	3012.75
0.0041	3510.34	1139.25	193.14	3910.92	1382.97	286.58
0.0042	3426.76	1112.12	188.54	3817.8	1350.04	279.76
0.0043	3347.07	1086.26	184.16	3729.02	1318.64	273.25
0.0044	3271	1061.57	179.97	3644.27	1288.67	267.04
0.0045	3198.31	1037.98	175.97	3563.28	1260.04	261.1
0.0046	3128.78	1015.41	172.15	3485.82	1232.64	255.43
0.0047	3062.21	993.81	168.48	3411.65	1206.42	249.99
0.0048	2998.42	973.11	164.97	3340.58	1181.28	244.79
0.0049	2937.22	953.25	161.61	3272.4	1157.18	239.79
0.055	261.68	84.93	14.4	291.54	103.09	21.36
0.1	143.92	46.71	7.92	160.35	56.7	11.75

Table 3.3 Some control limits of CQC_5 and CQC_6 charts with $\alpha = 0.0027$

α	CQC_1		CQC_2		CQC_3		CQC_4		CQC_5		CQC_6	
	UCL	LCL	UCL	LCL	UCL	LCL	UCL	LCL	UCL	LCL	UCL	LCL
0.0005	8294.05	0.25	10758.64	22.53	12864.8	117.88	14793.55	295.15	16610.71	542.54	18349.18	847.29
0.001	7600.9	0.5	9998.68	31.96	12051.4	149.7	13934.02	355.19	15709.91	632.49	17410.64	967.19
0.0015	7195.44	0.75	9551.73	39.24	11571.46	172.33	13425.68	396.28	15176.19	692.72	16853.76	1046.35
0.002	6907.76	1	9233.41	45.4	11228.87	190.53	13062.24	428.55	14794.15	739.37	16454.75	1107.1
0.0025	6684.61	1.25	8985.77	50.85	10961.88	206.03	12778.64	455.56	14495.75	778.02	16142.85	1157.11
0.003	6502.29	1.5	8782.93	55.8	10742.86	219.68	12545.76	479.01	14250.52	811.31	15886.37	1199.96
0.0035	6348.14	1.75	8611.05	60.36	10557.04	231.97	12348.01	499.87	14042.14	840.74	15668.31	1237.68
0.004	6214.61	2	8461.88	64.62	10395.58	243.2	12176.04	518.76	13860.82	867.23	15478.48	1271.52
0.0045	6096.83	2.25	8330.07	68.63	10252.77	253.59	12023.83	536.08	13700.25	891.41	15310.3	1302.29
0.005	5991.46	2.5	8211.97	72.43	10124.7	263.28	11887.24	552.13	13556.09	913.7	15159.24	1330.59
0.01	5298.32	5.01	7430.13	103.5	9273.79	337.86	10977.5	672.21	12594.09	1077.93	14149.76	1536.91
0.02	4605.17	10.05	6638.35	148.56	8405.95	436.05	10045.1	823.25	11604.63	1279.11	13108.48	1785.28
0.03	4199.71	15.11	6169.55	184.08	7888.7	507.98	9486.94	930.13	11010.3	1418.59	12481.41	1955.18
0.04	3912.02	20.2	5833.92	214.7	7516.6	567.21	9084.12	1016.24	10580.38	1529.53	12026.98	2089.14
0.05	3688.88	25.32	5571.64	242.21	7224.69	618.67	8767.27	1089.87	10241.59	1623.49	11668.33	2201.89
0.1	2995.73	51.29	4743.86	355.36	6295.79	817.69	7753.66	1366.32	9153.52	1970.15	10513.03	2613.01

Table 3.4 Some Control Limits of CQC_r charts with $\lambda_0 = 0.001$

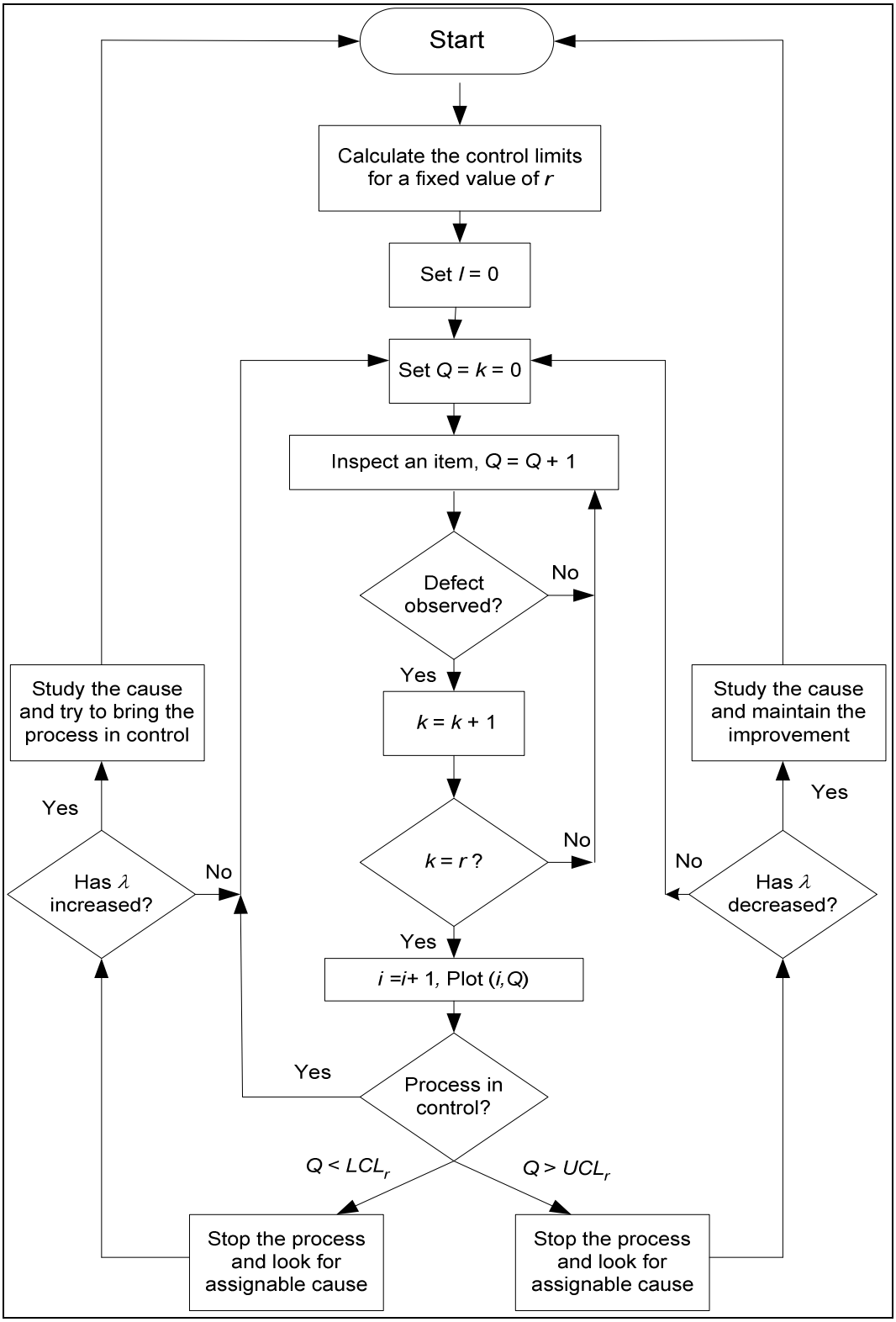

Figure 3.2 The decision rule for the CQC_r chart

3.3. Using the CQC_r charts for reliability monitoring

Failure process monitoring is an important issue for complex or repairable systems. It is also a common problem for a fleet of systems such as equipment or vehicles of the same type in a company. Control charts are widely used for process monitoring in the manufacturing industry. Little research is available on their use to monitor the failure process of components or systems, which is important for equipment performance monitoring. The Shewhart control charts for monitoring the number of defects, can be used for monitoring the number of failures per fixed interval; however, as pointed out before, they are not effective especially when the failure frequency becomes small. The cumulative quantity monitoring scheme between observations of defects can be easily adopted to monitor the failure process for exponentially distributed inter-failure time and the scheme can be easily extended to monitor inter-failure times that follow other distributions such as the Weibull distribution.

As a brief review of related research, process monitoring of reliability related process characteristics has attracted some attention recently. Katter *et al.* (1998) used the control chart to monitor the on-line welder condition. Steiner *et al.* (2001) showed the use of control chart to detect process changed for censored data. Cassady *et al.* (2000) introduced a combined control chart-preventive maintenance strategy. Haworth (1996) showed how the multiple regression control charts could be used to manage software maintenance processes. Kopnov *et al.* (1994) discussed bearing degradation in a process and obtained an optimal control limit by defining the degradation process, considering

the costs involved. Radaelli (1998) studied the time-between-event Shewhart chart and showed how they can be applied when the times are exponentially distributed. These studies mainly follow the standard approach.

As mentioned before, since the quantity produced between the observations of two defects is related to the time between failures in reliability study, the CQC chart approach can be readily adopted for process monitoring in reliability and maintenance. The control limits can be calculated using Equation (3.3). These control limits can then be utilized to monitor the failure times of components. After each failure the time can be plotted on the chart. If the plotted point falls between the calculated control limits, it indicates that the process is in the state of statistical control and no action is warranted. If the point falls above the upper control limit, it indicates that the process average, or the failure occurrence rate, may have decreased which resulted in an increase in the time between failures. This is an important indication of possible process improvement. If this happens the management should look for possible causes for this improvement and if the causes are discovered then action should be taken to maintain them. If the plotted point falls below the lower control limit, it indicates that the process average, or the failure occurrence rate, may have increased which resulted in a decrease in the failure time. This means that process may have deteriorated and thus actions should be taken to identify and remove them.

In either case the people involved can know when the reliability of the system is changed and by a proper follow up they can maintain and improve the reliability. Another

advantage of using the control chart is that it informs the maintenance crew when to leave the process alone, thus saving time and resources.

It can be noted here that the parameter λ should normally be estimated with the data from the failure process. Since λ_0 is the parameter in the exponential distribution, any traditional estimator can be used and we omit this discussion here.

Monitoring the failure occurrence process using the CQC chart is straightforward. However, again the decision regarding the process is based on only one observation, it may cause many false alarms or it is insensitive to process shift if the control limits are wide (with small value of α). Thus we can monitor using the time between r failures as in the case of CQC_r charts. A practical scenario is that when the reliability of a complex system is to be monitored and the failure of any components or incident is reported, the occurrence process can be modeled by a Poisson process. In fact, when components are replaced, we have a superposition of renewal processes. As mentioned before the superimposed process can be approximated by a Poisson process, and hence providing an important justification for the use of our model.

3.4 An illustrative example

An example is presented in this section to illustrate the charting procedure of CQC_r chart and to also illustrate the increased efficiency of the chart when r becomes more than 1.

Table 3.5 shows a set of failure time data. The first 30 times were simulated with the process average, λ, of 0.001 and the second 30 times were simulated with the process average changed to $\lambda = 0.003$. The accepted false alarm risk is $\alpha = 0.0027$.

Failure number	Time	Failure number	Time
1	1065.55	31	35.85
2	535.8	32	362.8
3	540.53	33	357.85
4	716.2	34	334.48
5	2525.43	35	80.13
6	1264.18	36	1939
7	479.44	37	77.88
8	1783.22	38	4.03
9	473.67	39	98.67
10	2265.42	40	17.19
11	2191.75	41	289.79
12	1097.26	42	63.99
13	597.59	43	2.46
14	971.16	44	697.68
15	3157.29	45	1167.33
16	2932.96	46	239.66
17	987.67	47	93.78
18	1816.18	48	680.45
19	117.21	49	4.83
20	190.65	50	102.91
21	943.99	51	479.05
22	1084.48	52	156.67
23	2306.54	53	1286.24
24	6.56	54	443.97
25	3111.51	55	360.03
26	283.86	56	414.66
27	659.39	57	128.9
28	683.48	58	36.1
29	36.14	59	197.31
30	754.16	60	418.12

Table 3.5 Failure time data of the components.

Figure 3.3 shows the CQC chart for the data in Table 3.5. It can be seen that the CQC chart fails to raise an alarm. The control limits of the CQC chart can be calculated using Equation (2.12) and are $UCL = 6607.7$ and $LCL = 1.4$.

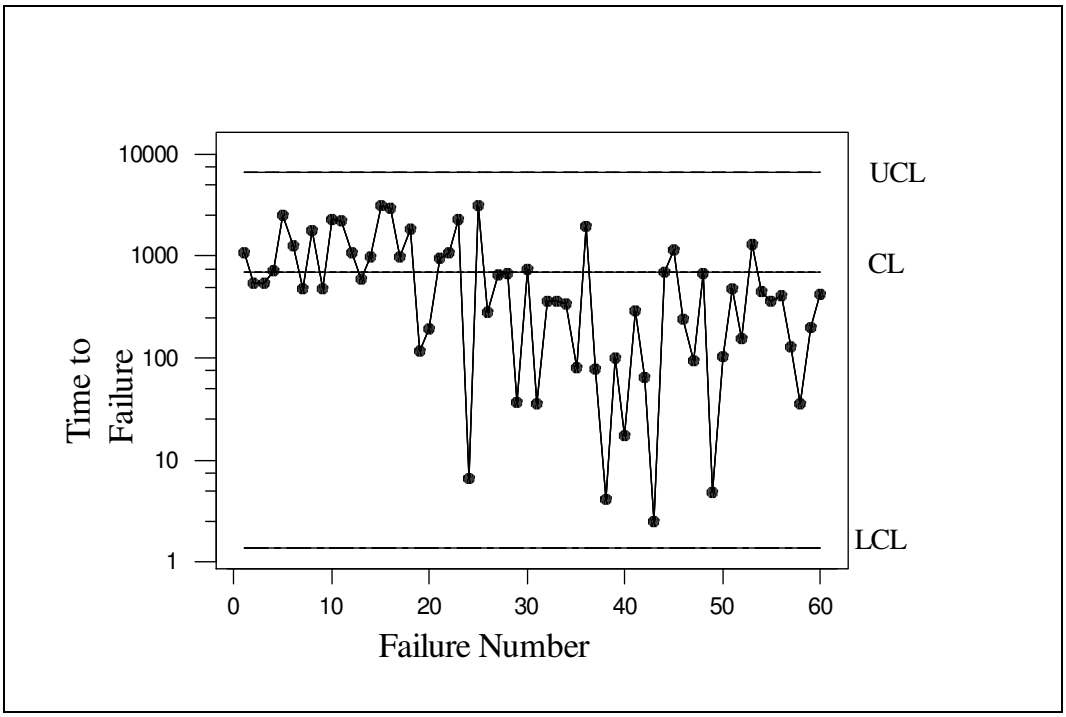

Figure 3.3 The CQC chart for the data in Table 3.5 and no alarm is raised.

Since CQC chart makes use of a single observation in decision making, a CQC_3 chart could be used if more observations are to be taken into consideration in an easy way. The data shown in Table 3.5 is converted into the data of Table 3.6 which shows the cumulative time to failure between every three failures, i.e. Q_3.

Observation number	Time to the accumulation of three failures	Observation number	Time to the accumulation of three failures
1	2141.88	11	756.5
2	4505.81	12	2353.61
3	2736.33	13	180.58
4	5554.43	14	370.97
5	4726.04	15	1867.47
6	5736.81	16	1013.89
7	1251.85	17	586.79
8	3397.58	18	1886.88
9	4054.76	19	903.59
10	1473.78	20	651.53

Table 3.6 Cumulative Failure Time between every three failures

The performance of CQC chart can be compared with the performance of CQC_3 chart by using the data of Table 3.6. The control limits of the CQC_3 charts can be calculated by solving the following equations:

$$1-\sum_{k=0}^{2} e^{-0.001UCL_3}\frac{(0.001UCL_3)^k}{k!}=0.99865$$

$$1-\sum_{k=0}^{2} e^{-0.001CL_3}\frac{(0.001CL_3)^k}{k!}=0.5$$

$$1-\sum_{k=0}^{2} e^{-0.001LCL_3}\frac{(0.001LCL_3)^k}{k!}=0.00135$$

Solving the above equations, the control limits of the CQC_3 chart are obtained as

$$UCL_3 = 10869.3,\ CL_3 = 2674.1,\ LCL_3 = 211.7$$

The CQC_3 chart is shown in Figure 3.4. As can be seen from the figure, the CQC_3 chart raises an alarm signifying process deterioration from $\lambda = 0.001$ to $\lambda = 0.003$. This can be compared with the CQC chart shown in Figure 3.3, which fails to raise an alarm.

Hence, by accumulating 3 failure times, the sensitivity of the chart to detect process changes can be improved as compared with CQC chart. On the other hand, it is a subjective issue what r should be used in CQC_r chart. Usually r should not be too large, as it may need to accumulate a long time before a decision is made. In the next section, we investigate the properties for CQC_3 chart and discuss the issue of chart sensitivity and implementation.

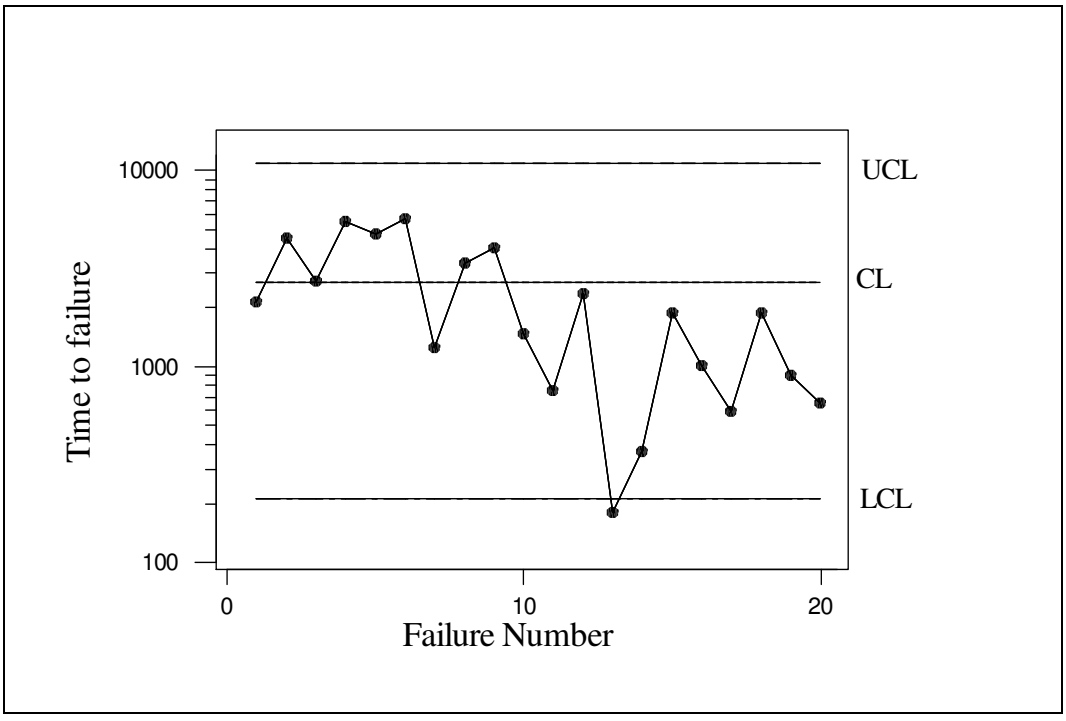

Figure 3.4 The CQC_3 chart for the data in Table 3.6

3.5. Some statistical properties of CQC_r chart

One of the most frequently used terms associated with the control charts for process monitoring is the average run length (ARL) which is generally defined as the average number of points that must be plotted on the control chart before a point indicates an out of control situation. A good control chart should have a large average run length when the process is in control and small average run length when the process shifts away from the target. This means that when the process runs in control, the control chart should raise few false alarms while on the other hand when the process runs out of control the control chart should raise frequent false alarms to indicate the shift in the process parameters. Due to these reasons it becomes important for any type of control chart to exhibit desirable average run length property. However for the CQC_r chart the ARL is not a good measure of the chart performance as in this case the out-of-control situation is very different from the traditional chart. A better measure of the chart performance is the Average item run length (AIRL), defined as, the number of items inspected to observe an out of control point.

Assume that the probability for the quantity Q_r falling within the control limits of the CQC_r chart can be denoted by β_r. Then β_r can be represented as:

$$\beta_r = F(UCL_r, r, \lambda) - F(LCL_r, r, \lambda) \tag{3.4}$$

where $F(t,r,\lambda)$ is the distribution of Q_r. Using Equation (3.2), the probability that the points do not fall between the control limits which is represented as (1-β_r) can be obtained as

$$1-\beta_r = 1-\left[\sum_{k=0}^{r-1} e^{-\lambda LCL_r}\frac{(\lambda LCL_r)^k}{k!} - \sum_{k=0}^{r-1} e^{-\lambda UCL_r}\frac{(\lambda UCL_r)^k}{k!}\right] \tag{3.5}$$

Thus the ARL of the CQC_r charts can be written as:

$$ARL_r = \frac{1}{1-\beta_r} = \frac{1}{1+\sum_{k=0}^{r-1} e^{-\lambda UCL_r}\frac{(\lambda UCL_r)^k}{k!} - \sum_{k=0}^{r-1} e^{-\lambda LCL_r}\frac{(\lambda LCL_r)^k}{k!}} \tag{3.6}$$

The average run length values of some CQC_r are shown in Table 3.7. It can be noticed from Table 3.7 that with increase in r the sensitivity of the CQC_r increases. However, it should be made clear that the average time to plot a single point on a CQC_r ($r > 1$) chart is r times that in the case of CQC_1 chart. Thus, the ARL behavior does not necessarily reflect the true performance of the chart and a better option is to use AIRL as a performance measure.

On an average only one out of 1/(1-β_r) points falls outside the control limits. If the process failure occurrence rate is λ, on average r defects will occur for r/λ (the mean of the Erlang distribution) items inspected. The average item run length of the CQC_3 chart ($AIRL_r$) can then be represented as:

$$AIRL_r = E(T) \times \frac{1}{(1-\beta_r)} \tag{3.7}$$

λ	CQC_1	CQC_2	CQC_3	CQC_4	CQC_5	CQC_6
0.001	1.01	1	1	1	1	1
0.002	1.01	1	1	1	1	1
0.005	1.03	1	1	1	1	1
0.008	1.05	1	1	1	1	1
0.01	1.07	1	1	1	1	1
0.02	1.14	1.01	1	1	1	1
0.05	1.39	1.08	1.02	1	1	1
0.08	1.7	1.19	1.06	1.02	1.01	1
0.1	1.94	1.29	1.11	1.04	1.02	1.01
0.2	3.75	2.13	1.59	1.33	1.2	1.12
0.5	26.73	15.63	10.79	8.1	6.41	5.27
0.8	162.83	134.48	115.46	101.09	89.7	80.42
1	370.37	370.37	370.37	370.37	370.37	370.37
1.2	505.09	454.75	404	359.82	322.37	290.64
1.5	482.18	332.49	236.66	175.36	134.45	105.98
1.8	410.59	235.02	143.92	94.39	65.45	47.44
2	370.37	191.77	108.24	66.56	43.87	30.54
5	148.55	34.05	10.95	4.85	2.75	1.87
8	93.03	14.74	4.15	1.96	1.32	1.1
10	74.53	10.09	2.82	1.46	1.12	1.02
20	37.51	3.5	1.26	1.02	1	1
25	30.11	2.62	1.11	1	1	1
50	15.31	1.35	1	1	1	1
75	10.38	1.1	1	1	1	1
100	7.91	1.03	1	1	1	1
1000	1.35	1	1	1	1	1

Table 3.7 Some ARL values of CQC_r charts

Substituting the values of $E(T)$ and $(1-\beta_r)$ Equation (3.7) can be written as:

$$AIRL_r = \frac{r}{\lambda\left[1+\sum_{k=0}^{r-1} e^{-\lambda UCL_r}\frac{(\lambda UCL_r)^k}{k!} - \sum_{k=0}^{r-1} e^{-\lambda LCL_r}\frac{(\lambda LCL_r)^k}{k!}\right]} \tag{3.8}$$

The UCL_r and LCL_r can be calculated as before. Throughout the thesis the $AIRL_r$ values of the CQC_r chart are obtained under the assumption of fixed shift model, *i.e.* the shift occurs either before plotting a point or after plotting a point on the CQC_r chart.

Some $AIRL_r$ values for λ_o=0.001 (process average) $\alpha = 0.0027$ are shown in Table 3.8.

λ	$AIRL_1$	$AIRL_2$	$AIRL_3$	$AIRL_4$
0.00001	106829	200749	300059	400004
0.00002	57062.4	101428	150219	200028
0.00005	27827.4	43196.7	61093.5	80327.5
0.00008	21203.3	29761	39806.2	51014.5
0.0001	19357.7	25767.9	33221.3	41665.5
0.0002	18726.8	21327.5	23819.2	26672.5
0.0005	53451.5	62504.3	64736.5	64815.6
0.0008	203557	336113	432901	505458
0.001	370495	740622	1110930	1481480
0.002	185310	191772	162343	133114
0.003	82471.3	58841.3	37421.5	25032.6
0.004	46421.4	25700.3	13791.3	8421.8
0.005	29729.7	13621.1	6567.1	3882.3
0.008	11636.7	3685	1555.5	979.4
0.01	7457.5	2018.7	845.2	585.8
0.02	1877	350.3	188.9	203.5
0.05	306.4	54	60.1	80
0.08	122.1	27.1	37.5	50
0.1	79.2	20.7	30	40

Table 3.8 Some AIRL values for CQC_r chart with λ_o=0.001 and $\alpha = 0.0027$

As it is evident from the table, when the process is in control the $AIRL_r$ value is quite large and when the process average shifts the $AIRL_r$ value decreases, thus proving that the CQC_r chart has a desirable $AIRL_r$ property. Figure 3.5 shows some $AIRL_r$ curves for λ_o=0.001 and $\alpha = 0.0027$.

From Table 3.8 it can be seen that $AIRL_r$ increases when $\lambda < 0.0002$, this is due to the effect of the term r/λ on the $AIRL_r$. When λ becomes small (approaches zero), it tends to increase the average run length. Also, $1/(1-\beta_r)$ tends to decrease the average item run length when the process improves but its effect is less dominant as compared to the other effect for small values of λ. Due to this when the process improves (*i.e.* λ decreases) the $AIRL_r$ first decreases and then increases.

From Figure 3.5 it can also be seen that as λ increases, the $AIRL_r$ drops more sharply than the traditional CQC chart thus the CQC_r charts (for r>1) are more sensitive to process deterioration than the CQC chart.

Chan *et al.* (2000) show the AIRL property of CQC chart with only lower control limit, which means that only the process deterioration was of interest. Figure 3.6 shows some of the $AIRL_r$ curves of some CQC_r charts having only a lower control limit with $\lambda_o = 0.001$ and $\alpha = 0.00135$.

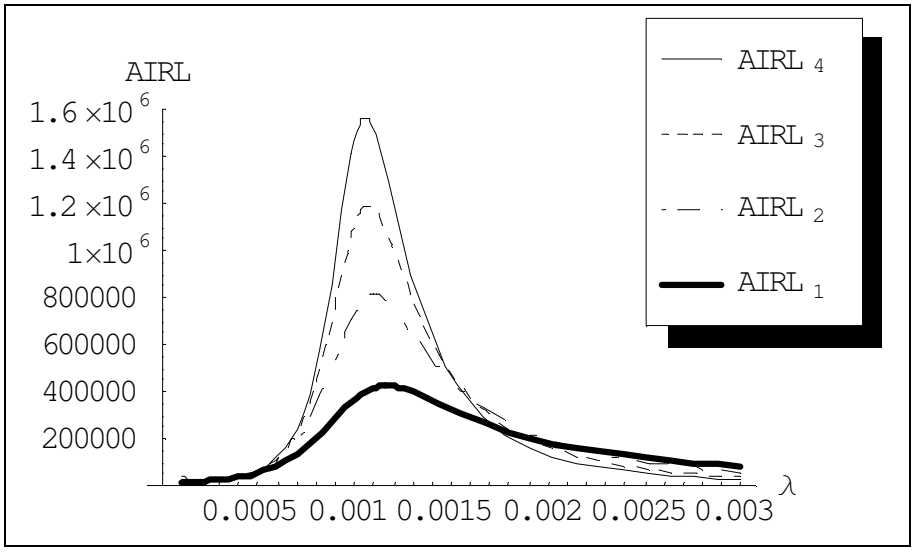

Figure 3.5 Some AIRL curves of CQC_r charts with $\lambda_o = 0.001$ and $\alpha = 0.0027$

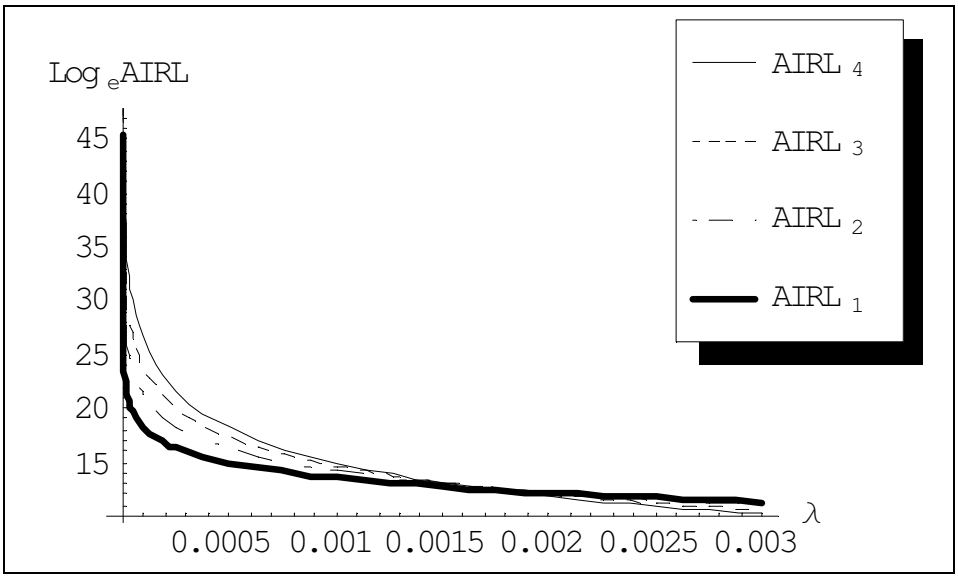

Figure 3.6 Some AIRL curves of CQC_r charts (with only a lower control limit) with $\lambda_o = 0.001$ and $\alpha = 0.00135$

3.6. Comparison of CQC_r chart and c chart

Control charts based on a Poisson distribution, namely the c chart or the u chart, are often used to monitor the number of defects in sampling units. However, as discussed earlier, this procedure requires a large number of defects and it is not appropriate when applied to a high quality process, *i.e.* when the defect rate becomes small. The c chart and the u chart are based on the normal approximation of the Poisson distribution and this assumption is often violated when the average number of failures is small. As a result of this the false alarm probability can be much higher than its anticipated value of 0.27%. Moreover, the lower control limit is usually set at zero, which is not useful as process improvement cannot be detected. Control charts based on binomial distribution also face similar problems, see, e.g., Xie and Goh (1993a). In this section the performance of the CQC_r chart is compared with the traditional Shewhart charts.

3.6.1. Average Item Run Length of the c chart

The probability limits of the traditional c chart are given as solutions of:

$$\sum_{x=0}^{UCL_c} \frac{e^{-n\lambda}(n\lambda)^x}{x!} = 1-\frac{\alpha}{2},\ \sum_{x=0}^{CL_c} \frac{e^{-n\lambda}(n\lambda)^x}{x!} = 0.5,\ \sum_{x=0}^{LCL_c} \frac{e^{-n\lambda}(n\lambda)^x}{x!} = \frac{\alpha}{2} \tag{3.9}$$

while the AIRL of the c chart, ($AIRL_c$), can be written as:

$$AIRL_c = \frac{n}{1-\sum_{x=LCL_c}^{UCL_c} \frac{e^{n\lambda}(n\lambda)^x}{x!}} \tag{3.10}$$

The choice of the sample size depends on the value of the predetermined in-control AIRL. Moreover, the in-control AIRL of the two charts should be same in order to give a fair basis for comparison. Thus the sample size of the c chart can be calculated by equating the two in-control AIRL*s* and then solving for *n*. Theoretically, the sample size can be calculated as r/λ. However, as the Poisson distribution is a discrete distribution, we cannot always get the in-control false alarm probability of 0.0027. In order to match the in-control AIRL*s* of the two charts the sample size should be calculated by iteration.

The AIRL values of the CQC_r charts are tabulated in Table 3.9 and the AIRL values of the corresponding c charts are listed in Table 3.10. The AIRL values have been calculated using the in-control defect rate as 0.001 and the false alarm probability of 0.0027. It can be seen that the two charts have the same in-control AIRL (marked in bold).

From Table 3.9 it can be seen that when λ decreases, the AIRL values of the CQC_r charts are smaller than those of the c charts. It is an indication that the CQC_r chart is more sensitive in detecting process improvements. For all the c charts listed in Table 3.10, the AIRL increases when the process improves from $\lambda = 0.001$, thus making them inadequate in detecting process improvement. This can be explained as follows: for the c charts with above parameters the lower control limit is taken as zero and hence only the upper control limit exists. As a result when the process improves the Type II error probability, β_c increases and approaches 1. This also explains the notation N.A. in Table 3.10 which means no solution or in other word the improvement detection is not possible.

λ	CQC1	CQC2	CQC3	CQC4	CQC5	CQC6
0.00001	106829	200749	300059.2	400003.9	500000.2	600000
0.00002	57062.4	101428	150218.7	200028.2	250003.2	300000
0.00004	32560.9	52640.4	75751.64	100184.8	125040.9	150008
0.00006	24772.9	37065.2	51471.15	67181.12	83497.3	100049
0.00008	21203.3	29761.3	39806.3	51014.48	62912.15	75157
0.0001	19357.7	25768.4	33221.44	41665.51	50805.73	60368.4
0.0002	18726.8	21328.5	23819.69	26672.49	29931.04	33564.6
0.0003	24127	26219	27219.13	28209.61	29393.39	30807.8
0.0004	34875.6	38493.1	39158.64	39203.13	39194.24	39299
0.0005	53450.8	62513.4	64741.55	64815.01	64146.87	63263.3
0.0006	84234.5	107890	117200.3	120616.8	121270	120550
0.0007	132948	191679	224177.8	242942.7	253770.1	259725
0.0008	203533	336188	432962.2	505450.9	560643.5	603132
0.0009	290179	543424	773730.9	984295	1.18E+06	1.35E+06
0.001	370370	740741	1.11E+06	1.48E+06	1.85E+06	2.22E+06
0.002	185185	191773	162363.5	133117.7	109662.7	91629.2
0.003	82415.7	58841.4	37425.85	25033.17	17952.76	13727.1
0.004	46390.2	25700.4	13792.84	8422.011	5851.445	4524.31
0.005	29709.7	13621.1	6567.777	3882.399	2753.11	2247.12
0.006	20645.7	8158.34	3674.863	2176.987	1618.656	1417.21
0.007	15178.5	5316.48	2296.786	1393.181	1100.322	1034.57
0.008	11628.9	3685.03	1555.661	979.4208	825.3149	827.342
0.009	9194.44	2677.35	1119.799	737.9013	662.7403	700.452
0.01	7452.52	2018.75	845.2739	585.7798	558.2727	614.611
0.02	1875.71	350.329	188.8745	203.4752	250.1134	300.001
0.04	475.263	80.0878	75.72133	100.001	125	150
0.06	214.068	40.392	50.01438	66.66667	83.33333	100
0.07	158.325	32.3218	42.85912	57.14286	71.42857	85.7143
0.08	122.025	27.0582	37.50027	50	62.5	75
0.1	79.1366	20.656	30	40	50	60

Table 3.9 The AIRL values of the CQC_r chart

λ	n (910)	n (1777.7)	n (2818)	n (3969)	n (4507)	n (5774)
0.00001	1.8E+15	1.60E+19	N.A.	N.A.	N.A.	N.A.
0.00002	5.6E+13	1.29E+17	N.A.	N.A.	N.A.	N.A.
0.00004	1.8E+12	1.E+15	3.85E+17	N.A.	N.A.	N.A.
0.00006	2.4E+11	6.26E+13	1.05E+16	1.43E+18	2.03E+19	N.A.
0.00008	5.7E+10	8.62E+12	8.33E+14	6.41E+16	6.25E+17	5.20E+19
0.0001	1.9E+10	1.87E+12	1.18E+14	5.92E+15	4.66E+16	1.86E+18
0.0002	6.4E+08	1.70E+10	2.96E+11	4.15E+12	1.72E+13	1.97E+14
0.0003	9E+07	1.16E+09	9.89E+09	6.89E+10	2.00E+11	1.15E+12
0.0004	2.3E+07	1.81E+08	9.55E+08	4.17E+09	9.59E+09	3.50E+10
0.0005	8160000	4.43E+07	1.65E+08	5.13E+08	9.94E+08	2.62E+09
0.0006	3540000	1.44E+07	4.10E+07	9.88E+07	1.68E+08	3.47E+08
0.0007	1760000	5.70E+06	1.31E+07	2.59E+07	3.97E+07	6.79E+07
0.0008	974226	2.61E+06	5.05E+06	8.51E+06	1.20E+07	1.77E+07
0.0009	582350	1.33E+06	2.24E+06	3.32E+06	4.38E+06	5.76E+06
0.001	**370341**	**7.41E+05**	**1.11E+06**	**1.48E+06**	**1.85E+06**	**2.22E+06**
0.002	24029.3	2.55E+04	23974.7	22296.7	22722.2	21245.2
0.003	6427.07	6173.3	5988.6	6173.1	6461.6	7045.5
0.004	3020.98	3137.1	3561.3	4322.2	4765.3	5871.7
0.005	1906.32	2270.7	2995.9	4016.2	4532.9	5778.5
0.006	1430.33	1960.9	2855.9	3973.8	4508.9	5774.1
0.007	1195.13	1843.5	2825.0	3969.4	4507.1	5774.0
0.008	1069.26	1800.1	2819.1	3969.0	4507.0	5774.0
0.009	999.186	1784.9	2818.2	3969.0	4507.0	5774.0
0.01	959.594	1779.9	2818.0	3969.0	4507.0	5774.0
0.02	910.065	1777.7	2818.0	3969.0	4507.0	5774.0
0.04	910	1777.7	2818.0	3969.0	4507.0	5774.0
0.06	910	1777.7	2818.0	3969.0	4507.0	5774.0
0.07	910	1777.7	2818.0	3969.0	4507.0	5774.0
0.08	910	1777.7	2818.0	3969.0	4507.0	5774.0
0.1	910	1777.7	2818.0	3969.0	4507.0	5774.0

Table 3.10 The AIRL values of the c chart

Another interesting observation is that for CQC_r charts the AIRL increases when $\lambda <$ 0.0002 (for r = 1-4) and when $\lambda <$ 0.0003 (for r = 5-6). This happens due to the effect of the term r/λ on the $AIRL_r$. When λ becomes small (approaches zero), it tends to increase

the AIRL. On the other hand, the term $1/(1-\beta_r)$ tends to decrease the AIRL when the process improves but its effect is less dominant as compared to the other effect for small values of λ. Due to this when the process improves (*i.e.* λ decreases) the $AIRL_r$ first decreases and then increases. It can also be seen that a CQC_r chart with a large value of r is more sensitive to small shifts in the process and is less sensitive to large shifts.

When λ increases, *i.e.* when the process deteriorates, it can be seen that the AIRL performance of the c chart is superior to that of a corresponding CQC_r chart especially for small deterioration. When the magnitude of shift increases the CQC_r chart outperforms the c chart in terms of sensitivity. Also, in case of the c chart, its AIRL cannot be less than the selected sample size as a result of which the c chart will end up producing more items with defects when the process shift occurs.

3.6.2. An example

Table 3.11 shows the number of items (quantity) inspected to observe a defect. The first 30 points were simulated using the in-control defect rate of $\lambda = 0.001$, while the next 15 points were simulated using $\lambda = 0.0001$ and the last 15 points were simulated using $\lambda = 0.01$. Using this data set we will illustrate the charting procedure of the CQC_r and the c chart. For this purpose the data set in Table 3.11 is converted to record the cumulative quantity inspected to observe 3 defect (Table 3.12) and the number of defects observed in a sample of 2818 (Table 3.13).

2465.6	2189	2883.9	301.7	1577.5	626.2	398.8	6758	1538.3	671
1282.5	445.6	47.8	709.2	986.8	699.8	1569.6	1738.3	2893.5	750.6
147.6	971.5	729.4	115.3	251.2	1322.5	852.7	1887.3	559.8	312.2
1707.6	3921	19694	1820.3	14831.1	5072.7	9625.7	22265.4	20215.3	22731.1
1202.4	5906.6	89.8	9735.6	3142.5	546.4	71.5	152.8	66.1	35.2
53.2	212.7	91.7	65.6	29.6	81.3	134.6	37.8	65.9	17.3

Table 3.11 Quantity inspected to observe one defect (read across for consecutive data points)

7538.5	2505.3	8695.1	2399	1743.8	4007.7	3791.7	1816.3	2426.4	2759.3
25322.5	21724.1	52106.4	29840.1	12967.9	770.8	154.6	370	245.4	121

Table 3.12 Quantity inspected till the occurrence of 3 defects (read across for consecutive data points)

1	1	2	3	0	0	3	4	3	1	3	4	2	4	0	1	0	0	0	0
0	0	1	1	0	0	0	0	1	0	1	0	0	1	0	0	0	0	0	0
0	1	0	0	0	0	0	0	1	0	0	0	0	0	0	0	1	1	0	2
0	0	1	3	13															

Table 3.13 Number of defects observed per sample (read across for consecutive data points)

Solving Equations (3.3) and (3.8) with $\alpha = 0.0027$, the control limits of the CQC_3 chart and the c chart are obtained as

$UCL_3 = 10869.3$; $CL_3 = 2674.1$; $LCL_3 = 211.7$ and $UCL_c = 8$; $CL_c = 2$; $LCL_c = 0$ respectively. The CQC_3 chart and the c charts with the computed limits are shown in Figures 3.7 and 3.8 respectively.

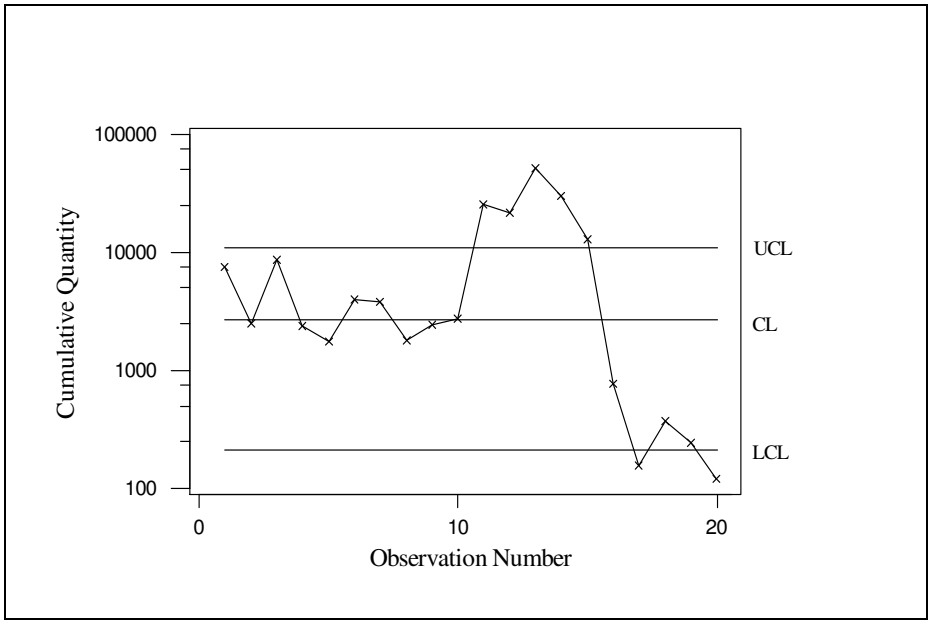

Figure 3.7 The CQC_3 chart

When the process improves from $\lambda = 0.001$ to $\lambda = 0.0001$, CQC_3 chart raises an alarm on the very first out-of-control point. On the other hand the absence of lower control limit renders the c chart incapable of detecting the shift. This is perhaps the biggest demerit associated with the control charts based on the normal approximation assumption. As the figure shows a number of meaningless zeroes are plotted on the c chart.

Another alternative to monitor the defects in a Poisson process is to use a CUSUM chart. The CUSUM chart has been shown to be very useful in detecting small shifts in the process. The important advantage associated with the CUSUM charts and the CQC_r charts is that they are free from the sample size constraint and are thus superior to the c and the u chart. The CUSUM scheme is studied in detail in the next chapter and its performance is compared to that of the CQC_r charts.

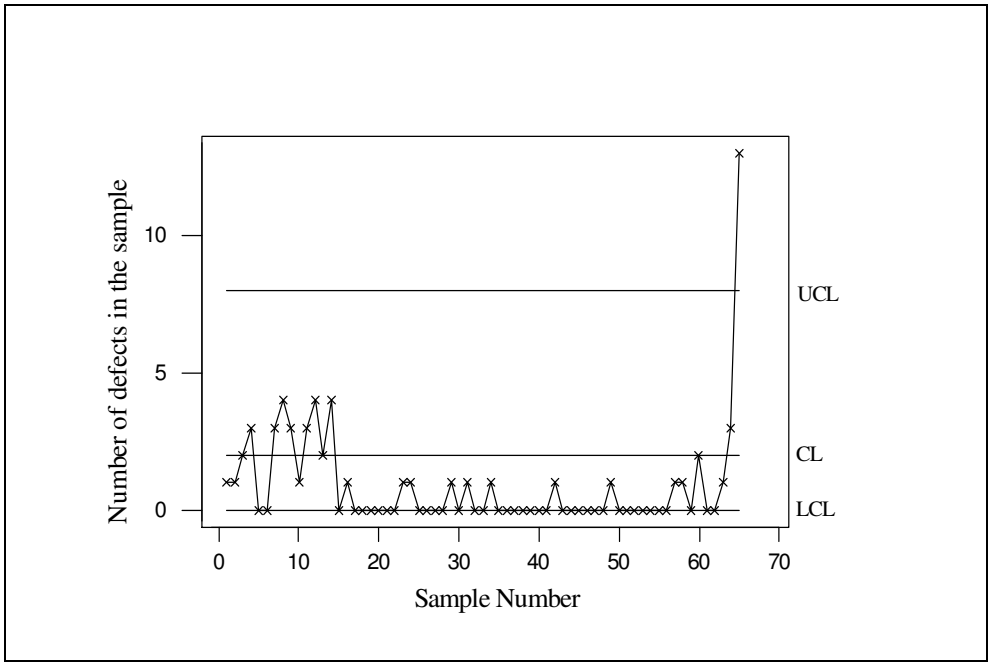

Figure 3.8 The c chart

Chapter 4

Control Charts for Monitoring the Inter-arrival Times

4.1. Overview of Exponential CUSUM Charts

A time-between-events CUSUM can be defined in the following manner: If X_1, X_2,… be the inter-arrival times then, as mentioned in 2.7, the time-between-events CUSUM for detecting an increase or decrease in the inter-arrival times can be respectively defined as

$$S_i^+ = \max\{S_{i-1}^+ + (X_i - k)\}$$
$$S_i^- = \min\{S_{i-1}^- + (X_i - k)\}$$

where, k is the reference value and can be treated as the reference value of the Wald sequential probability ratio test; see Moustakides (1986) and Reynolds and Stoumbos (1998). The value of the reference value k can be calculated for any given in-control defect rate, λ_0, and an out-of-control defect rate, λ_d, that the CUSUM scheme is designed to detect quickly as; see Lucas (1985):

$$k = \frac{\ln(\lambda_d) - \ln(\lambda_0)}{\lambda_d - \lambda_0} \tag{4.1}$$

The control limits of the CUSUM scheme are denoted by h and the decision on the statistical control of the process is taken depending on whether $S_t^- \leq -h$ or $S_t^+ \geq h$. Once the reference value k has been calculated, a suitable value of h can be found out to give an acceptable in-control average run length. The average run length of the CUSUM

scheme can be calculated by the Markov chain approach, see Brook and Evans (1972) and Lucas (1985).

When the random variable is continuous, the Markov chain method gives an approximate answer; however, this answer can be brought reasonably close to the exact values by grouping the possible values of the random variable into discrete class intervals. The width of the interval is given by:

$$w = \frac{2h}{t-1} \tag{4.2}$$

where, t is the number of states in the Markov chain process.

The transition probabilities are defined as:

$$p_r = \Pr(rw - \frac{1}{2}w < X - k \le rw + \frac{1}{2}w \text{ , and } F_r = \Pr(X - k \le rw + \frac{1}{2}w \tag{4.3}$$

where, $r = j - i$, where i is the state before transition and j is the state after transition. The transition probability matrix can then be written as:

$$P=\begin{bmatrix} F_0 & p_1 & \cdots & p_j & \cdots & p_{h-1} & 1-F_{h-1} \\ F_{-1} & p_0 & \cdots & p_{j-1} & \cdots & p_{h-2} & 1-F_{h-2} \\ \vdots & \vdots & & \vdots & & \vdots & \vdots \\ F_{-i} & p_{1-i} & \cdots & p_{j-i} & \cdots & p_{h-1-i} & 1-F_{h-1-i} \\ \vdots & \vdots & & \vdots & & \vdots & \vdots \\ F_{1-h} & p_{2-h} & \cdots & p_{j-(h-1)} & \cdots & p_0 & 1-H \\ 0 & 0 & \cdots & 0 & \cdots & 0 & 1 \end{bmatrix}$$

Using the Markov chain result:

$$(I-R)\mu=1 \tag{4.4}$$

where, I is the $h \times h$ identity matrix and R is the matrix obtained from the transition probability matrix P by deleting the last row and column and μ is a vector of factorial moments.

The first element of the vector μ gives the average run length for the CUSUM chart.

4.2. Numerical comparison based on ARL and ATS performance

The case of process deterioration and improvement are considered separately. To detect the process deterioration, the performance of the lower CUSUM is compared to that of the CQC chart and CQC_r chart having only a lower control limit. Similarly the performance of the upper CUSUM chart is compared to that of the CQC chart and CQC_r chart with only an upper control limit. An in-control average run length of 370 is used for both cases, which translates to a false alarm probability of approximately 0.0027 for the CQC_r charts with single limit. The in-control average time to signal (ATS_0) is also fixed

as 370 for which the false alarm probability of the CQC_r charts can be calculated as $0.0027r/\lambda_0$ (where $\lambda_0 = 1$).

4.2.1. Case I: Process Deterioration

The in-control value of the defect rate is assumed to be 1 and say that the user is interested in quickly identifying a shift to 1.4, 1.9 and 2.5. The reference value *k* for the three CUSUM charts, now onwards referred to as Lower CUSUM 1(LC-1), Lower CUSUM 2 (LC-2) and Lower CUSUM 3 (LC-3) respectively, can be calculated using Equation (4.1). The appropriate value of *h* can then be calculated to give an in-control ARL_0 of approximately 370. The *k* and *h* values for the three CUSUM charts are found out to be, (0.84, 7.16), (0.71, 4.13) and (0.61, 2.783) respectively. The Markov chain approach (with 151 states) was then used to calculate the ARL for different values of defect rate. Table 4.1 shows the ARL values of the three CUSUM charts along with the ARL values of CQC, CQC_2, CQC_3 and CQC_4 charts.

It can be seen from the table that the CQC_r charts are out-performed by the CUSUM charts. LC-1 chart gives a satisfactorily low ARL for small deteriorations in process while the LC-2 and LC-3 charts give better performance for moderate and larger shifts. Among the CQC_r charts, the control chart with large *r* performs better than those with small *r*. The performance of CQC_4 chart is quite close to that of the CUSUM charts and in fact is better than LC-1 and LC-2 charts for large shifts.

However it is not appropriate to use the ARL as a performance measure as it does not take into account the time needed to plot one point on the control chart. Moreover, the time needed to plot one point on CQC_r chart is r times the time needed to plot one point on CQC chart Thus to give a better picture of the chart performance, average time to signal (ATS) is now used as the yardstick for comparison in place of ARL. Table 4.2 shows the ATS values for all the seven charts mentioned above. Again it can be seen that the CQC_r charts perform worse than the CUSUM chart. For large process deteriorations, however, the performance of CQC_4 chart is somewhat similar to the CUSUM charts.

λ	CQC	CQC_2	CQC_3	CQC_4	LC-1	LC-2	LC-3
1	370.37	370.37	370.37	370.37	370	370.23	370.3
1.1	336.75	307.62	283.89	264.4	164.1	190.74	211.5
1.2	308.73	259.78	223.08	195.1	91.84	111.32	131.2
1.3	285.02	222.46	178.99	148.02	61.07	72.38	87.47
1.4	264.69	192.77	146.19	114.99	45.65	51.47	62.18
1.5	247.08	168.76	121.25	91.17	36.87	39.3	46.7
1.6	231.67	149.07	101.91	73.57	31.33	31.71	36.74
1.7	218.07	132.7	86.66	60.3	27.58	26.69	30.05
1.8	205.98	118.96	74.47	50.11	24.88	23.19	25.38
1.9	195.17	107.3	64.58	42.16	22.85	20.65	21.99
2	185.44	97.32	56.47	35.86	21.27	18.74	19.47
2.1	176.63	88.71	49.75	30.8	20.02	17.26	17.55
2.2	168.62	81.23	44.13	26.7	18.99	16.08	16.03
2.3	161.31	74.69	39.39	23.33	18.13	15.12	14.83
2.4	154.61	68.93	35.36	20.54	17.41	14.33	13.84
2.5	148.45	63.84	31.9	18.21	16.8	13.67	13.03
2.6	142.76	59.32	28.92	16.25	16.26	13.1	12.34
2.7	137.49	55.28	26.33	14.58	15.8	12.61	11.76
2.8	132.6	51.66	24.07	13.15	15.39	12.19	11.26
2.9	128.04	48.39	22.09	11.92	15.02	11.82	10.83
3	123.79	45.44	20.35	10.86	14.7	11.49	10.45

Table 4.1 ARL values when the process deteriorates from $\lambda_0 = 1$

λ	CQC	CQC_2	CQC_3	CQC_4	LC-1	LC-2	LC-3
1	370.37	370.37	370.37	370.37	370	370.23	370.33
1.1	306.13	280.25	260.56	245.48	149.22	173.4	192.27
1.2	257.27	217.4	189.49	169.55	76.54	92.77	109.29
1.3	219.24	172.21	141.68	121.24	46.97	55.68	67.28
1.4	189.07	138.86	108.48	89.28	32.61	36.76	44.42
1.5	164.72	113.7	84.76	67.44	24.58	26.2	31.13
1.6	144.79	94.36	67.42	52.07	19.58	19.82	22.96
1.7	128.28	79.22	54.47	40.99	16.22	15.7	17.68
1.8	114.44	67.21	44.62	32.83	13.82	12.89	14.1
1.9	102.72	57.55	37	26.69	12.03	10.87	11.58
2	92.72	49.69	31.02	22	10.64	9.37	9.74
2.1	84.11	43.23	26.27	18.36	9.53	8.22	8.36
2.2	76.65	37.87	22.45	15.49	8.63	7.31	7.29
2.3	70.14	33.37	19.34	13.2	7.88	6.58	6.45
2.4	64.42	29.58	16.79	11.35	7.26	5.97	5.77
2.5	59.38	26.35	14.67	9.85	6.72	5.47	5.21
2.6	54.91	23.59	12.91	8.61	6.25	5.04	4.75
2.7	50.92	21.22	11.42	7.58	5.85	4.67	4.36
2.8	47.36	19.16	10.16	6.72	5.5	4.35	4.02
2.9	44.15	17.36	9.08	5.99	5.18	4.08	3.73
3	41.26	15.79	8.16	5.37	4.9	3.83	3.48

Table 4.2 ATS values when the process deteriorates from $\lambda_0 = 1$

4.2.2. Case II: Process Improvement

The in-control value of the defect rate is again assumed to be 1 and say that the user is interested in quickly identifying a shift to 0.9, 0.5 and 0.1. The reference value *k* and the appropriate value of *h* were then calculated to give an in-control ARL_0 of approximately 370. The *k* and *h* values for the two CUSUM charts, now onwards referred to as Upper CUSUM-1 (UC-1), Upper CUSUM-2 (UC-2) and Upper CUSUM-3 (UC-3) respectively, are found out to be (1.05, 13.82), (1.39, 6.81) and (2.56, 3.58) respectively.

Table 4.3 shows the ARL values of charts when the process improves. Clearly the UC-1 chart identifies the shift to $\lambda = 0.9$ faster than the other charts. UC-1 chart picks up the small changes faster than the rest followed by the CQC_4 chart. For moderate and large shifts, however, the CQC_r charts perform better than the CUSUM charts.

λ	CQC	CQC_2	CQC_3	CQC_4	UC-1	UC-2	UC-3
1	370.37	370.37	370.37	370.37	370.08	370.86	370.21
0.95	275.56	258.21	245.98	236.22	205.1	237.02	268.22
0.9	205.01	180.41	164.08	151.68	126.63	154.19	194.36
0.85	152.52	126.35	109.99	98.11	85.43	102.48	140.91
0.8	113.48	88.72	74.13	63.98	61.62	69.8	102.26
0.75	84.43	62.48	50.25	42.1	46.59	48.83	74.33
0.7	62.81	44.15	34.3	27.99	36.41	35.1	54.14
0.65	46.74	31.31	23.58	18.81	29.12	25.91	39.55
0.6	34.77	22.3	16.35	12.81	23.66	19.59	29
0.55	25.87	15.96	11.45	8.85	19.42	15.13	21.37
0.5	19.25	11.48	8.11	6.21	16.04	11.89	15.83
0.45	14.32	8.32	5.81	4.45	13.28	9.46	11.8
0.4	10.65	6.07	4.23	3.25	10.99	7.6	8.86
0.35	7.92	4.47	3.14	2.44	9.06	6.14	6.7
0.3	5.9	3.33	2.37	1.89	7.41	4.96	5.1
0.25	4.39	2.52	1.85	1.52	5.98	4	3.9
0.2	3.26	1.93	1.48	1.27	4.73	3.2	3
0.15	2.43	1.52	1.24	1.12	3.63	2.52	2.3
0.1	1.81	1.24	1.09	1.03	2.66	1.94	1.77
0.05	1.34	1.07	1.01	1	1.78	1.44	1.34
0.01	1.06	1	1	1	1.15	1.08	1.06

Table 4.3 ARL values when the process improves from $\lambda_0 = 1$

Table 4.4 shows the ATS values of the three CUSUM charts listed along with the ATS values of the CQC_r charts (r = 1-4). Clearly the UC-1 chart identifies the shift to $\lambda = 0.9$ faster than the other charts. UC-1 chart picks up the small changes faster than the rest

followed by the UC-2 chart. For moderate shifts (the middle portion of the table) UC-2 gives the best performance followed by the CQC_4 chart. The table also shows that the ATS of the charts first decreases as the process improves and then increases. This is due to the effect of the term r/λ on the ATS (Equation (3.7)) as explained in section 3.5. When λ becomes small, it tends to increase the ATS. The second term in Equation (3.8) tends to decrease the ATS when the process improves but its effect is less dominant as compared to the other effect for small values of λ. Due to this when the process improves (*i.e.* λ decreases) the ATS first decreases and then increases. As a result for large shifts, the CQC chart and the CUSUM (particularly UC-3) charts perform better than the rest.

λ	CQC	CQC_2	CQC_3	CQC_4	UC-1	UC-2	UC-3
1	370.37	370.37	370.36	370.37	370.08	370.86	370.21
0.95	290.06	282.5	276.7	271.97	215.89	249.49	282.34
0.9	227.79	216.53	208.17	201.55	140.7	171.32	215.96
0.85	179.44	166.87	157.84	150.88	100.51	120.56	165.78
0.8	141.85	129.38	120.71	114.22	77.02	87.25	127.83
0.75	112.57	100.99	93.21	87.55	62.12	65.1	99.1
0.7	89.73	79.43	72.75	68.04	52.02	50.14	77.34
0.65	71.9	63.03	57.49	53.72	44.8	39.86	60.85
0.6	57.95	50.51	46.06	43.16	39.43	32.65	48.34
0.55	47.03	40.95	37.5	35.4	35.31	27.51	38.85
0.5	38.49	33.66	31.11	29.71	32.08	23.78	31.66
0.45	31.82	28.11	26.37	25.63	29.52	21.03	26.23
0.4	26.63	23.95	22.96	22.82	27.48	19.01	22.15
0.35	22.64	20.91	20.64	21.12	25.88	17.54	19.14
0.3	19.65	18.84	19.3	20.47	24.69	16.54	16.99
0.25	17.55	17.69	19.01	21.03	23.91	16	15.6
0.2	16.32	17.59	20.05	23.28	23.65	15.98	14.98
0.15	16.19	19.09	23.34	28.51	24.2	16.79	15.36
0.1	18.07	24.03	31.83	40.76	26.55	19.39	17.66
0.05	26.88	42.24	60.6	80.14	35.66	28.75	26.82
0.01	106.09	200.52	300.03	400	115.02	108.3	106.26

Table 4.4 ATS values when the process improves from $\lambda_0 = 1$

4.3. Implementing the charts

This section discusses some of the implementation issues associated with the CQC, CUSUM and the CQC_r charts. The CQC and the CQC_r charts plot the time or the quantity observed till the occurrence of an event (defect or failure) while the CUSUM charts plots the difference of the observed quantity from the reference value. One of the drawbacks associated with the CUSUM chart is the extensive computing required. In the case of CQC and the CQC_r charts, the calculation of lower and upper control limits is much easier compared to the calculation of k and h for the CUSUM charts.

Issues	CQC	CQC_r	CUSUM
Information required	Time/Quantity between events	Time/Quantity between events	Time/Quantity between events
Parameters	False alarm probability	• r • False alarm probability	• Reference Value (k) • Decision Interval (h)
Value Plotted	Time/Quantity between events	Time/Quantity between r events	Deviations from the reference value
Calculation required	Control limits	Control Limits	• Reference Value (k) • Decision Interval (h)
Sensitivity	Comparatively less sensitive	Sensitive to moderate and large shifts	Sensitive to small shifts

Table 4.5 Implementation Issues

Thus if ease of design is an issue, then the CQC_r charts may turn out to be better alternative compared to the CUSUM charts. Even from operation point of view, the CQC_r charts appear more promising due to their resemblance to the Shewhart chart

charts. The optimum CUSUM design discussed in this chapter requires extensive computing. On the other hand for the case of CQC_r charts a simple algorithm can be written to calculate the control limits and the average run length. Most of the calculations in this chapter were done using the statistical software, MATHEMATICA.

4.4. An example

The charting procedure of the three charts for times between events will be illustrated with an example here. Table 4.6 shows some time between events. The first 36 values (across) correspond to a historical in-control defect rate of $\lambda_0 = 1$. The last 24 points were simulated when the process average is shifted to $\lambda = 0.9$, which means that the process has improved. Suppose the user is interested in detecting the process improvement only.

0.367	1.078	0.732	0.681	0.805	0.373
1.42	0.514	1.649	0.508	2.193	0.368
0.471	0.89	0.095	0.233	0.262	0.727
0.461	0.641	0.318	0.163	1.819	1.304
3.362	0.674	0.384	0.268	0.531	0.197
0.822	1.788	0.927	1.518	1.115	0.744
0.289	0.236	0.967	0.424	7.304	1.249
0.265	2.065	1.439	0.827	0.521	0.137
1.59	0.039	0.063	2.363	0.476	2.15
0.759	0.055	1.515	0.086	1.922	0.823

Table 4.6 Time between events data (read across for consecutive values)

Using Equation (2.12), the upper control limit of the CQC chart (for $\alpha = 0.0027$) can be found as

$$Q_U = -\frac{\ln(\alpha)}{\lambda_0} = 5.91$$

The reference value of the CUSUM chart designed to detect the shift from $\lambda_0 = 1$to $\lambda =$ 0.9 can be calculated using Equation (4.1) can then be found as

$$k = \frac{\ln(0.9) - \ln(1)}{0.9 - 1} = 1.05$$

Once the reference value is known, an appropriate value for the decision interval can be found out so that it gives a desired in-control ATS performance. The value of *h* for an in-control ATS of 370 is 13.82.

Since the CQC chart makes use of a single observation in decision making, a CQC_r chart could be used if more observations are to be taken into consideration in an easy way. The data shown in Table 4.6 is converted into the data of Table 4.7 which shows the cumulative time between every three occurrences, *i.e.* Q_3. The control limits of the CQC_3 chart can be calculated by using Equation (3.3) and solving it with the help of some statistical or mathematical package. Using MATHEMATICA the upper control limit of the CQC_3 chart can be calculated as 8.67. The CQC chart, CUSUM chart and the CQC_r chart are shown in Figures 4.1, 4.2 and 4.3 respectively.

2.177	1.859	3.583	3.069	1.456	1.222	1.42	3.286	4.42	0.996
3.537	3.377	1.492	8.977	3.769	1.485	1.692	4.989	2.329	2.831

Table 4.7 Cumulative time between every three events

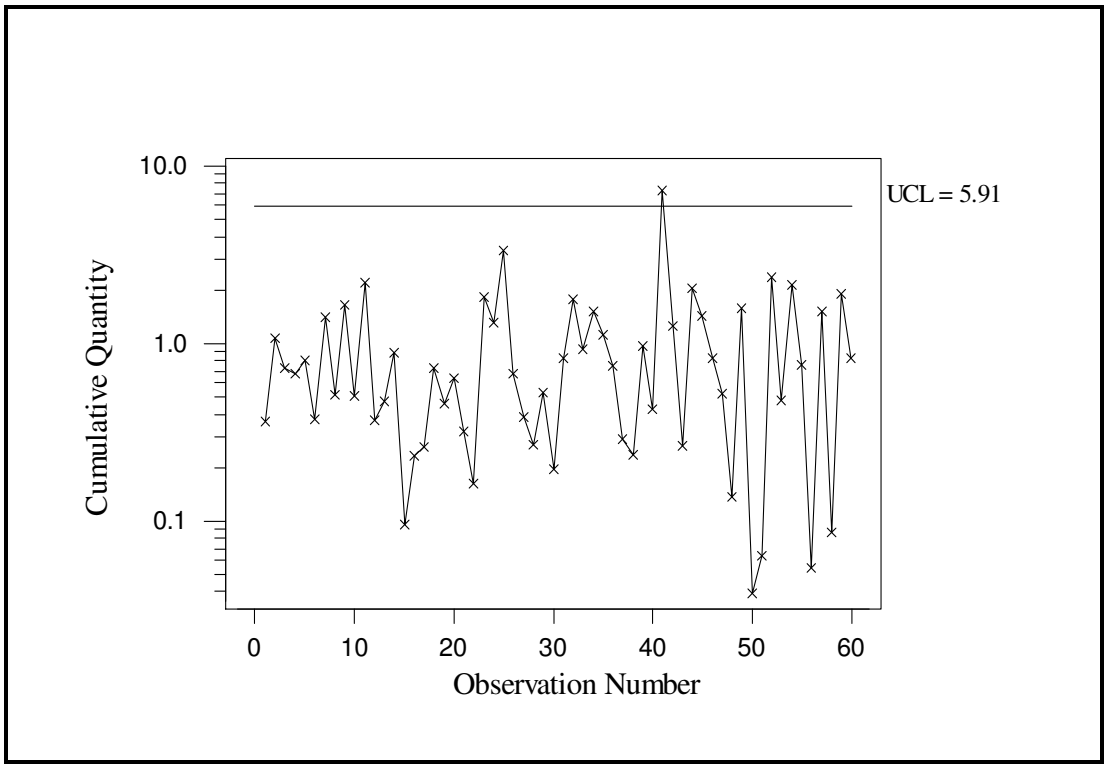

Figure 4.1 The CQC chart for data in Table 4.6

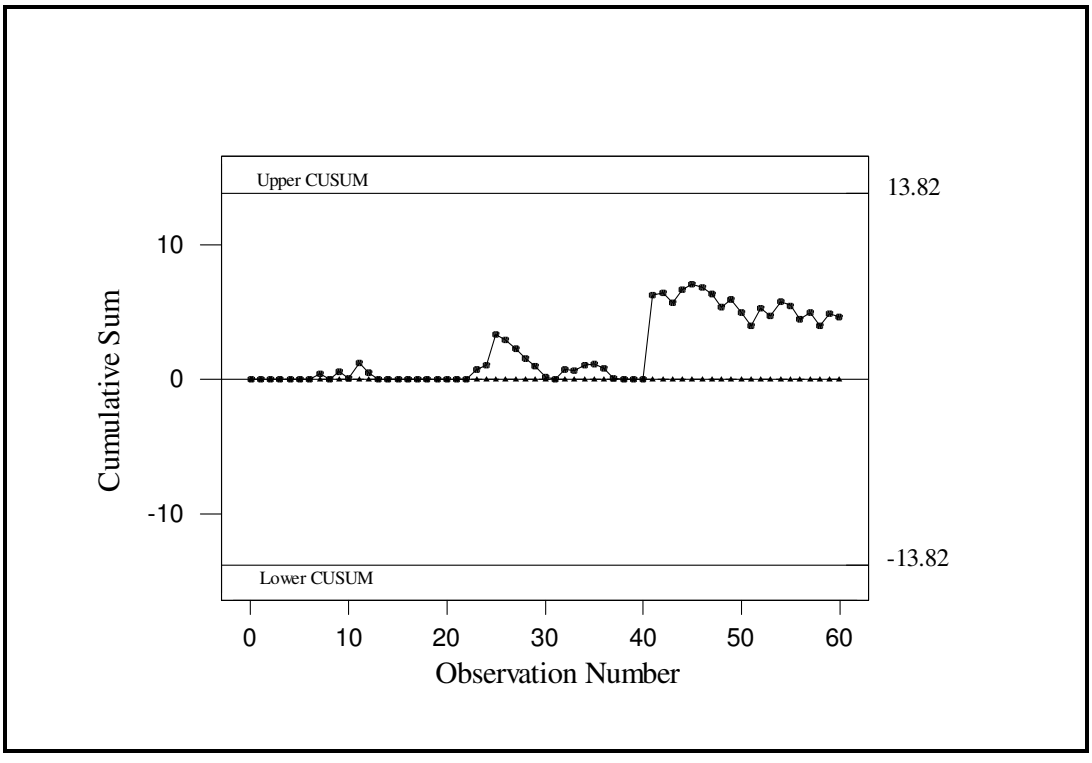

Figure 4.2 The CUSUM chart for data in Table 4.6

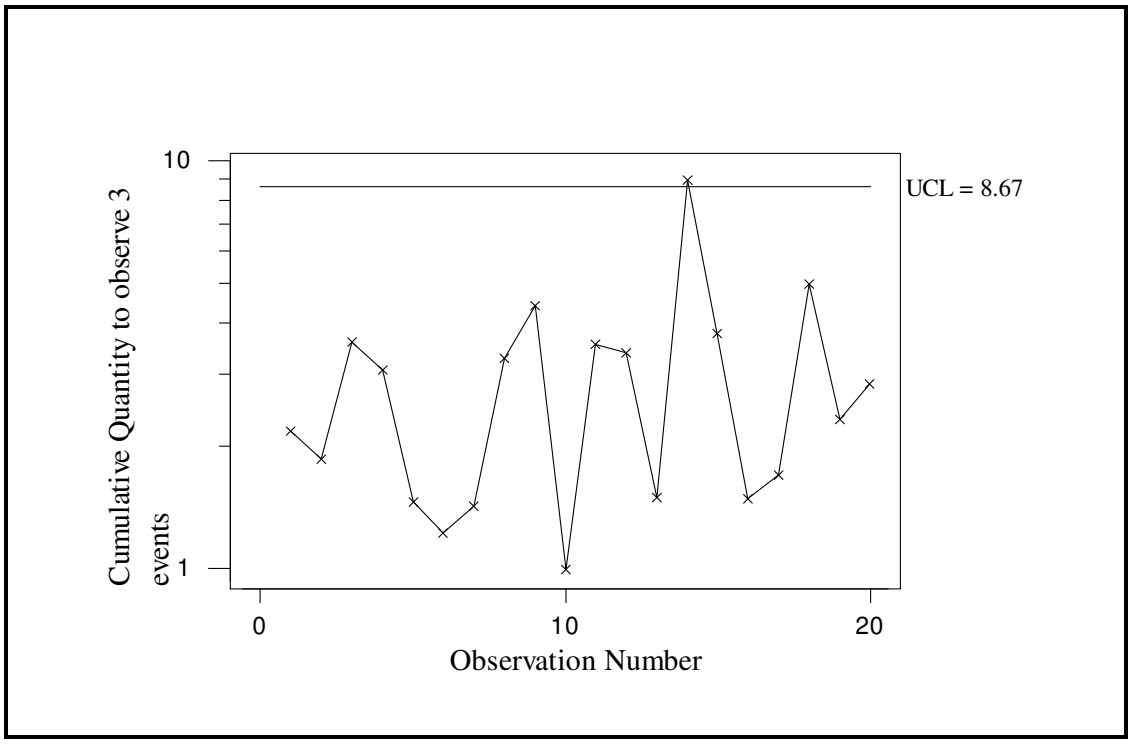

Figure 4.3 The CQC_3 chart data in Table 4.7

Interestingly both the CQC and the CQC_3 charts raise an alarm while the CUSUM chart does not. However, the pattern on the CUSUM chart does point out a shift in the process.

4.5. Detecting the shift when the underlying distribution changes

4.5.1. Case I: Weibull Distribution

In this section the performance of the CUSUM charts and CQC_r charts arte studied when the underlying distribution can no longer be modeled by the exponential distribution. We have assumed that the underlying distribution can be modeled by the Weibull distribution. It should be noted that although similar ideas could be used for other

distributions, the Weibull distribution is probably the most widely used one and it is very flexible for modeling increasing or decreasing failure rate.

Even though the scale parameter (θ) is more likely to change but sometimes the shape parameter (β), which depends on the material property, can also change. In this study we have only concentrated on the change in shape parameter, and the scale parameter is fixed as 1. For Weibull distribution, the mean is given by

$$\mu = E[T] = \theta\Gamma(1+1/\beta) \tag{4.5}$$

and the variance is given by

$$\sigma^2 = \theta^2\left\{\Gamma(1+2/\beta) - [\Gamma(1+1/\beta)]^2\right\} \tag{4.6}$$

It can be seen that the mean and the variance are strongly affected by the scale and shape parameter. When the shape parameter increases, both the mean and the variance reduce. However the decrease in variance is quite significant compared to the decrease in mean. Table 4.8 shows the ARL values of the charts when the shape parameter increases. As can be seen with the increase in shape parameter the chances of point falling within the limits increases. Thus the control charts will have larger out-of-control ARLs as

compared to the in-control ARLs. Same is the case for the Average time to signal, shown in Table 4.9.

β	CQC	CQC_2	CQC_3	CQC_4	LC-1	LC-2	LC-3
1	370.37	362.02	366.33	368.34	370	370.23	370.33
1.1	668.62	668	683.41	681.19	396.66	495.81	556.8
1.2	1207.36	1233.33	1274.04	1295.18	428.72	680.56	865.39
1.3	2180.54	2343.78	2192.89	2150.86	468.14	960	1391.93
1.4	3938.43	3858.76	4716.23	4076.24	517.32	1394.87	2318.26
1.5	7113.84	8328.59	9077.33	10775.54	579.35	2091.6	3997.87
1.6	12849.8	17053.16	20597.06	15780.21	658.4	3241.43	7134.44
1.7	23210.9	27664.47	23863.44	32366.8	760.21	5196.67	13161.73
1.8	41926.9	45016.36	55224.28	64330.38	893.01	8622.67	25066.73
1.9	75734.8	70173.18	124862	166029.2	1068.74	14807.8	49207.2
2	136804	135287	207234	256074.3	1305.07	26308.73	99394.64

Table 4.8 ARL values when the shape parameter increases

β	CQC	CQC_2	CQC_3	CQC_4	LC-1	LC-2	LC-3
1	370.37	362.45	367.8	373.98	370	370.23	370.33
1.1	645.16	507.15	503.31	493.4	382.74	478.41	537.27
1.2	1135.71	650.1	635.13	611.01	403.28	640.18	814.03
1.3	2013.9	783.3	755.4	729.48	432.36	886.64	1285.55
1.4	3589.58	917.65	880.04	852.73	471.5	1271.31	2112.92
1.5	6421.98	1067.11	1021.39	976.83	523.01	1888.18	3609.05
1.6	11520.8	1219.61	1150.66	1099.29	590.3	2906.18	6396.56
1.7	20709.81	1332.77	1260.79	1247.81	678.3	4636.7	11743.49
1.8	37285.05	1473.91	1391.62	1375.16	794.15	7668.03	22291.52
1.9	67204.26	1645.28	1534.33	1478.71	948.36	13139.9	43664.65
2	121239.4	1715.03	1665.17	1631.86	1156.59	23315.5	88086.22

Table 4.9 ATS when the shape parameter increases

When the shape parameter decreases, the variance increases thus resulting in a decrease in the ARL and the control charts will be able to detect the decrease in the shape

parameter. Table 4.10 lists the ARL values when the shape parameter increases and the CQC_4 chart detects the shifts fastest. In fact, in general all the CQC_r charts perform better than the CUSUM charts (except for the CQC chart which outperforms the CUSUM charts only for $\beta \leq 0.3$).

β	CQC	CQC_2	CQC_3	CQC_4	UC-1	UC-2	UC-3
1	370.37	366.56	395.84	384.36	370.08	370.28	370.21
0.9	141.37	123.68	120.86	115.35	172.48	145.38	138.05
0.8	63.12	53.6	45.03	42.99	90.61	67.04	61.18
0.7	32.14	23.92	20.77	17.77	51.56	35.27	31.25
0.6	18.27	12.59	10.13	8.73	30.81	20.54	17.92
0.5	11.38	7.41	5.79	4.8	18.98	12.93	11.27
0.4	7.66	4.76	3.64	3.07	11.97	8.65	7.65
0.3	5.5	3.41	2.55	2.15	7.76	6.08	5.52
0.2	4.17	2.51	1.94	1.65	5.21	4.47	4.18
0.1	3.3	2	1.57	1.36	3.66	3.42	3.31

Table 4.10 ARLs when the shape parameter decreases

This is again a very good example of the case where the ARL values do not actually represent the correct information. Table 4.11 shows the ATS values for the control charts when the shape parameter decreases. From the table it can be noticed that as the shape parameter becomes very small the average time to signal becomes very large. This can be explained as follows: as the shape parameter decreases, no doubt the variability increases but at the same time the mean increases resulting in an increase in the ATS. For $\beta \leq 0.3$, the increase in mean in somewhat gradual but after that as the shape parameter further decreases, the mean increases very steeply as a result of which the time to plot a point become quite large and thus the ATS increases. In general, for $\beta \leq 0.3$ the CQC chart and the UC-3 chart give the best and almost identical performance.

β	CQC	CQC_2	CQC_3	CQC_4	UC-1	UC-2	UC-3
1	370.37	376.93	356.88	375.82	370.08	370.28	370.21
0.9	148.75	159.35	159.32	169.79	181.48	152.96	145.26
0.8	71.52	82.36	84.55	89.8	102.67	75.96	69.32
0.7	40.68	45.51	50.17	52.08	65.26	44.64	39.56
0.6	27.48	31.4	33.47	36.5	46.35	30.91	26.96
0.5	22.76	26.05	28.62	30.52	37.95	25.86	22.55
0.4	25.46	28.81	32.18	35.62	39.79	28.73	25.42
0.3	50.92	59.56	66.95	73.96	71.84	56.28	51.08
0.2	499.88	555.79	615.58	734.34	625.05	535.83	502.17
0.1	11982152	13283098	11148821	15190426	13291052	12401015	12020158

Table 4.11 ATS when the shape parameter decreases

4.5.2. Case II: lognormal distribution

The lognormal distribution is a widely used distribution in the field of economics. It is also used in modeling the processing time and repair times in the manufacturing industry. In this section the properties of the CQC_r chart are studied when the underlying distribution changes from exponential to lognormal.

The normal and lognormal distributions are closely related. If X is distributed lognormal with parameters μ and σ^2, then the natural logarithm of X is distributed normal with parameters μ and σ^2.

The probability density function and the cumulative distribution function of the log normal distribution are:

$$f(x;\mu,\sigma) = \frac{1}{x\sigma\sqrt{2\pi}} e^{\frac{-(\ln(x)-\mu)^2}{2\sigma^2}} \tag{4.7}$$

$$F(x;\mu,\sigma) = \frac{1}{\sigma\sqrt{2\pi}} \int_0^x \frac{e^{\frac{-(\ln(t)-\mu)^2}{2\sigma^2}}}{t} dt \tag{4.8}$$

The mean and variance of the lognormal distribution are:

$$\text{Mean} = e^{\left(\mu+\frac{\sigma^2}{2}\right)} \tag{4.9}$$

$$\text{Variance} = e^{(2\mu+2\sigma^2)} - e^{(2\mu+\sigma^2)} \tag{4.10}$$

It can be seen that the mean and the variance are affected by changes in the parameters μ and σ^2. When either μ or σ increases, both the mean and the variance increase.

Figures 4.4 and 4.5 show the effect of changes in parameter μ or σ on the operation characteristic of the CQC chart with an in control parameter of 1 and false alarm probability of 0.0027. As μ or σ decreases the Type II error probability increases. However the decrease in μ is more significant than the decrease in σ. Due to the increase in type II error the chart will take longer time to raise an alarm. In fact for small values of μ and σ the type II error probability is close to one and makes it practically impossible for the chart to detect this shift.

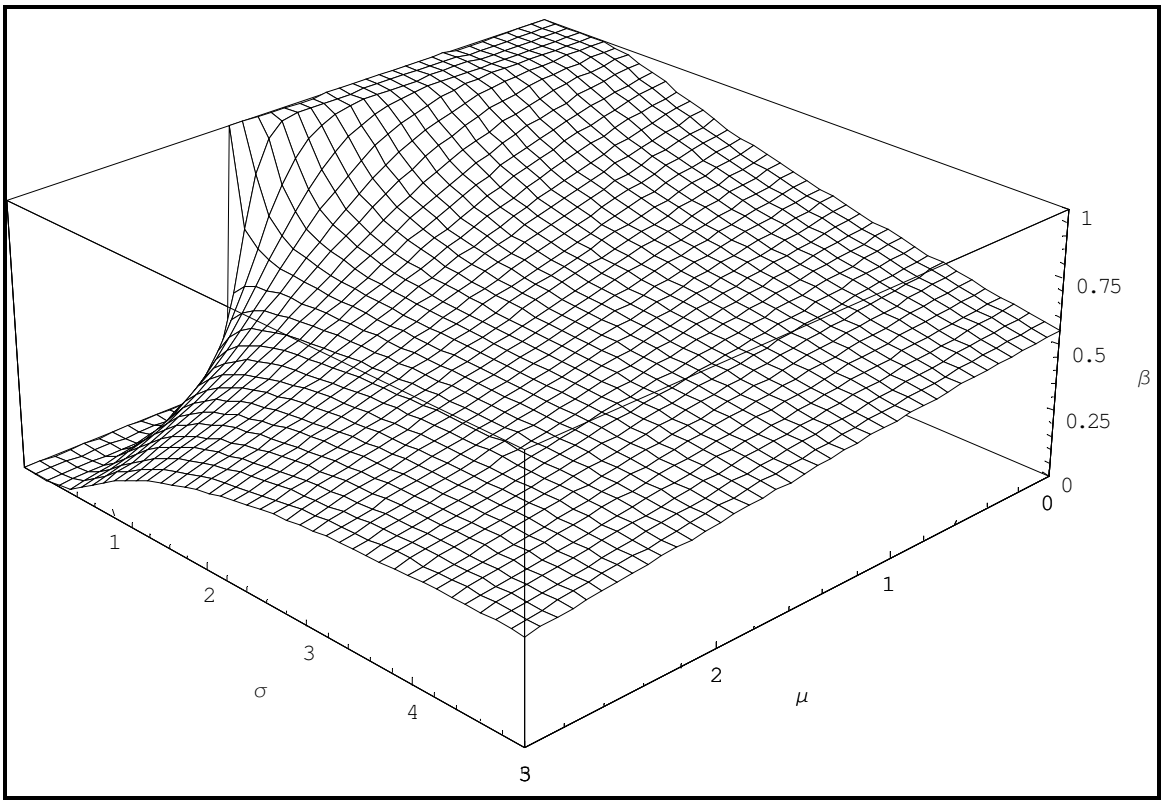

Figure 4.4 The Type II error probability of CQC chart (top view)

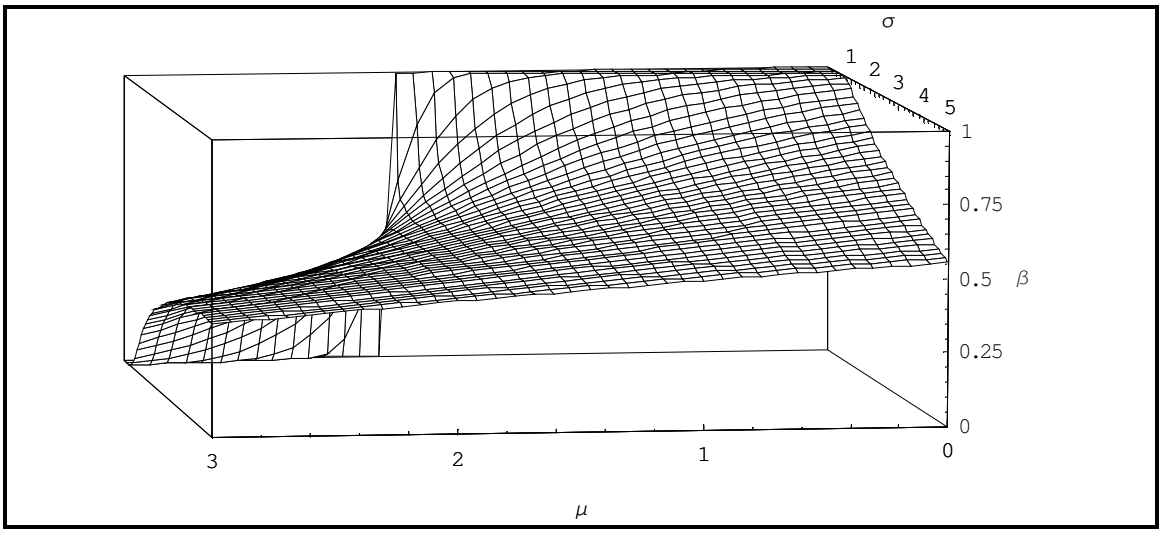

Figure 4.5 The Type II error probability of the CQC chart (side view)

Tables 4.12 and 4.13 show the ARL values of the CQC chart for different values of μ and σ. Tables 4.14 and 4.15 show the computed values of the ARLs for CQC_2 chart. The in control defect rate and false alarm probability for both the charts were fixed at 1 and 0.0027 respectively.

The ARLs were computed for charts having only an upper control limit. The reason why the lower control limit case was not used is that as the mean or standard deviation decrease, the probability of a point to fall below the lower control limit of either chart becomes very small and hence the chart will take too long to indicate the shift. For example, for $\mu = 0$ and $\sigma = 1$, the ARL of the CQC chart with a lower control limit is about 595908103.62. As μ and σ decrease the ARL further increases. The ARLs of the CQC_2 charts were calculated by simulation. For each set of value of μ and σ 100000 following lognormal distribution were simulated.

$\mu\backslash\sigma$	0.5	0.55	0.6	0.65	0.7	0.75	0.8	0.85	0.9	0.95	1
0.7	64.15	39.9	27.57	20.53	16.16	13.26	11.23	9.76	8.65	7.79	7.11
0.68	72.81	44.42	30.23	22.25	17.35	14.12	11.89	10.27	9.07	8.13	7.4
0.65	82.83	49.53	33.2	24.14	18.64	15.06	12.6	10.83	9.51	8.5	7.71
0.63	94.44	55.33	36.51	26.23	20.06	16.08	13.36	11.42	9.98	8.88	8.03
0.6	107.92	61.93	40.22	28.54	21.61	17.18	14.18	12.05	10.48	9.29	8.37
0.58	123.6	69.44	44.38	31.09	23.3	18.37	15.06	12.72	11.02	9.73	8.73
0.55	141.89	78.01	49.03	33.91	25.15	19.66	16	13.45	11.59	10.19	9.1
0.53	163.24	87.8	54.26	37.03	27.18	21.07	17.03	14.22	12.19	10.67	9.5
0.5	188.25	99	60.14	40.5	29.4	22.59	18.13	15.05	12.84	11.19	9.93
0.48	217.57	111.83	66.77	44.34	31.85	24.25	19.32	15.94	13.53	11.74	10.37
0.45	252.04	126.57	74.23	48.62	34.53	26.06	20.61	16.9	14.26	12.32	10.85
0.43	292.64	143.52	82.66	53.38	37.48	28.03	21.99	17.92	15.05	12.94	11.35
0.4	340.57	163.04	92.19	58.68	40.73	30.18	23.5	19.02	15.89	13.6	11.88
0.38	397.26	185.57	102.98	64.59	44.32	32.52	25.13	20.21	16.78	14.3	12.44
0.35	464.45	211.61	115.21	71.2	48.27	35.08	26.89	21.48	17.74	15.04	13.03
0.33	544.26	241.77	129.1	78.58	52.63	37.88	28.8	22.86	18.77	15.84	13.66
0.3	639.27	276.74	144.89	86.84	57.46	40.94	30.87	24.33	19.86	16.68	14.33
0.28	752.61	317.37	162.87	96.1	62.8	44.29	33.12	25.93	21.04	17.58	15.04
0.25	888.1	364.66	183.38	106.49	68.71	47.97	35.57	27.65	22.3	18.54	15.79
0.23	1050.43	419.8	206.79	118.16	75.26	52	38.23	29.5	23.66	19.56	16.59
0.2	1245.33	484.19	233.55	131.29	82.54	56.42	41.12	31.5	25.11	20.66	17.44
0.18	1479.85	559.54	264.21	146.07	90.62	61.28	44.27	33.67	26.67	21.82	18.34
0.15	1762.64	647.84	299.36	162.73	99.61	66.63	47.7	36.01	28.34	23.07	19.3
0.13	2104.4	751.53	339.73	181.54	109.61	72.52	51.45	38.54	30.14	24.4	20.31
0.1	2518.32	873.48	386.17	202.8	120.76	79	55.53	41.28	32.08	25.82	21.4
0.08	3020.74	1017.18	439.65	226.85	133.2	86.15	59.99	44.25	34.16	27.35	22.55
0.05	3631.94	1186.8	501.35	254.09	147.09	94.04	64.87	47.47	36.4	28.98	23.78
0.03	4377.09	1387.38	572.62	285	162.61	102.76	70.21	50.97	38.82	30.73	25.09
0	5287.58	1624.99	655.08	320.1	179.98	112.4	76.05	54.76	41.43	32.6	26.49

Table 4.12 ARL of CQC chart when the distribution changes to lognormal

$\mu\backslash\sigma$	0.5	0.55	0.6	0.65	0.7	0.75	0.8	0.85	0.9	0.95	1
0.7	146.39	93.48	66.47	51.07	41.58	35.37	31.15	28.2	26.11	24.63	23.61
0.675	162.05	101.48	71.08	53.98	43.53	36.75	32.16	28.96	26.7	25.09	23.96
0.65	179.8	110.37	76.14	57.13	45.63	38.22	33.23	29.76	27.31	25.56	24.33
0.625	199.93	120.25	81.67	60.54	47.88	39.79	34.37	30.61	27.96	26.06	24.73
0.6	222.83	131.27	87.75	64.23	50.3	41.46	35.57	31.51	28.64	26.59	25.14
0.575	248.91	143.56	94.42	68.24	52.9	43.24	36.85	32.45	29.35	27.14	25.57
0.55	278.67	157.29	101.75	72.6	55.69	45.14	38.2	33.45	30.11	27.72	26.02
0.525	312.7	172.65	109.82	77.33	58.7	47.18	39.64	34.5	30.9	28.33	26.49
0.5	351.69	189.87	118.72	82.47	61.94	49.34	41.16	35.61	31.73	28.97	26.99
0.475	396.44	209.19	128.53	88.08	65.42	51.66	42.78	36.79	32.61	29.64	27.51
0.45	447.91	230.91	139.38	94.19	69.19	54.14	44.5	38.03	33.53	30.34	28.05
0.425	507.23	255.37	151.37	100.85	73.25	56.8	46.33	39.34	34.51	31.08	28.62
0.4	575.72	282.95	164.66	108.13	77.64	59.64	48.28	40.73	35.53	31.85	29.21
0.375	654.96	314.09	179.39	116.09	82.38	62.68	50.34	42.2	36.61	32.67	29.84
0.35	746.84	349.33	195.74	124.8	87.51	65.95	52.55	43.75	37.74	33.52	30.49
0.325	853.57	389.25	213.92	134.34	93.07	69.45	54.89	45.4	38.94	34.41	31.18
0.3	977.82	434.55	234.16	144.8	99.09	73.21	57.39	47.14	40.2	35.35	31.89
0.275	1122.76	486.05	256.72	156.28	105.62	77.25	60.05	48.99	41.53	36.34	32.64
0.25	1292.18	544.69	281.9	168.9	112.72	81.59	62.9	50.94	42.94	37.38	33.43
0.225	1490.63	611.57	310.03	182.79	120.42	86.27	65.93	53.02	44.42	38.47	34.25
0.2	1723.58	687.96	341.52	198.08	128.8	91.3	69.17	55.22	45.98	39.62	35.11
0.175	1997.58	775.39	376.81	214.94	137.92	96.71	72.63	57.56	47.63	40.82	36.02
0.15	2320.57	875.59	416.4	233.54	147.85	102.56	76.33	60.04	49.37	42.08	36.96
0.125	2702.1	990.65	460.89	254.1	158.69	108.86	80.28	62.67	51.21	43.42	37.95
0.1	3153.75	1122.97	510.95	276.84	170.51	115.67	84.52	65.48	53.15	44.82	38.99
0.075	3689.54	1275.43	567.36	302.03	183.43	123.02	89.06	68.45	55.2	46.29	40.08
0.05	4326.53	1451.37	631	329.95	197.56	130.97	93.92	71.62	57.38	47.84	41.22
0.025	5085.45	1654.77	702.91	360.95	213.01	139.58	99.13	75	59.68	49.47	42.42
0	5991.61	1890.33	784.28	395.4	229.95	148.9	104.73	78.59	62.11	51.19	43.67

Table 4.13 ATS of CQC chart when the distribution changes to lognormal

$\mu\backslash\sigma$	0.5	0.55	0.6	0.65	0.7	0.75	0.8	0.85	0.9	0.95	1
0.7	25.23	16.95	12.59	9.64	7.92	6.75	5.94	5.16	4.7	4.3	3.97
0.65	33.91	21.93	15.69	11.6	9.29	7.78	6.75	5.77	5.21	4.72	4.33
0.6	48.55	29.09	19.87	14.16	11.1	9.18	7.54	6.5	5.78	5.14	4.67
0.55	68.99	38.53	23.87	17.31	13.03	10.51	8.7	7.41	6.36	5.69	5.13
0.5	98.47	49.53	30.69	21.7	15.64	12.37	9.8	8.32	7.24	6.33	5.65
0.45	138.31	68.22	39.71	26.01	19.13	14.66	11.37	9.47	8.04	6.94	6.16
0.4	196.33	91.62	53.03	33.43	23.48	17.07	13.14	11.04	9.19	7.78	6.9
0.35	308.72	136.24	66.21	42.21	28.25	20.56	15.69	12.59	10.58	8.8	7.69
0.3	404.78	184.13	94.37	53.97	35.02	24.73	18.17	14.36	11.65	9.91	8.37
0.25	821.84	265.16	122.4	67.55	43.3	30.04	20.99	16.81	13.33	11.15	9.43
0.2	805.4	372.36	165.92	87.28	52.58	35.89	25.86	19.49	15.57	12.85	10.48
0.15	1738.67	575.1	215.28	116.95	68.9	45.33	30.46	22.82	17.98	14.39	11.9
0.1	2262.32	824.69	314.59	146.2	90.15	52.88	38.96	26.5	20.78	16.41	13.49
0.05	3480.93	1061.66	457.39	188.3	115.87	66.64	45.52	31.84	23.47	18.44	15.13
0	7320	1873.79	561.28	271.6	133.67	82.03	53.54	37.48	27.69	21.89	17.03

Table 4.14 ARL of CQC_2 chart when the distribution changes to lognormal

$\mu\backslash\sigma$	0.5	0.55	0.6	0.65	0.7	0.75	0.8	0.85	0.9	0.95	1
0.7	115.4	79.44	60.7	48.03	40.77	35.97	32.73	29.86	28.32	27.15	26.31
0.65	147.56	97.76	71.99	54.97	45.5	39.46	35.38	31.8	29.87	28.33	27.25
0.6	200.27	123.12	86.39	63.72	51.74	44.22	37.77	34	31.6	29.51	28.14
0.55	270.34	155.25	99.31	74.16	57.9	48.23	41.48	36.79	33.15	30.9	29.38
0.5	367.46	190.19	121.26	88.08	66.06	53.9	44.7	39.37	35.76	32.77	30.6
0.45	491.24	249	149.34	101.25	76.68	60.79	49.21	42.72	37.85	34.26	31.94
0.4	663.9	318.3	189.2	123	89.33	67.55	54.2	47.12	41.07	36.66	33.93
0.35	992.3	449.2	225.8	148	102.5	77.49	61.22	51.16	44.84	39.22	36.07
0.3	1238	577.8	304.3	179.8	121	88.29	67.45	55.64	47.31	41.9	37.53
0.25	2393.57	790.56	376.05	214.85	141.91	102.05	74.46	61.84	51.29	45.08	39.89
0.2	2233.92	1056.13	484.44	263.65	164.38	115.87	87.34	68.17	57.11	48.96	42.09
0.15	4570.87	1551.29	599.89	335.97	205.02	139.18	97.56	76.15	62.55	52.47	45.63
0.1	5679.71	2121.51	832.66	399.73	254.83	154.71	117.76	84.2	68.78	56.85	49.05
0.05	8283.69	2592.54	1147.2	488.82	311.46	185.21	131.64	96.11	74.05	61.12	52.58
0	16541.83	4356.4	1347.29	671.23	342.59	217.31	147.32	107.41	83.26	68.54	56.28

Table 4.15 ATS of CQC_2 chart when the distribution changes to lognormal

Chapter 5

Optimal Control Limits for the run length control charts

5.1. The ARL behavior of the run length type charts

The average run length, defined earlier as the number of plotted points until an out of control signal, is commonly used to measure the chart performance. One would want the average run length to be large at the in-control process average and any change in the process average should be notified by a decrease in the average run length. However, the ARL behavior of any control chart based on a skewed distribution is inherently different from the one based on normal distribution. Compared to the normal distribution where the ARL is maximum at the in-control process parameter and decreases as the process shifts from its desired state on either side, the ARL of a control chart based on a skewed distribution, say exponential or geometric distribution, first increases and then decreases when the process deteriorates. This can be seen from Figure 5.1, which shows the CQC_r chart with the maximum ARL not at the process average but is reached at a higher value. Such behavior may lead to misinterpretation that the process is well in control, or even improved.

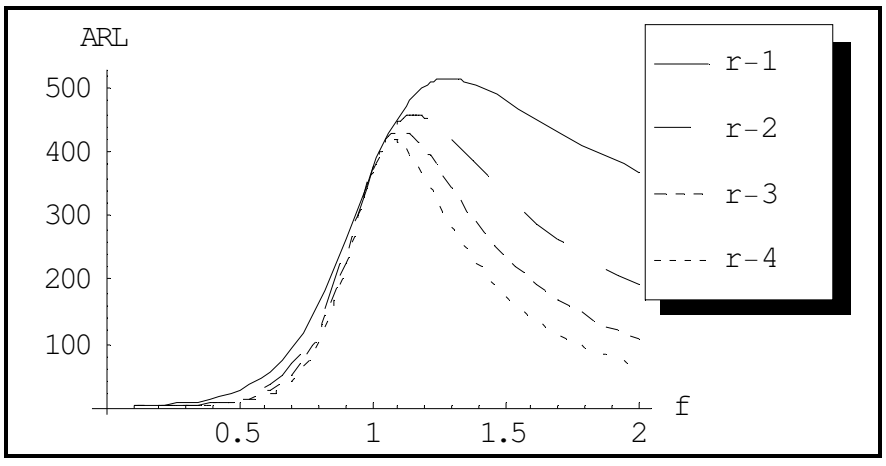

Figure 5.1 The behavior of the average run length in the CQC_r chart ($\alpha = 0.0027$)

From Figure 5.1 it can be seen that the theoretical in-control average run length of 370 (for $\alpha = 0.0027$) is attained not just at the in-control parameter λ_0 but also at an out of control parameter. The out of control parameter depends only on the in-control parameter and can be easily found out. Figure 5.2 plots the ratio *f*, which has the same ARL as the in-control ARL against the *r* (the parameter of the Erlang Distribution). From the figure it can be seen that any shift in the region $1 < f \leq 2$ (100% deterioration) for CQC_1 chart will not be detected quickly. The effect is less harmful for higher values of *r* and as *r* increases the value of *f* approaches 1.

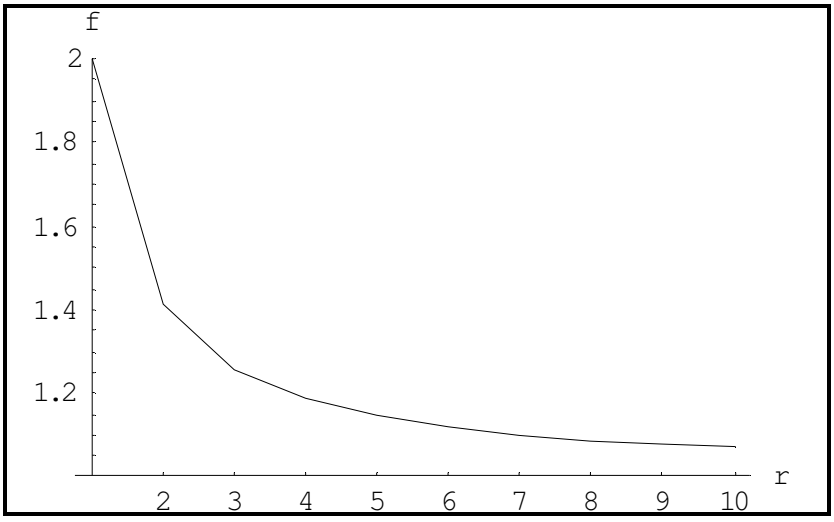

Figure 5.2 The effect of *r* on the ARL of CQC_r charts for process deterioration ($\alpha = 0.0027$)

A similar problem lies with the Shewhart charts for attributes. Some researchers have studied this problem and have suggested alternative methods. Ryan and Schwertman (1997) proposed modifying the limits in order to obtain positive lower control limit for

the attribute charts. Winterbottom (1993) suggested a procedure to modify the limits and thus unbias the p charts. Some other related discussions can be found in Acosta-Meija (1999) and Xie and Goh (1993a). Xie *et al.* (2000a) suggested an optimizing procedure for the geometric charts so that the average run length is maximized at the in-control process average. However, Xie *et al.* (2000a) did not discuss the decrease in sensitivity of the chart towards process improvements due to the optimizing procedure.. In this chapter a general optimizing procedure is devised for the run length type charts based on erlang and negative binomial distribution and also addresses the issue of specifying a proper false alarm probability to improve the sensitivity of the chart towards process changes.

5.2. The optimizing procedure for maximizing the ARL

To resolve this undesirable property associated with the ARL of the run length charts, suitable control limits need to be calculated to give the maximum ARL at the desired process level. Once the ARL expression for the CQC_r charts has been derived, Equation (3.6), the λ value at which the ARL is maximum can be found. Based on the procedure developed by Xie *et al.* (2000a) the maximum ARL at $\lambda = \lambda_0$ by taking the derivatives of ARL, and equating it to zero, the λ^* value at which the ARL is maximized can be calculated. To do we need to solve these two equations for z_2 and z_1:

$$\frac{\int_{z_2}^{\infty} t^{r-1}e^{-t}dt}{\int_{0}^{\infty} t^{r-1}e^{-t}dt} = 1-\frac{\alpha}{2} \tag{5.1}$$

$$\frac{\int_{z_1}^{\infty} t^{r-1} e^{-t} dt}{\int_{0}^{\infty} t^{r-1} e^{-t} dt} = \frac{\alpha}{2} \tag{5.2}$$

As found out by Xie *et al.* (2000a) the adjusted control limits are the product of old control limits and a factor, henceforth referred to as the adjustment factor (A_f), which depends only on the false alarm probability α. After solving Equations (5.1) and (5.2), the Adjustment factor for control charts based on Erlang Distribution can be calculated as:

$$A_f = \frac{\ln\left[\frac{z_1^{\,r}}{z_2^{\,r}}\right]}{z_1 - z_2} \tag{5.3}$$

For the case of $r = 1$, Equations (5.1) and (5.2) can be solved to obtain:

$$z_1 = -\ln\left[\frac{\alpha}{2}\right], \text{ and } \quad z_2 = -\ln\left[1 - \frac{\alpha}{2}\right]$$

Using Equation (5.3) the A_f for CQC_1 chart can be found out to be:

$$A_f = \frac{\ln\left[\frac{\ln(\alpha/2)}{\ln(1-\alpha/2)}\right]}{\ln\left[\frac{1-\alpha/2}{\alpha/2}\right]}$$

The adjustment factor can also be written as:

$$A_f = \frac{\ln\left[\frac{\ln(1-\alpha/2)}{\ln(\alpha/2)}\right]}{\ln\left[\frac{\alpha/2}{1-\alpha/2}\right]}$$

which is same as that obtained by Xie *et al.* (2000a) for the case of control charts based on geometric distribution. Some values of the adjustment factors for different values of false alarm probabilities are shown in Table 5.1.

α	A_f				
	CQC_1 chart	CQC_2 chart	CQC_3 chart	CQC_4 chart	CQC_5 chart
0.001	1.267	1.153	1.106	1.081	1.065
0.002	1.28	1.157	1.108	1.082	1.066
0.003	1.288	1.159	1.109	1.082	1.066
0.004	1.294	1.161	1.11	1.083	1.066
0.005	1.299	1.162	1.11	1.083	1.067
0.006	1.303	1.164	1.111	1.083	1.067
0.007	1.307	1.164	1.111	1.084	1.067
0.008	1.31	1.165	1.111	1.084	1.067
0.009	1.313	1.166	1.112	1.084	1.067

0.01	1.315	1.167	1.112	1.084	1.067
0.011	1.318	1.167	1.112	1.084	1.067
0.012	1.32	1.168	1.112	1.084	1.067
0.013	1.322	1.168	1.113	1.084	1.068
0.014	1.324	1.169	1.113	1.085	1.068
0.015	1.326	1.169	1.113	1.085	1.068
0.016	1.327	1.17	1.113	1.085	1.068
0.017	1.329	1.17	1.113	1.085	1.068
0.018	1.331	1.17	1.114	1.085	1.068
0.019	1.332	1.171	1.114	1.085	1.068
0.02	1.333	1.171	1.114	1.085	1.068
0.021	1.335	1.171	1.114	1.085	1.068
0.022	1.336	1.172	1.114	1.085	1.068
0.023	1.337	1.172	1.114	1.085	1.068
0.024	1.338	1.172	1.114	1.085	1.068
0.025	1.34	1.172	1.114	1.085	1.068
0.026	1.341	1.173	1.114	1.085	1.068
0.027	1.342	1.173	1.115	1.085	1.068
0.028	1.343	1.173	1.115	1.086	1.068
0.029	1.344	1.173	1.115	1.086	1.068
0.03	1.345	1.174	1.115	1.086	1.068
0.031	1.346	1.174	1.115	1.086	1.068
0.032	1.347	1.174	1.115	1.086	1.068
0.033	1.347	1.174	1.115	1.086	1.068
0.034	1.348	1.174	1.115	1.086	1.068
0.035	1.349	1.174	1.115	1.086	1.068
0.036	1.35	1.175	1.115	1.086	1.068
0.037	1.351	1.175	1.115	1.086	1.068
0.038	1.352	1.175	1.115	1.086	1.068
0.039	1.352	1.175	1.115	1.086	1.068
0.04	1.353	1.175	1.116	1.086	1.068
0.041	1.354	1.175	1.116	1.086	1.068
0.042	1.355	1.176	1.116	1.086	1.068
0.043	1.355	1.176	1.116	1.086	1.068
0.044	1.356	1.176	1.116	1.086	1.069
0.045	1.357	1.176	1.116	1.086	1.069
0.046	1.357	1.176	1.116	1.086	1.069
0.047	1.358	1.176	1.116	1.086	1.069
0.048	1.359	1.176	1.116	1.086	1.069
0.049	1.359	1.177	1.116	1.086	1.069
0.05	1.36	1.177	1.116	1.086	1.069

Table 5.1 Values of Adjustment Factors for different values of false alarm probabilities

The ARL curves for the CQC_r chart with adjusted control limits are shown in Figure 5.3. As expected the adjusted limits give a better performance with the maximum ARL attained at the process average.

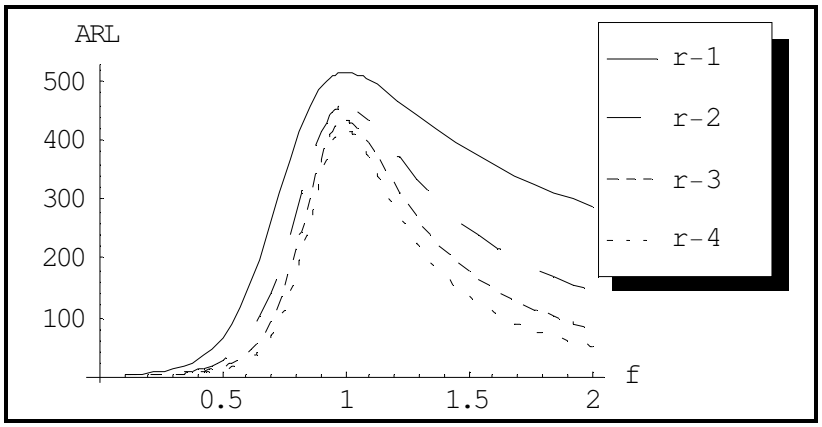

Figure 5.3 ARL curves after adjusting the limits ($\alpha = 0.0027$)

5.3. The inspection error and modification of CCC chart

The process monitoring technique based on the cumulative count of conforming (CCC) items between two nonconforming ones, or the so-called CCC chart, have been shown to be very useful, especially for high quality processes, see, e.g. Woodall (1997), Goh (1987a,b), Glushkovsky (1994), Kaminsky *et al.* (1992). Related discussions can be found in Wu and Spedding (1999) and Lai *et al.* (2000). However, as in the case of traditional Shewhart charts, the assumption of 100% error free inspection is also made in the study of the CCC charts. In reality this is hardly the case. Inspection errors and their impact on control charts have been discussed in Ryan (1989) and Johnson *et al.* (1991).

Burke *et al.* (1995) showed that when the process nonconforming is estimated from the sample, the estimated value might deviate from the true value due to the presence of inspection errors. Based on the relationship between the true and observed values of the process fraction nonconforming Lu *et al.* (2000) computed the adjusted control limits for the CCC chart in presence of inspection errors. Other studies on the inspection errors can be found in Case (1980), Lindsay (1985), Cheng and Chung (1994), Huang *et al.* (1989), and Suich (1988).

Furthermore, as shown in section 5.1 there is an undesirable property of the CCC chart; the average time to alarm might increase in the beginning when the process deteriorates. This simply means that by the time the deterioration will be detected, many nonconforming items would have been already produced. Xie *et al.* (2000a) pointed out this, and they developed a procedure to determine an optimal set of control limits, which would provide maximum average run length when the process is in control, but again under the assumption of 100% error free inspection.

5.3.1. The control limits and ARL of the CCC chart in presence of inspection errors

There are two types of inspection errors that need to be considered, a conforming item being classified as nonconforming and a nonconforming item being classified as conforming. When inspection errors are present, the observed (estimated) process fraction nonconforming will be different from the true value. Denote by p_o and p_t the observed (estimated) and the true process fraction nonconforming value respectively,

Burke *et al.* (1995) showed the relationship between the observed (estimated) and true value of fraction nonconforming as:

$$p_o = (1-\psi)p_t + \theta(1-p_t) \tag{5.4}$$

where θ and ψ are the probability of classifying a conforming item as nonconforming and the probability of classifying a nonconforming item as conforming.

When there are inspection errors, the control limits can be modified based on the inspection error. Equation (5.4) can also be represented as:

$$p_t = (p_o - \theta)/(1-\theta-\psi) \tag{5.5}$$

Using the above relationship it can be shown that the control limits of the CCC chart in the presence of inspection errors can be derived as follows:

$$UCL_a = \ln\{\frac{0.5\alpha_{desired}\, p_t}{p_o}\}/\ln[1-p_o] \tag{5.6}$$

$$CL_a = \ln(0.5)/\ln[1-p_o] \tag{5.7}$$

$$LCL_a = \ln\{1-\frac{0.5\alpha_{desired}\, p_t}{p_o}\}/\ln[1-p_o] \tag{5.8}$$

In the above formulae $\alpha_{desired}$ is the desired false alarm probability when the process is in control. It should be noted that generally $\alpha_{desired}$ is taken as 0.0027, which is equivalent to the standard 3-sigma control limits. With these control limits, the false alarm probability will be equal to $\alpha_{desired}$ (Lu *et al.*, 2000).

The average run length (ARL), is now given by

$$ARL = \frac{1}{1-(1-p_o)^{LCL-1}+(1-p_o)^{UCL}} \tag{5.9}$$

In Table 5.2 some ARL values are given for a process for different values of $\alpha_{desired}$ with average fraction nonconforming = 50 ppm, $\psi = 0.2$ and $\theta = 0.0001$. Some ARL curves are also shown in Figure 5.4.

It is also of interest to investigate the ARL property for different values of inspection errors. In Table 5.3 some ARL values are given for a process with fixed α(=0.0027) and average fraction nonconforming 50 ppm but for different values of the inspection errors. Some ARL curves are shown in Figure 5.5 for different values of inspection errors.

p_t (ppm)	$\alpha_{desired}$ = 0.0027	$\alpha_{desired}$ = 0.01	$\alpha_{desired}$ = 0.05
10	330	113	30
20	483	150	37
30	686	195	43
40	936	243	50
50	1213	291	56
60	1485	335	62
70	1716	370	67
80	1883	395	70
90	1982	409	72
100	2023	415	73
120	1993	409	73
140	1895	391	71
160	1782	369	68
200	1572	327	61
300	1203	250	47
400	974	203	38
500	818	170	32

Table 5.2 Some numerical value of the ARL for different values of observed fraction nonconforming and desired false alarm rate.

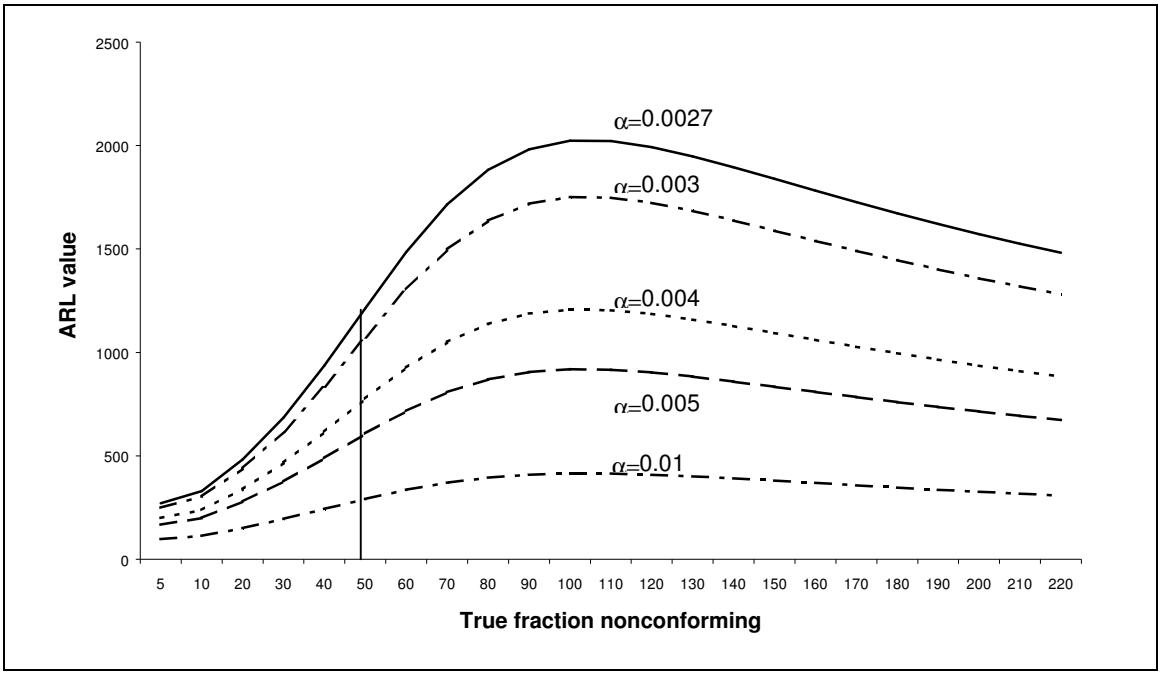

Figure 5.4 Some ARL Curves with p=50ppm, $\psi = 0.2, \theta = 0.0001$

p_t (ppm)	$\theta = 0.00001$ $\psi = 0.5$	$\theta = 0.00006$ $\psi = 0.5$	$\theta = 0.00006$ $\psi = 0.2$
10	14	208	136
20	34	296	231
30	78	406	377
40	158	533	575
50	262	665	800
60	339	786	1003
70	363	881	1140
80	353	944	1205
90	330	976	1213
100	306	985	1188
120	264	959	1101
140	231	907	1008
160	206	851	924
200	168	748	791
300	116	571	580
400	88	461	458
500	72	387	378

Table 5.3 Some numerical value of the ARL for different values of observed fraction nonconforming and inspection errors.

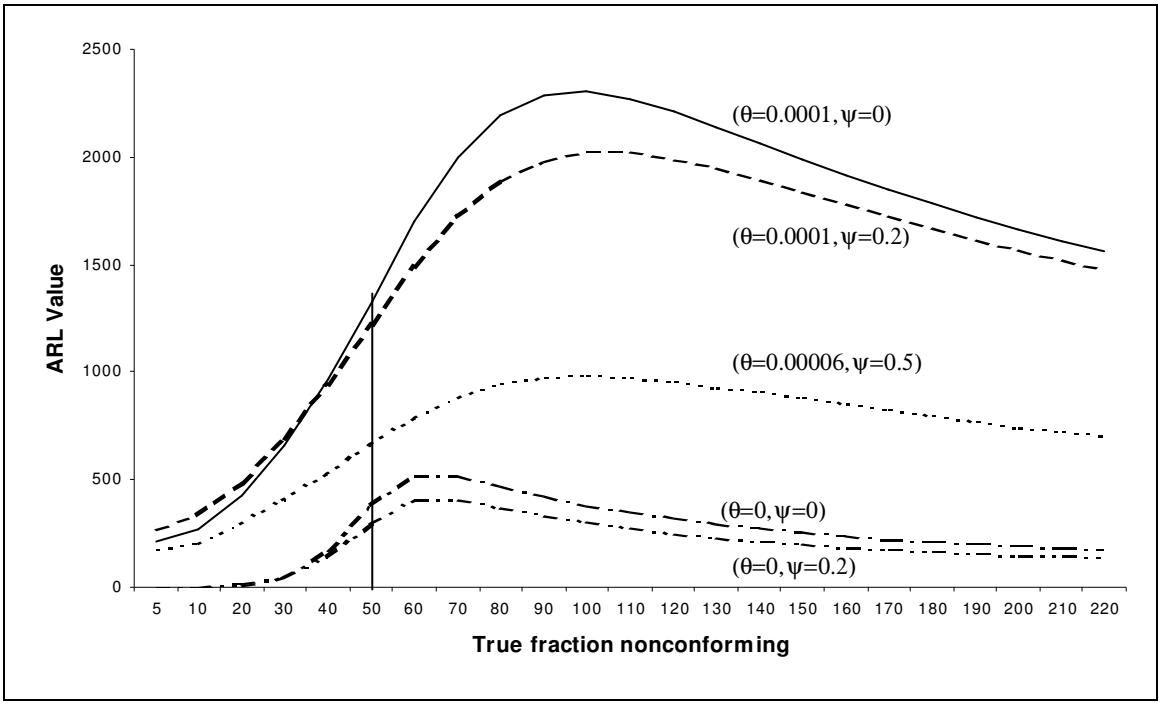

Figure 5.5 ARL curves with p=50ppm, $\alpha = 0.0027$ for different values of inspection errors

5.3.2 The behavior of ARL in CCC chart

It is evident from both Figures 5.4 & 5.5 that maximum ARL value is reached at a value of fraction nonconforming, which is greater than the average fraction nonconforming of the process. This means that when the process deteriorates, it will take a longer time to observe an out-of-control signal, a property that is highly undesirable. This is a general problem associated with the ARL of the control charts based on skewed distributions as pointed out before. Thus with the existing ARL expression it will take longer time for an alarm to be raised when the process deteriorates than when the process is in a state of statistical control.

We can actually compute the relative differences between the maximum ARL and the ARL at the normal process fraction nonconforming level (called nominal level here)

$$\text{Relative Error (ARL)} = \frac{ARL_{\max} - ARL_0}{ARL_0}$$

and also the relative difference between the p at which ARL reaches its maximum, and the nominal level,

$$\text{Relative Error } (p) = \frac{p_{\max} - p_0}{p_0}$$

Table 5.4 and 5.5 give some values of the two relative errors for different values of false alarm rate (with fixed inspection errors $\theta = 0.0001, \psi = 0.2$) and for different values of inspection errors (with fixed $\alpha_{desired} = 0.0027$) respectively.

p_t (ppm)	$\alpha_{desired} = 0.0027$					$\alpha_{desired} = 0.005$				
	ARL_o	Observed Maximum (ppm)	Maximum ARL value	Relative Error (p)	Relative Error (ARL)	ARL_o	Observed Maximum (ppm)	Maximum ARL value	Relative Error (p)	Relative Error (ARL)
20	2861	70	5881	2.5	1.0556	1340	60	2208	2	0.6478
30	1889	80	3418	1.67	0.8094	921	80	1446	1.67	0.57
40	1457	90	2503	1.25	0.7179	723	90	1110	1.25	0.5353
50	1213	100	2023	1	0.6678	608	100	919	1	0.5115
100	757	170	1209	0.7	0.5971	385	170	567	0.7	0.4727
150	617	240	977	0.6	0.5835	314	240	458	0.6	0.4586
200	550	300	874	0.5	0.5891	279	300	407	0.5	0.4588

Table 5.4 Some values of the fraction nonconforming at which the maximum ARL is reached for different values of false alarm rate.

It should be noted here that although the inspection error θ has a large effect on the ARL, this type of error could be easily rectified. An item that is considered nonconforming will probably be checked again and if it turns out to be a conforming item, it will not be counted as nonconforming. This inspection procedure has been called "repetitive testing" in Greenberg and Stokes (1995). A nonconforming item when considered conforming will normally be just passed as one of the many conforming items. Hence, when considering inspection error for high-quality, the focus will be on the inspection error P, the probability that a nonconforming item is considered conforming because as pointed out, the number of conforming items heavily outnumber the number of nonconforming ones in a high-quality environment (process).

p_t (ppm)	$\theta = 0.00001, \psi = 0.5$					$\theta = 0.00001, \psi = 0$				
	ARL_o	Observed Maximum (ppm)	Maximum ARL value	Relative Error (p)	Relative Error (ARL)	ARL_o	Observed Maximum (ppm)	Maximum ARL value	Relative Error (p)	Relative Error (ARL)
20	373	30	521	0.5	0.3968	565	30	802	0.5	0.4195
30	311	50	424	0.67	0.3633	504	40	716	0.33	0.4206
40	280	60	388	0.5	0.3857	474	50	662	0.25	0.3966
50	262	70	363	0.4	0.3855	457	70	651	0.4	0.4245
100	225	140	311	0.4	0.3822	426	130	618	0.3	0.4507
150	214	200	296	0.33	0.3832	422	200	622	0.33	0.4739
200	208	270	290	0.35	0.3942	423	270	635	0.35	0.5012

Table 5.5 Some values of the fraction nonconforming at which the maximum ARL is reached for different values of inspection errors.

To resolve this undesirable property associated to the ARL of the CCC chart, we can find suitable control limits by using Equation (5.3). In fact, the p value for maximum ARL is given by:

$$p = 1 - \exp\left(\frac{\ln(1-p_o)\ln\left[\frac{(\alpha_d p_t / 2p_o)(1-p_o)}{(1-\alpha_d p_t / 2p_o)}\right]}{\ln\left[\frac{\ln\{(1-\alpha_d p_t / 2p_o)/(1-p_o)\}}{\ln(\alpha_d p_t / 2p_o)}\right]}\right) \tag{5.10}$$

Now substituting this value in Equations (5.6) and (5.8) we get the control limits as

$$UCL_a^* = \frac{\ln\left(\frac{0.5\alpha_d p_t}{(1-\psi)p_t + (1-p_t)\theta}\right)\ln\left[\frac{\ln\{(1-\alpha_d p_t / 2p_o)/(1-p_o)\}}{\ln(\alpha_d p_t / 2p_o)}\right]}{\ln[1-(1-\psi)p_t - (1-p_t)\theta]\ln\left[\frac{(\alpha_d p_t / 2p_o)(1-p_o)}{(1-\alpha_d p_t / 2p_o)}\right]} \tag{5.11}$$

and

$$LCL_a^* = \frac{\ln(1-\frac{0.5\alpha_d p_t}{(1-\psi)p_t+(1-p_t)\theta})\ln[\frac{\ln\{(1-\alpha_d p_t/2p_o)/(1-p_o)\}}{\ln(\alpha_d p_t/2p_o)}]}{\ln[1-(1-\psi)p_t-(1-p_t)\theta]\ln[\frac{(\alpha_d p_t/2p_o)(1-p_o)}{(1-\alpha_d p_t/2p_o)}]} \quad (5.12)$$

For a fixed value of p_0, Equations (5.11) and (5.12) can be used to compute the control limits. With these control limits, the ARL will decrease when the process is shifted from the value p_0.

5.3.3. Implementation procedure

Although the Equations (5.11) and (5.12) look complicated, the implementation is straightforward. A close look at the above two formulas shows that it can be broken into two parts, the formula of the old control limits multiplied with a factor. The factor, which we will refer to as *Adjustment Factor*, can be written as:

$$A_f = \frac{\ln[\frac{\ln\{(1-\alpha_d p_t/2p_o)/(1-p_o)\}}{\ln(\alpha_d p_t/2p_o)}]}{\ln[\frac{(\alpha_d p_t/2p_o)(1-p_o)}{(1-\alpha_d p_t/2p_o)}]} \quad (5.13)$$

Some values of the adjustment factor are given in Table 5.6 for a process with average fraction nonconforming of 50 ppm for different values of false alarm rate and inspection errors. From the table it can be observed that the inspection error θ has much larger effects on the average run length than the inspection error ψ. This becomes even clearer in section 5.3.5, when we compare the current and the proposed methods. From Table 5.6 we can see that when the inspection errors are absent (or ignored) then the adjustment factor increases with increase in false alarm rate. This also holds true for the case when inspection error θ is zero (third column in Table 5.6). But this does not hold for the case when inspection error θ is present (columns four, five and six). Adjustment factors first decrease and then increase with $\alpha_{desired}$. It should be noted that θ tends to increase the process fraction nonconforming while ψ tends to decrease it.

$\alpha_{desired}$	$\theta = 0$ $\psi = 0$	$\theta = 0$ $\psi = 0.2$	$\theta = 0.0001$ $\psi = 0$	$\theta = 0.0001$ $\psi = 0.2$	$\theta = 0.00006$ $\psi = 0.5$
0.0015	1.2839	1.2848	1.3655	1.3460	1.2923
0.0020	1.2873	1.2892	1.3344	1.3236	1.2907
0.0025	1.2904	1.2929	1.3209	1.3136	1.2909
0.005	1.3025	1.3064	1.3043	1.3019	1.2967
0.006	1.3061	1.3104	1.3033	1.3016	1.2992
0.007	1.3094	1.3138	1.3032	1.3020	1.3016
0.008	1.3123	1.3169	1.3036	1.3028	1.3038
0.01	1.3173	1.3223	1.3050	1.3046	1.3078

Table 5.6 Values of the adjustment factor for a process with average fraction nonconforming = 50 ppm, $\psi = 0.2$ and $\theta = 0.0001$

Figure 5.6 illustrates the charting procedure for the CCC chart in presence of inspection errors. The procedure includes the proposed method for finding the optimal set of control limits to maximize the ARL value at the process average. Before starting the chart the

count of conforming items (n) is set to zero. An item is inspected and if it is conforming the value of n is increased by 1 and another item is taken. This process goes on until the first nonconforming item is encountered. The value of n is plotted on the chart. If a plotted point falls below the lower control limit, it indicates that the process fraction nonconforming might have increased. In such a case investigation should be carried out to locate any assignable causes for the possible deterioration. If assignable causes are identified then they should be removed and the process should be brought back to its original state. If a plotted point falls above the upper control limit, it indicates that the process might have improved. In such a case again a search for assignable causes should be performed and if found the causes should be retained, and a new control chart should be started with improved fraction nonconforming.

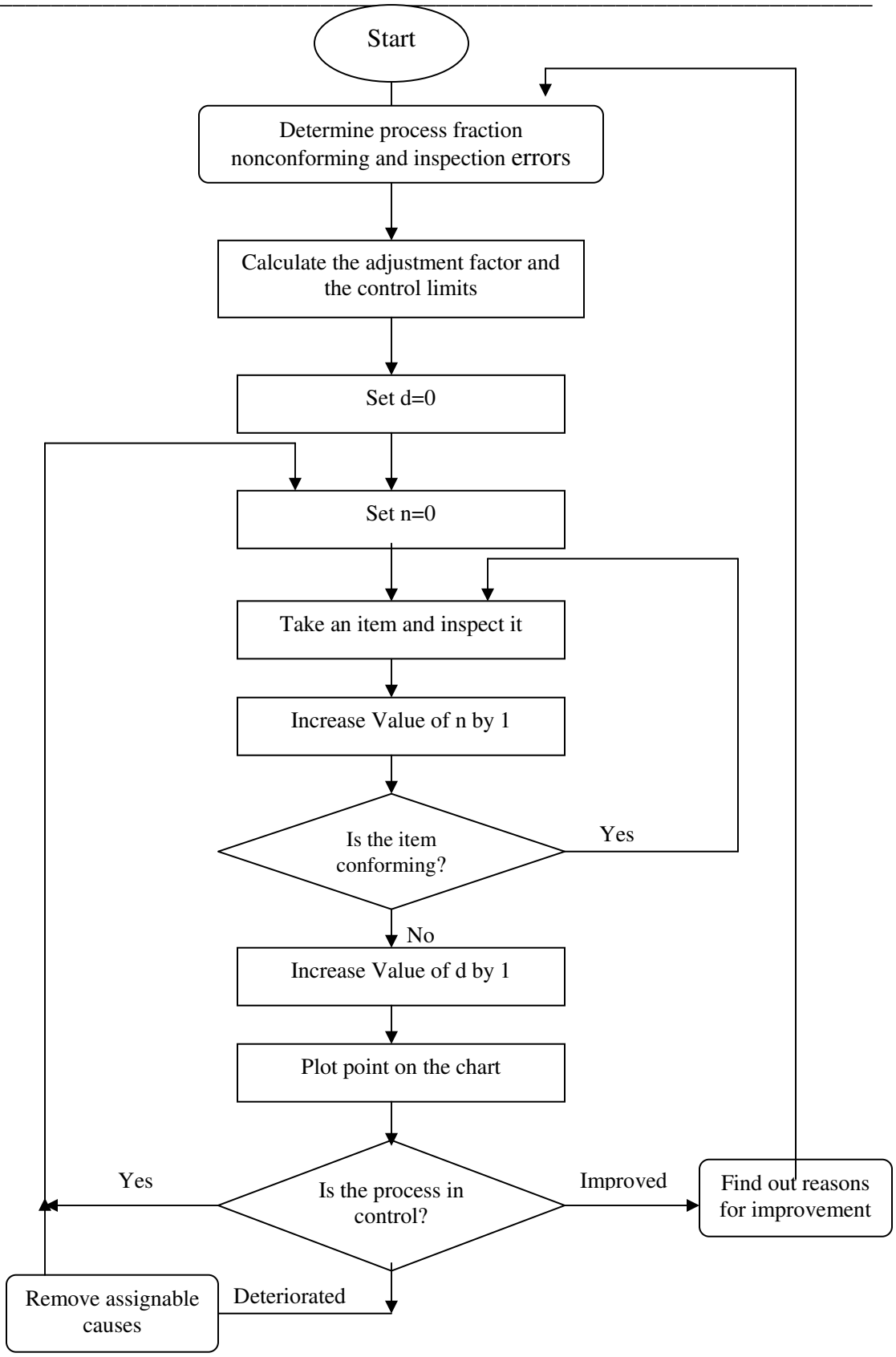

Figure 5.6 Implementation Procedure

5.3.4. An application example

Here an example is used to illustrate the usefulness of the proposed procedure. A process has average fraction nonconforming of 500ppm, $\alpha = 0.1$ and inspection errors $\theta = 0.0002, \psi = 0.1$. The control limits calculated by the current method in the presence of inspection errors are 60 (*LCL*) and 5011 (*UCL*) and the proposed limits are 83 (*LCL*) and 6905 (*UCL*). The data in Table 5.7 represent the number of conforming items observed before observing a nonconforming one. The first 15 observations were simulated for *p*=500ppm while the second 15 observations were simulated for *p*=5000ppm.

Nonconforming item No.	Count of conforming items	Process average	Nonconforming item No.	Count of conforming items	Process average
1	3211	p=500ppm	16	70	p=5000ppm
2	612	p=500ppm	17	904	p=5000ppm
3	899	p=500ppm	18	234	p=5000ppm
4	10497	p=500ppm	19	342	p=5000ppm
5	1760	p=500ppm	20	95	p=5000ppm
6	26	p=500ppm	21	406	p=5000ppm
7	3334	p=500ppm	22	99	p=5000ppm
8	4830	p=500ppm	23	536	p=5000ppm
9	3711	p=500ppm	24	40	p=5000ppm
10	3518	p=500ppm	25	103	p=5000ppm
11	5351	p=500ppm	26	480	p=5000ppm
12	2477	p=500ppm	27	231	p=5000ppm
13	4307	p=500ppm	28	103	p=5000ppm
14	382	p=500ppm	29	82	p=5000ppm
15	115	p=500ppm	30	102	p=5000ppm

Table 5.7 Number of conforming items observed before observing a nonconforming item (for *p*=500ppm, $\alpha = 0.1, \theta = 0.0002$ and $\psi = 0.1$)

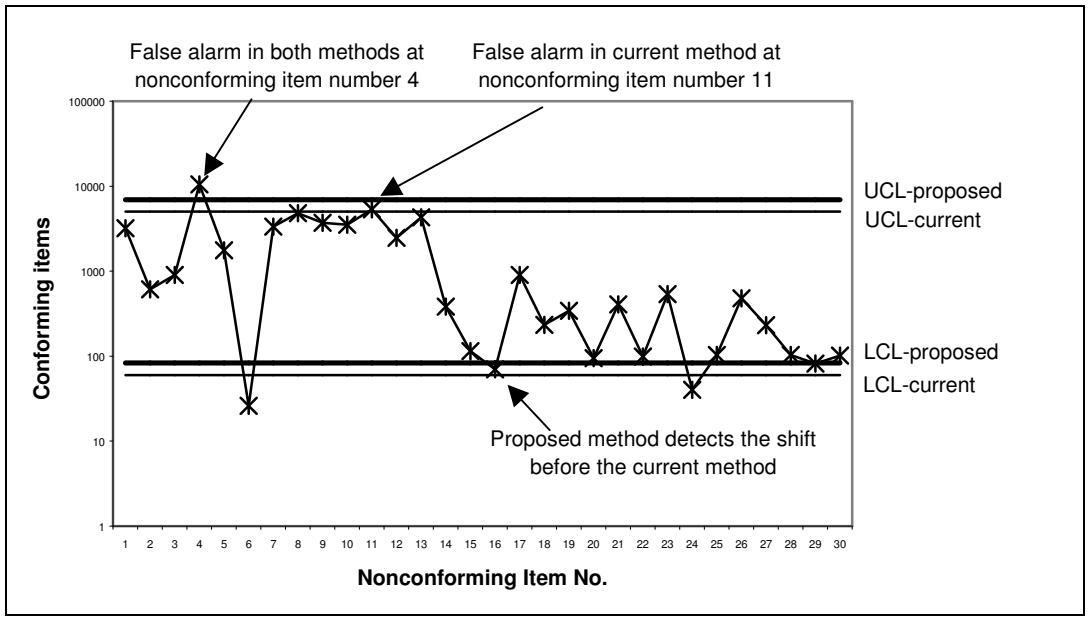

Figure 5.7 The CCC chart for the data set in Table 5.6

It can be seen in Figure 5.7 that the chart based on current method raises two false alarms while the proposed method raises only one false alarm. Also as expected, the proposed method identifies the shift much quickly than the current method when the process average changes from 500ppm to 5000pppm.

5.3.5. Statistical comparison of chart performance

The proposed method makes sure that whenever there is a shift in the process fraction nonconforming level, irrespective of whether the process deteriorates or improves, it will be indicated by a change in the average run length value. This is a very important property for a control chart. As noted before, because of the skewness of the geometric

distribution, the CCC chart has the undesirable property that it will show fewer alarms initially when the process deteriorates.

Figures 5.8 and 5.9 show the ARL curves for the data set presented in section 5.3.1. It is evident that maximum value of ARL is reached at the process average fraction nonconforming (50 ppm in this case). Table 5.8 shows a comparison between the current and the proposed method in terms of the average run length value at different process levels.

The last column in Table 5.8 shows the percent reduction in the false alarm signal achieved when we use the proposed method instead of the current method. At process average 50 ppm, the current method raises the false alarm signal at every 1213 points while the proposed method raises a signal at every 1862 points which translates to almost 54 percent reduction in the false alarm signal.

When the process shifts to 90 ppm, the ARL value for the proposed method is 1641 and for the current method is 1982. Thus, the out-of-control ARL is also improved, in this instance by a reduction of 17%.

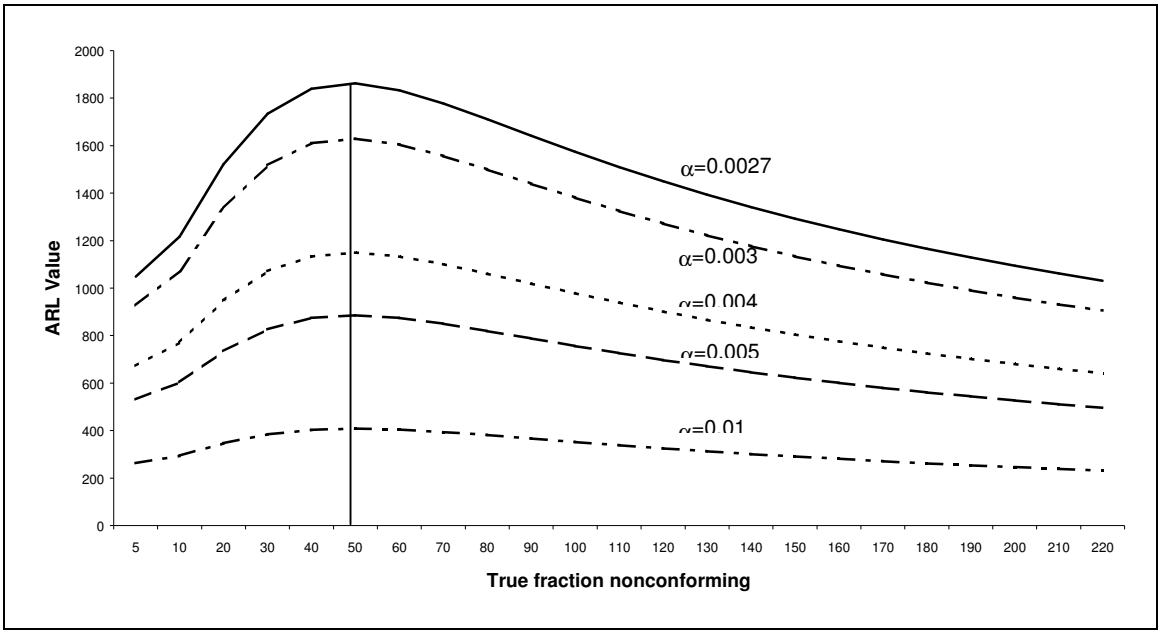

Figure 5.8 ARL curves with p=50ppm, $\psi = 0.2, \theta = 0.0001$ with maximum ARL at p=50ppm (for the proposed method)

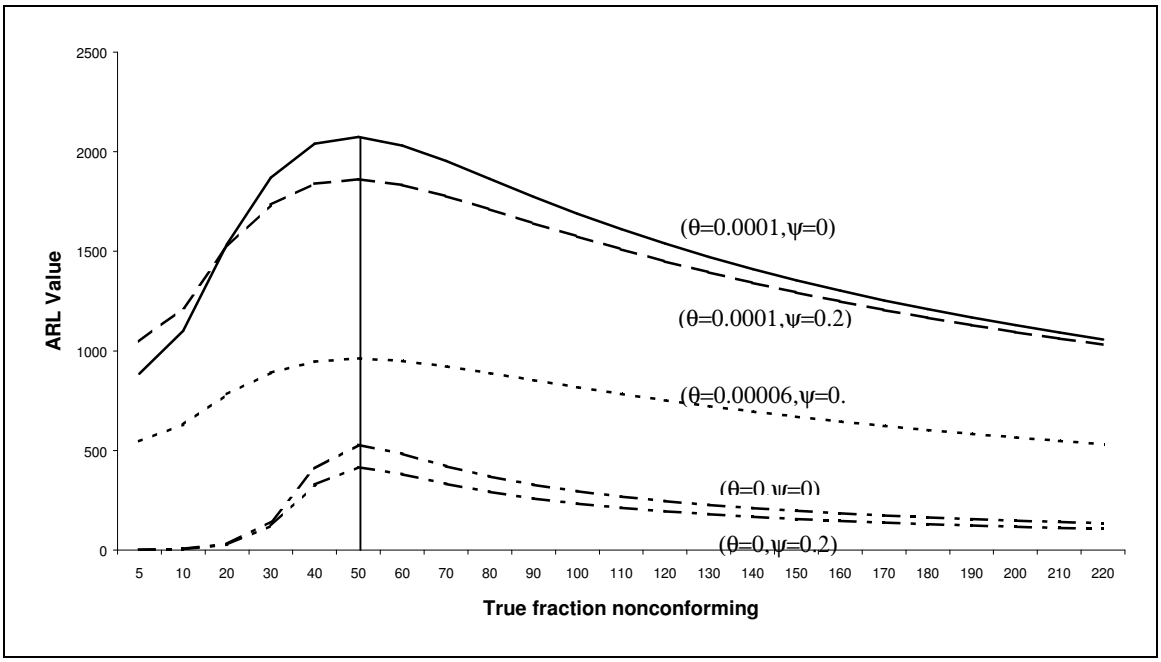

Figure 5.9 ARL curves with p=50ppm, $\alpha = 0.0027$ for different values of inspection errors with maximum ARL value p=50ppm.

Process Average (ppm)	Current Method			Proposed Method			Increase in the in-control ARL (%)
	LCL_c	UCL_c	ARL_c	LCL_p	UCL_p	ARL_p	
20	2	72113	2861	3	96370	4784	67.21426
30	3	64729	1889	3	85376	3011	59.39651
40	3	59100	1457	4	77615	2269	55.73095
50	3	54550	1213	5	71522	1862	53.50371
60	4	50745	1056	5	66499	1607	52.17803
70	4	47492	947	5	62239	1431	51.10876
80	4	44666	867	5	58555	1304	50.40369
90	4	42180	806	5	55325	1207	49.75186
100	4	39973	757	5	52462	1132	49.53765
200	4	26421	550	5	34943	815	48.18182

Table 5.8 A comparison of current and proposed methods for given process average, $\alpha = 0.0027$, $\psi = 0.2$ and $\theta = 0.0001$

5.4. Attaining the desired false alarm probability

The maximizing procedure described in the previous section results in the optimal set of control limits for the control charts based on skewed distributions, however, adjusting the limits results in a smaller false alarm probability than that specified. As a result of that the chart becomes less sensitive to small process deteriorations as compared to the chart without the adjusted limits. Figure 5.10 shows the ARL curves with and without the adjusted limits. As can be seen from the figure, any shift in the region between the drawn lines will be picked up faster by the control chart without the adjusted limits. This region in which the control chart with adjusted limits performs worse than the control charts without the adjusted limits can be found out by equating the ARLs of the two charts and then solving for *f*. The *f* values for CQC_r charts are shown in Table 5.9.

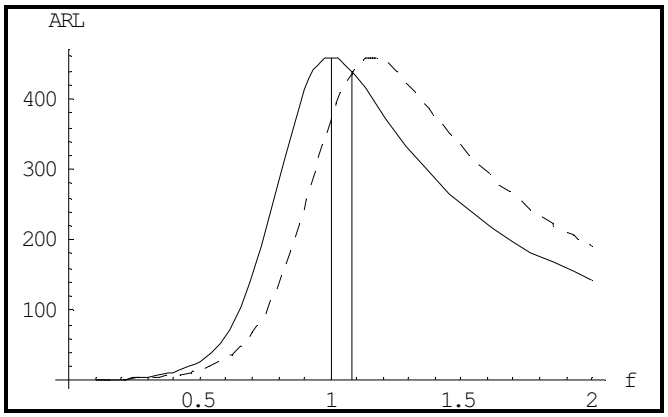

Figure 5.10 The effect of the maximizing procedure on the anticipated false alarm

α	f				
	CQC_1 chart	CQC_2 chart	CQC_3 chart	CQC_4 chart	CQC_5 chart
0.001	1.142	1.079	1.055	1.041	1.033
0.002	1.148	1.081	1.055	1.042	1.033
0.003	1.151	1.082	1.055	1.042	1.033
0.004	1.153	1.082	1.056	1.042	1.034
0.005	1.155	1.083	1.056	1.042	1.034
0.006	1.157	1.083	1.056	1.042	1.034
0.007	1.158	1.083	1.056	1.042	1.034
0.008	1.159	1.084	1.056	1.042	1.034
0.009	1.16	1.084	1.056	1.042	1.034
0.01	1.161	1.084	1.056	1.042	1.034
0.011	1.162	1.084	1.056	1.042	1.034
0.012	1.163	1.084	1.056	1.042	1.034
0.013	1.163	1.085	1.057	1.042	1.034
0.014	1.164	1.085	1.057	1.042	1.034
0.015	1.165	1.085	1.057	1.042	1.034
0.016	1.165	1.085	1.057	1.042	1.034
0.017	1.166	1.085	1.057	1.042	1.034
0.018	1.166	1.085	1.057	1.042	1.034
0.019	1.167	1.085	1.057	1.042	1.034
0.02	1.167	1.085	1.057	1.042	1.034
0.021	1.168	1.085	1.057	1.042	1.034
0.022	1.168	1.086	1.057	1.043	1.034
0.023	1.168	1.086	1.057	1.043	1.034
0.024	1.169	1.086	1.057	1.043	1.034
0.025	1.169	1.086	1.057	1.043	1.034
0.026	1.17	1.086	1.057	1.043	1.034

0.027	1.17	1.086	1.057	1.043	1.034
0.028	1.17	1.086	1.057	1.043	1.034
0.029	1.171	1.086	1.057	1.043	1.034
0.03	1.171	1.086	1.057	1.043	1.034
0.031	1.171	1.086	1.057	1.043	1.034
0.032	1.171	1.086	1.057	1.043	1.034
0.033	1.172	1.086	1.057	1.043	1.034
0.034	1.172	1.086	1.057	1.043	1.034
0.035	1.172	1.086	1.057	1.043	1.034
0.036	1.173	1.086	1.057	1.043	1.034
0.037	1.173	1.086	1.057	1.043	1.034
0.038	1.173	1.087	1.057	1.043	1.034
0.039	1.173	1.087	1.057	1.043	1.034
0.04	1.173	1.087	1.057	1.043	1.034
0.041	1.174	1.087	1.057	1.043	1.034
0.042	1.174	1.087	1.057	1.043	1.034
0.043	1.174	1.087	1.057	1.043	1.034
0.044	1.174	1.087	1.057	1.043	1.034
0.045	1.175	1.087	1.057	1.043	1.034
0.046	1.175	1.087	1.057	1.043	1.034
0.047	1.175	1.087	1.057	1.043	1.034
0.048	1.175	1.087	1.057	1.043	1.034
0.049	1.175	1.087	1.057	1.043	1.034
0.05	1.175	1.087	1.057	1.043	1.034

Table 5.9 Some ARL values of the adjustment method and existing methods (α=0.0027)

A large run length at the in-control process level is a desirable property, however in this case it means that the higher in-control average run length means smaller false alarm probability which means a higher Type II error than before. For example for the specified false alarm probability, α_s, of 0.0027, the use of adjusted control limits gives an actual false alarm probability, α_a, of 0.00194. In other words it means that the actual false alarm probability is less than that specified. One way to deal with this problem is to appropriately select α_s so that α_a can take the desired value. This can be done by equating the false alarm probability with adjusted limits to α_a and then solving for α_s. For example in order to obtain a desired (actual) false alarm probability of 0.0027, the specified false

alarm probability, α_s, should be approximately 0.00372 for CQC_1 chart and about 0.00333 for CQC_2 chart. Table 5.10 shows some values of actual (desired) false alarm probability and the corresponding false alarm probability that should be specified in order to obtain the desired false alarm probability. The ARL performance of the existing, adjustment and method is also shown in Figure 5.11. The continuous line represents the chart with optimized limits and adjusted false alarm probability.

α_a	α_s				
	CQC_1 chart	CQC_2 chart	CQC_3 chart	CQC_4 chart	CQC_5 chart
0.001	0.0014	0.0013	0.0012	0.0011	0.0011
0.002	0.0028	0.0025	0.0023	0.0023	0.0022
0.003	0.0041	0.0037	0.0035	0.0034	0.0033
0.004	0.0054	0.0049	0.0046	0.0045	0.0044
0.005	0.0068	0.0061	0.0057	0.0056	0.0055
0.006	0.0081	0.0072	0.0069	0.0067	0.0065
0.007	0.0093	0.0084	0.008	0.0077	0.0076
0.008	0.0106	0.0095	0.0091	0.0088	0.0087
0.009	0.0119	0.0107	0.0102	0.0099	0.0097
0.01	0.0132	0.0119	0.0113	0.011	0.0108
0.011	0.0144	0.013	0.0124	0.0121	0.0119
0.012	0.0157	0.0141	0.0135	0.0131	0.0129
0.013	0.0169	0.0153	0.0146	0.0142	0.014
0.014	0.0182	0.0164	0.0157	0.0153	0.015
0.015	0.0194	0.0175	0.0168	0.0163	0.0161
0.016	0.0207	0.0187	0.0179	0.0174	0.0171
0.017	0.0219	0.0198	0.0189	0.0185	0.0182
0.018	0.0231	0.0209	0.02	0.0195	0.0192
0.019	0.0243	0.022	0.0211	0.0206	0.0203
0.02	0.0256	0.0232	0.0222	0.0217	0.0213
0.021	0.0268	0.0243	0.0233	0.0227	0.0224
0.022	0.028	0.0254	0.0243	0.0238	0.0234
0.023	0.0292	0.0265	0.0254	0.0248	0.0245
0.024	0.0304	0.0276	0.0265	0.0259	0.0255
0.025	0.0316	0.0287	0.0276	0.027	0.0266
0.026	0.0328	0.0298	0.0286	0.028	0.0276
0.027	0.034	0.031	0.0297	0.0291	0.0287
0.028	0.0352	0.0321	0.0308	0.0301	0.0297

0.029	0.0364	0.0332	0.0319	0.0312	0.0307
0.03	0.0376	0.0343	0.0329	0.0322	0.0318
0.031	0.0388	0.0354	0.034	0.0333	0.0328
0.032	0.04	0.0365	0.0351	0.0343	0.0339
0.033	0.0412	0.0376	0.0361	0.0354	0.0349
0.034	0.0424	0.0387	0.0372	0.0364	0.036
0.035	0.0436	0.0398	0.0383	0.0375	0.037
0.036	0.0447	0.0408	0.0393	0.0385	0.038
0.037	0.0459	0.0419	0.0404	0.0396	0.0391
0.038	0.0471	0.043	0.0414	0.0406	0.0401
0.039	0.0483	0.0441	0.0425	0.0417	0.0411
0.04	0.0494	0.0452	0.0436	0.0427	0.0422
0.041	0.0506	0.0463	0.0446	0.0437	0.0432
0.042	0.0518	0.0474	0.0457	0.0448	0.0442
0.043	0.053	0.0485	0.0467	0.0458	0.0453
0.044	0.0541	0.0496	0.0478	0.0469	0.0463
0.045	0.0553	0.0506	0.0489	0.0479	0.0473
0.046	0.0564	0.0517	0.0499	0.049	0.0484
0.047	0.0576	0.0528	0.051	0.05	0.0494
0.048	0.0588	0.0539	0.052	0.051	0.0504
0.049	0.0599	0.055	0.0531	0.0521	0.0515
0.05	0.0611	0.0561	0.0541	0.0531	0.0525

Table 5.10 Some values of desired and specified false alarm probabilities

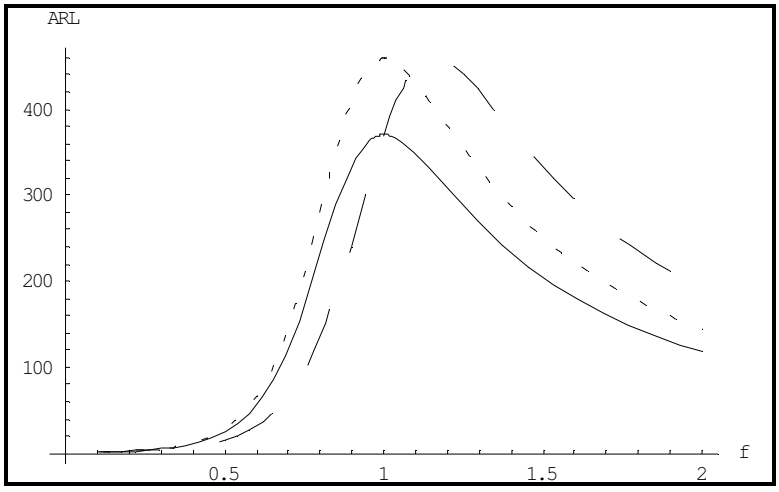

Figure 5.11 The ARL curves for the three methods

Chapter 6

Process Monitoring with Estimated Parameters

6.1. The effect of inaccurate control limits

The motive behind using the control chart is to detect changes in the process. Shewhart control charts have undergone many modifications with time to enhance their detection power. Some of these modifications are using variable sampling schemes (Aparisi and Haro (2001), Zimmer *et al.* (2000)) and using the pattern recognition techniques (Perry *et al.* (2001), Yang and Yang (2002)). The first step in implementing in any control chart is to determine the control limits, which in turn requires the determination of process model parameter(s) involved. The observations are then plotted on the control chart and inference about the state of the process is made.

Most of the research done on control charts is based on the assumption that an accurate estimation of the parameter is available. However, an estimate of process parameters can be far from accurate. There is always uncertainty involved when a preliminary sample is taken to estimate the parameter of the process and many authors have addressed this issue, Proschan and Savage (1960), Hillier (1969), Quesenberry (1993), Chen (1997, 1998), Woodall (1997), Braun (1999), Woodall and Montgomery (1999), Bischak and Silver (2001), Yang *et al.* (2002a). He *et al.* (2002) studied the effect of estimation error in a near zero defect production process.

The average run length, defined as the number of plotted points until an out of control signal, is commonly used to measure the chart performance. One would want the average run length to be large at the in-control process average and any change in the process

average should be notified by a decrease in the average run length. However, due to the skewness of the exponential distribution, the average run length of the CQC chart first increases and then decreases when the process deteriorates. This problem can be solved by adjusting the limits as shown in section (5.2). Again this is done under the assumption that parameters are known or an accurate estimate is available.

The CQC chart proposed by Chan *et al.* (2000) plots the quantity produced before observing one defect. For any production process, the occurrence of defects is a random event. Under fairly general conditions, the occurrence process can be modeled by Poisson process. It then follows that the quality produced between the occurrence of two defects is exponential distributed with mean of $1/\lambda$. The control limits of CQC chart cam be calculated using Equation (2.12)

In case the actual parameter is not known then it needs to be estimated and the control limits can then be expressed as:

$$\begin{aligned} UCL &= \frac{\ln(1/\alpha)}{\hat{\lambda}} \\ CL &= \frac{\ln 2}{\hat{\lambda}} \\ LCL &= \frac{\ln[1/(1-\alpha/2)]}{\hat{\lambda}} \end{aligned} \tag{6.2}$$

These control limits are then used to plot the CQC chart.

Figure 6.1 shows a typical CQC chart. The data was simulated for λ = 0.0001. The continuous lines show the control limits calculated with the actual estimate (Equation (6.1)). Suppose that the actual defect rate was not known and a preliminary sample was used to estimate the parameter and it was found out to be 0.0002. From sampling point of view the situation can be seen as one in which 2 defects were observed in a sample of 10000. The dashed lines show the estimated control limits (Equation (6.2)).

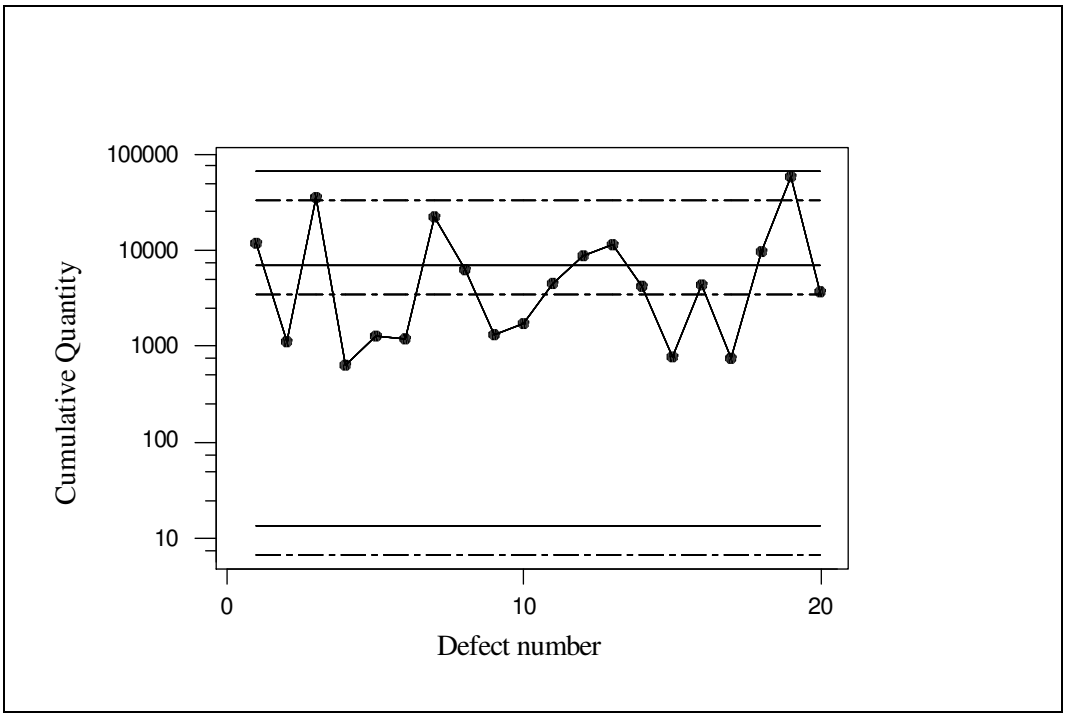

Figure 6.1 A CQC chart with actual (continuous) and estimated (dotted) control limits

As can be seen, when estimated control limits are used, two points fall above the control limits. According to the common practice a search for assignable cause(s) should be

performed and if any assignable cause is found then it should be removed, and in case there are no assignable causes then the point(s) should be treated as false alarm(s). Considerable amount of time and effort is used up by such search actions. Imagine stopping the production to conduct the search. The two points above the upper control limit point towards a 'possible' process improvement, but, in fact, they are due to incorrectly placed control limits. Thus, apart from the two alternatives, namely presence and absence of an assignable cause, there is also a third possibility that the parameter and hence the control limits may be inaccurate. Figure 6.2 shows the decision path when an out of control point is observed.

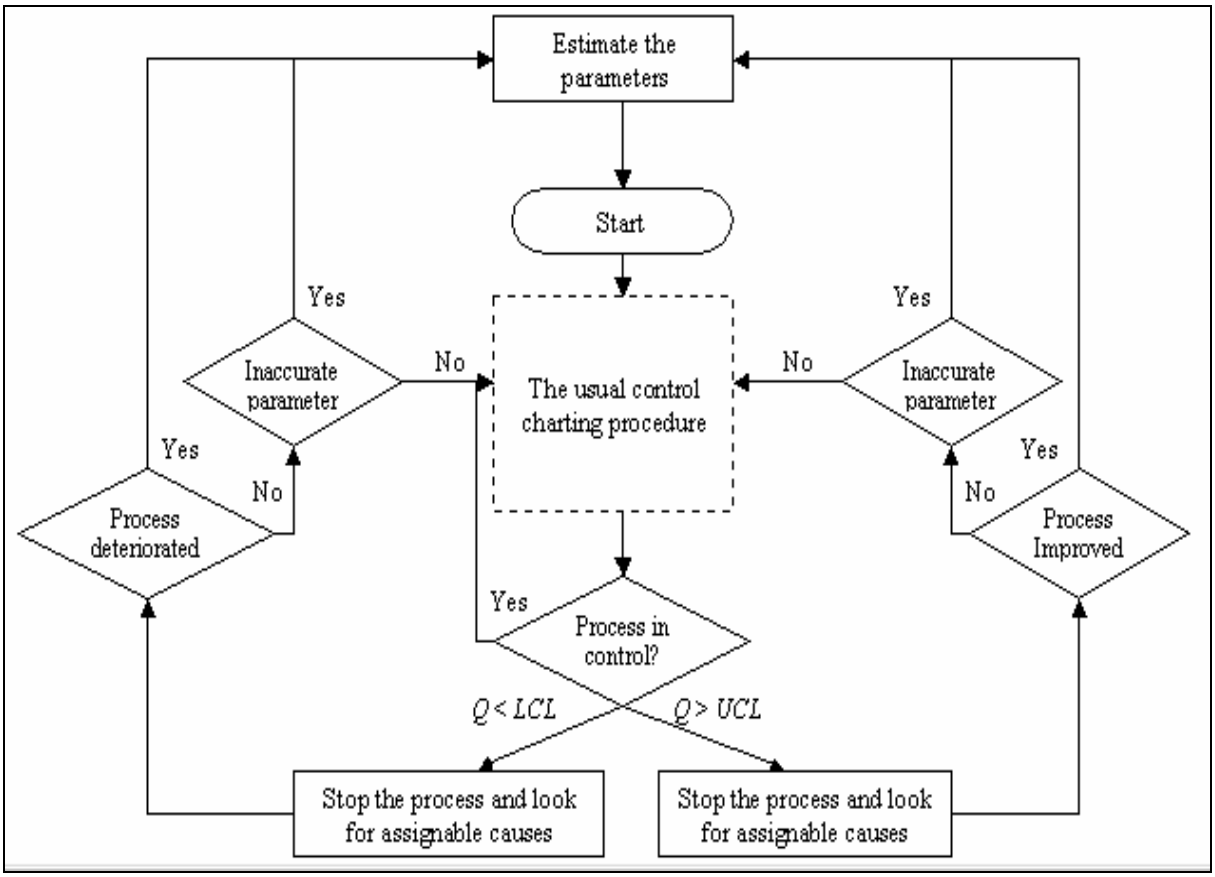

Figure 6.2 Decision path for an out of control situation

6.2. Estimated control limits and their effect on chart properties

As seen from the example in the previous section, the accurate estimation of the control limits is actually a problem of the accurate estimation of the parameter. In this section, first, the estimation of the parameter, λ, and then, the effect of estimation error on the chart properties are discussed.

6.2.1. Estimation of λ

Often the parameter λ is estimated by taking a preliminary sample. For example, when a sample of m items is taken and the total number of defects observed is x, then the process parameter can be calculated as

$$\hat{\lambda} = \frac{x}{m} \tag{6.3}$$

This value is treated as an estimate of the actual process parameter λ_0 and then it is used to compute the control limits, given by Equation (6.2). Thus, using Equation (6.2) and (6.3), the estimated control limits can be represented as:

$$\begin{aligned} UCL &= \frac{\ln(1/\alpha)}{x/m} \\ CL &= \frac{\ln 2}{x/m} \\ LCL &= \frac{\ln[1/(1-\alpha/2)]}{x/m} \end{aligned} \tag{6.4}$$

Using these control limits the control chart is then plotted and the decision about the statistical control of the process is made based on whether the plotted point falls within or outside the control limits.

6.2.2. Properties of the CQC chart with estimated parameter

Let Q_i be a cumulative quantity observed and assume that the process parameter has shifted from λ_0 to λ. Define the event E_i as,

$$E_i = \{\, Q_i > U\hat{C}L(X) \text{ or } Q_i < L\hat{C}L(X) \,\}$$

Then, $P(E_i)$ is the alarm rate (AR), which becomes the false alarm rate (FAR) when $\lambda = \lambda_0$. The AR can then be calculated by using the following conditional argument

$$P(E_i) = \sum_{x=0}^{\infty} P(E_i \mid X = x)P(X = x) = \sum_{x=0}^{\infty} P(E_i \mid X = x)\frac{e^{-m\lambda_0}(m\lambda_0)^x}{x!} \tag{6.5}$$

where,

$$P(E_i \mid X = x) = P\{\, Q_i > U\hat{C}L(X) \mid X = \mathrm{x}\} + P\{\, Q_i < L\hat{C}L(X) \mid X = \mathrm{x}\}$$

$$= (\alpha/2)^{m\lambda/x} + 1 - (1-\alpha/2)^{m\lambda/x}. \tag{6.6}$$

and Equation (6.5) can also be written as

$$P(E_i) = \sum_{x=1}^{\infty} P(E_i \mid X = x) \frac{e^{-m\lambda_0} (m\lambda_0)^x}{x!} + e^{-m\lambda_0} \tag{6.7}$$

All the events E_i are dependent on the same estimated control limits and unless the estimated limits are very close to the true limits, the false alarm probability can be far from the desired level. Due of this, the decision about the process, whether in-control or out of control, will not reflect the exact status of the process.

6.2.3. Zero defect samples

As mentioned before, the CQC chart is very effective in a high quality environment where the defect rate is quite small. In such a process it is very common that the preliminary sample taken contains no defects. On encountering such a problem the usual practice is to take another sample as no information is obtained from the previous sample. Due to this reason it would be wise that the first term obtained by expanding Equation (6.5), which is same as the last term in Equation (6.7), be omitted from the calculations for the alarm rate and future calculations. If that term is included in the calculations then it will give unusually high values of alarm rate (Yang *et al.* (2002a)). Equation (6.5) can then be written as:

$$P(E_i) = \sum_{x=1}^{\infty} P(E_i \mid X = x) \frac{e^{-m\lambda_0} (m\lambda_0)^x}{x!} \tag{6.8}$$

Table 6.1 provides the probability of obtaining zero defects in a sample of size *m* for different values of process average (λ_0).

$m \setminus \lambda_0$	0.00001	0.00005	0.0001	0.0002	0.0005	0.0008	0.001
100	0.999	0.99501	0.99005	0.9802	0.95123	0.92312	0.90484
200	0.998	0.99005	0.9802	0.96079	0.90484	0.85214	0.81873
500	0.99501	0.97531	0.95123	0.90484	0.7788	0.67032	0.60653
1000	0.99005	0.95123	0.90484	0.81873	0.60653	0.44933	0.36788
2000	0.9802	0.90484	0.81873	0.67032	0.36788	0.2019	0.13534
5000	0.95123	0.7788	0.60653	0.36788	0.08209	0.01832	0.00674
10000	0.90484	0.60653	0.36788	0.13534	0.00674	0.00034	0.00005
20000	0.81873	0.36788	0.13534	0.01832	0.00005	1.13E-07	2.06E-09
50000	0.60653	0.08209	0.00674	0.00005	1.39E-11	4.25E-18	1.93E-22
100000	0.36788	0.00674	0.00005	2.06E-09	1.93E-22	1.80E-35	3.72E-44
200000	0.13534	0.00005	2.06E-09	4.25E-18	3.72E-44	3.26E-70	1.38E-87
1000000	0.00005	1.93E-22	3.72E-44	1.38E-87	7.12E-218	3.67E-348	5.076E-435
2000000	2.06E-09	3.72E-44	1.38E-87	1.92E-174	5.08E-435	1.35E-695	2.58E-869
∞	0	0	0	0	0	0	0

Table 6.1 Probability of obtaining zero defect in a sample

It can be seen from the table that the probability value is very high for small sample size and low defect rate. This further strengthens the fact that if it is included in the calculations then it will lead towards unusually high alarm rates. The table also shows that the probability of obtaining zero defect approaches zero as the sample size becomes large.

6.2.4. The case when samples contain at least one defect

The alarm rate (AR) or the false alarm rate (FAR) can be calculated using Equation (6.8). Table 6.2 provides FAR values for different combinations of λ_0 and m, and Table 6.3 provides AR values when the process parameter is shifted from λ_0 = 0.0002. Table 6.2 shows that for a sample size of 100, the false alarm rate is quite small for small values of λ_0. This is due to the fact that for small values of m and λ_0 most of the times no defects will be observed. The possible solution is to take a substantial sample size so that there is sufficient possibility of occurrence of at least one defect. So for λ_0=0.00001 (a high yield process) a sample of around 100000 is required. In such a case the false alarm will decrease with increase in λ_0 for a fixed sample size and will decrease with increase in m for a fixed defect rate.

$m \setminus \lambda_0$	0.00001	0.00005	0.0001	0.0002	0.0005	0.0008	0.001
100	0.00099	0.00483	0.00932	0.01736	0.03521	0.04587	0.05012
200	0.00197	0.00932	0.01736	0.03019	0.05012	0.05426	0.05292
500	0.00483	0.02095	0.03521	0.05012	0.0493	0.03691	0.03089
1000	0.00932	0.03521	0.05012	0.05292	0.03089	0.02166	0.01864
2000	0.01736	0.05012	0.05292	0.03691	0.01864	0.01366	0.01187
5000	0.03521	0.0493	0.03089	0.01864	0.01038	0.00792	0.00698
10000	0.05012	0.03089	0.01864	0.01187	0.00698	0.00541	0.00487
20000	0.05292	0.01864	0.01187	0.00792	0.00487	0.00406	0.00379
50000	0.03089	0.01038	0.00698	0.00487	0.00357	0.00324	0.00314
100000	0.01864	0.00698	0.00487	0.00379	0.00314	0.00297	0.00292
200000	0.01187	0.00487	0.00379	0.00324	0.00292	0.00284	0.00281
1000000	0.00487	0.00314	0.00292	0.00281	0.00274	0.00273	0.00272
2000000	0.00379	0.00292	0.00281	0.00275	0.00272	0.00271	0.00271
∞	0.0027	0.0027	0.0027	0.0027	0.0027	0.0027	0.0027

Table 6.2 Values of FAR with Estimated Control Limits, $\alpha = 0.0027$

The same argument holds true for the case of AR, shown in Table 6.3. It can be noted from the table that for substantial sample size, the AR first decreases and then increases when the process deteriorates. This is due to the skewness of exponential distribution.

$m \setminus \lambda$	0.00001	0.00005	0.00008	0.0001	**0.0002**	0.0003	0.0004	0.0008	0.001
100	0.01967	0.01916	0.01879	0.01854	**0.01736**	0.01626	0.01522	0.01171	0.01027
200	0.0387	0.03673	0.03532	0.0344	**0.03019**	0.0265	0.02326	0.01382	0.01066
500	0.09215	0.08102	0.07358	0.06901	**0.05012**	0.03647	0.0266	0.00776	0.00431
1000	0.17025	0.1326	0.11007	0.09728	**0.05292**	0.0293	0.01659	0.00238	0.00119
2000	0.29273	0.18345	0.13045	0.10446	**0.03691**	0.01492	0.00693	0.00119	0.00099
5000	0.49281	0.19936	0.11101	0.07813	**0.01864**	0.00638	0.00316	0.00267	0.00328
10000	0.60217	0.19011	0.09593	0.06368	**0.01187**	0.00434	0.00329	0.00537	0.0067
20000	0.65818	0.18816	0.086	0.05334	**0.00792**	0.00359	0.00367	0.00696	0.00869
50000	0.69637	0.18863	0.07788	0.04472	**0.00487**	0.00262	0.00309	0.00608	0.0076
100000	0.70819	0.18984	0.0748	0.04124	**0.00379**	0.00231	0.00286	0.00569	0.00711
200000	0.71361	0.19079	0.07323	0.03937	**0.00324**	0.00218	0.00278	0.00553	0.00691
1000000	0.71772	0.19175	0.07199	0.03782	**0.00281**	0.00209	0.00271	0.00542	0.00677
2000000	0.71822	0.19189	0.07184	0.03762	**0.00275**	0.00208	0.00271	0.0054	0.00675
∞	0.71872	0.19202	0.07168	0.03742	**0.0027**	0.00207	0.0027	0.00539	0.00673

Table 6.3 Values of AR with Estimated Control Limits: $\alpha = 0.0027$, $\lambda_0 = 0.0002$

6.2.5. The effect of estimated parameter on the run length

As discussed earlier the control chart should be able to raise an alarm when the process average shifts in step. At the same time it should raise minimum false alarms when the process is in control. The average number of points plotted on the control chart until a plotted point falls outside the control limits is termed as the run length. This section discusses the effect of estimated parameter on the run length of the CQC chart.

Denote the run length by R and $P(E_i \mid X)$ defined in Equation (6.6) by $p(X)$. Following a conditional argument the unconditional distribution of R can be represented as

$$\begin{aligned} f_R(r;\lambda_0,\lambda) &= \sum_{x=1}^{\infty}\left[1-p(X)\right]^{r-1} p(X)P(X=x) \\ &= \sum_{x=1}^{\infty}\left[1-p(X)\right]^{r-1} p(X)\frac{e^{-m\lambda_0}(m\lambda_0)^x}{x!}. \end{aligned} \tag{6.9}$$

Due to the reasons mentioned in Section 6.2.3, the case $x = 0$ has been omitted from the Equation (6.9). The expected value of the run length, *i.e.* the average run length (ARL), and the standard deviation of the run length (SDRL) can be represented as:

$$ARL(\lambda_0,\lambda) = E_X[1/p(X)] \tag{6.10}$$

$$SDRL(\lambda_0,\lambda) = \sqrt{Var_X[1/p(X)] + E_X[(1-p(X))/p^2(X)]}, \tag{6.11}$$

The quantity $E_X[1/p(X)]$ and $E_X[1/p^2(X)]$ in Equations (10) and (11) can be calculated by using the distribution of X.

$$E_X[1/p(X)] = \sum_{x=1}^{\infty} \frac{1}{p(x)} \frac{e^{-m\lambda_0}(m\lambda_0)^x}{x!}$$
$$E_X[1/p^2(X)] = \sum_{x=1}^{\infty} \frac{1}{p^2(x)} \frac{e^{-m\lambda_0}(m\lambda_0)^x}{x!} \quad (6.12)$$

In case the parameter is known or an accurate estimate is available, the relationship between $SDRL_0$, the in control standard deviation of run length, and ARL_0, the in control average run length, takes the form:

$$SDRL_0(\lambda_0, \lambda) = \sqrt{ARL_0(ARL_0 - 1)} \quad (6.13)$$

In such case, for $\alpha = 0.0027$ and $\lambda = \lambda_0$, the $ARL_0 \cong SDRL_0 \cong 370$. When the control limits are estimated, a decision about how large the sample size should be, can be made on the basis of the above mentioned in control value of ARL and SDRL.

Table 6.4 shows some values of ARL and SDRL for fixed value of λ_0, when the control limits are estimated. The table shows the manner in which the estimated limits have an impact on the run length. As discussed in Section 6.2.4, the ARL and SDRL value for small sample sizes are not reliable. In general the estimated limits tend to decrease the ARL and the SDRL value from their usual value. Another impact of the dependence of events E_i is that SDRL is greater than ARL. This is also due to the geometric distribution of the run length. Yang *et al.* (2002a) have given an excellent explanation for this

behavior. The last row shows that for an infinitely large sample size, the in control ARL and SDRL value take the expected value of 370.

m \ λ	0.00001	0.00005	0.00008	0.0001	**0.0002**	0.0003	0.0004	0.0008	0.001
100	0.02	0.02	0.02	0.02	**0.02**	0.02	0.03	0.03	0.04
	0.14	0.15	0.15	0.15	**0.17**	0.18	0.2	0.28	0.33
200	0.04	0.04	0.04	0.04	**0.05**	0.06	0.07	0.11	0.15
	0.2	0.21	0.23	0.23	**0.28**	0.33	0.39	0.72	0.96
500	0.1	0.11	0.12	0.13	**0.18**	0.25	0.35	1.28	2.44
	0.31	0.37	0.43	0.46	**0.69**	1.01	1.45	5.69	11
1000	0.19	0.25	0.3	0.34	**0.65**	1.23	2.35	26.9	61.09
	0.43	0.61	0.78	0.91	**1.91**	3.83	7.51	89.1	202.86
2000	0.37	0.6	0.87	1.12	**3.96**	13.97	44.45	131.71	119.73
	0.57	1.13	1.77	2.36	**9.29**	34.15	110.54	312.62	271.85
5000	0.82	2.47	6	11.02	**141.81**	202.06	209.51	174.07	145.39
	0.8	3.71	10.35	20.11	**284.51**	368.5	328.67	286.33	245.32
10000	1.29	9.49	49.38	109.76	**217.31**	277.68	283.45	183.73	148.24
	1.03	17.5	109.48	250.05	**321.43**	366.14	366.22	255.68	208.38
20000	1.6	34.99	68.93	105.27	**277.52**	347.33	329.95	185.4	148.53
	1.37	138.2	184.89	227.48	**366.33**	398.27	379.91	226.13	181.29
50000	1.48	10.68	37.11	69.72	**326.28**	414.19	359.59	185.56	148.55
	1.21	44.67	108.77	163.87	**391.59**	434.49	385.49	202.71	162.18
100000	1.42	6.48	21.7	45.55	**348.23**	445.87	366.91	185.56	148.55
	0.81	10.73	46.57	93.1	**398.62**	455.29	381.9	194.09	155.27
200000	1.41	5.68	16.72	34.18	**360.56**	464.03	369.21	185.56	148.55
	0.76	5.84	21.84	49.68	**396.71**	468.54	377.16	189.63	151.7
1000000	1.39	5.29	14.39	27.89	**369.32**	478.77	370.22	185.56	148.55
	0.74	4.85	14.44	29.03	**380.86**	479.46	371.52	185.98	148.79
2000000	1.39	5.25	14.16	27.29	**369.98**	480.5	370.3	185.56	148.55
	0.74	4.76	13.92	27.55	**376.06**	480.62	370.7	185.52	148.42
∞	1.39	5.21	13.95	26.73	**370.37**	482.18	370.37	185.56	148.55
	0.74	4.68	13.44	26.22	**369.87**	481.68	369.87	185.06	148.05

Table 6.4 Values of ARL (upper entry) and SDRL (lower entry) with Estimated Control Limits, $\lambda_0 = 0.0002$

6.3. The optimal limits of the CQC chart with estimated parameter

Table 6.4 proves the undesirable behavior of the ARL of CQC chart, *i.e.* the ARL first increases and then decreases as the process deteriorates. To obtain the optimal ARL

performance we would once again follow the optimizing procedure discussed in previous chapter to get the *estimated adjusted control limits* as:

$$\hat{LCL}_a(X) = -\frac{\ln(1-\alpha/2)}{\hat{\lambda}} \frac{\ln\left[\frac{\ln(\alpha/2)}{\ln(1-\alpha/2}\right]}{\ln\left(\frac{1-\alpha/2}{\alpha/2}\right)},$$
$$\hat{UCL}_a(X) = -\frac{\ln(\alpha/2)}{\hat{\lambda}} \frac{\ln\left[\frac{\ln(\alpha/2)}{\ln(1-\alpha/2}\right]}{\ln\left(\frac{1-\alpha/2}{\alpha/2}\right)} \tag{6.14}$$

By replacing the old estimated limits by the estimated adjusted limits the FAR, AR, ARL and SDRL can be easily tabulated. Tables 6.5, 6.6 show the FAR and AR, respectively, when the estimated adjusted control limits are used.

Comparing the values in Table 6.2 and Table 6.5 it can be seen that for a fixed λ_0, the false alarm probability approaches the desired value of 0.0027 much faster when the adjusted control limits are used. For a sample size of 100000 and process average of 0.0001, use of old control limits gives a false alarm of 0.0049 which is around 81% more than the desired level of 0.0027. For the same parameters the use of adjusted control limits results in a false alarm of 0.0028, which is around 44% more than the false alarm probability of 0.00194 for known parameters. This shows that the use of adjusted control limits gives a better performance. Comparing Table 6.3 and Table 6.6, it can be seen that

the alarm rate increases on either side (provided the sample size is large enough) when the adjusted limits are used.

$m \setminus \lambda_0$	0.00001	0.00005	0.0001	0.0002	0.0005	0.0008
100	0.00099	0.00478	0.00914	0.01672	0.03208	0.0396
200	0.00196	0.00914	0.01672	0.02802	0.04178	0.04096
500	0.00478	0.01999	0.03208	0.04178	0.03285	0.02161
1000	0.00914	0.03208	0.04178	0.03765	0.01738	0.01158
2000	0.01672	0.04178	0.03765	0.02161	0.0097	0.0069
5000	0.03208	0.03285	0.01738	0.0097	0.00541	0.00434
10000	0.04178	0.01738	0.0097	0.00606	0.00389	0.0031
20000	0.03765	0.0097	0.00606	0.00434	0.00283	0.00246
50000	0.01738	0.00541	0.00389	0.00283	0.00226	0.00213
100000	0.0097	0.00389	0.00283	0.00235	0.00209	0.00203
200000	0.00606	0.00283	0.00235	0.00213	0.00202	0.00199
1000000	0.00283	0.00209	0.00202	0.00198	0.00195	0.00195
2000000	0.00235	0.00202	0.00198	0.00196	0.00195	0.00194
∞	0.00194	0.00194	0.00194	0.00194	0.00194	0.00194

Table 6.5 Values of FAR with estimated adjusted control limits, $\alpha = 0.0027$.

$m \setminus \lambda$	0.00001	0.00005	0.00008	0.0001	**0.0002**	0.0003	0.0004	0.0008
100	0.01963	0.01898	0.01851	0.0182	**0.01672**	0.01537	0.01412	0.01008
200	0.03856	0.03605	0.03428	0.03314	**0.02802**	0.02369	0.02004	0.01028
500	0.0913	0.07738	0.06837	0.06297	**0.04178**	0.02781	0.01859	0.00397
1000	0.16722	0.12132	0.09558	0.08161	**0.03765**	0.01796	0.00896	0.00109
2000	0.28299	0.15577	0.10121	0.07661	**0.02161**	0.00767	0.00339	0.00099
5000	0.4597	0.14941	0.07445	0.04945	**0.0097**	0.0034	0.00229	0.00337
10000	0.54661	0.13551	0.06018	0.03712	**0.00606**	0.00332	0.0036	0.00689
20000	0.59317	0.12812	0.04993	0.0284	**0.00434**	0.0036	0.00451	0.00893
50000	0.63011	0.12272	0.04139	0.02126	**0.00283**	0.00299	0.00392	0.00782
100000	0.6425	0.12111	0.03793	0.01839	**0.00235**	0.00277	0.00366	0.00731
200000	0.64836	0.12046	0.03607	0.01682	**0.00213**	0.00268	0.00356	0.00711
1000000	0.65286	0.12004	0.03451	0.0155	**0.00198**	0.00262	0.00349	0.00696
2000000	0.65341	0.12	0.03431	0.01533	**0.00196**	0.00261	0.00348	0.00694
∞	0.65396	0.11996	0.03411	0.01515	**0.00194**	0.00261	0.00347	0.00692

Table 6.6 Values of AR with estimated adjusted control limits: $\alpha = 0.0027$, λ_0=0.0002

Table 6.7 shows some values of ARL (upper entry) and SDRL (lower entry) when the adjusted limits are used in place of the old control limits. As can been seen the ARL decreases when the process average shifts unlike previously (see Table 6.4) where the ARL first increases and then decreases when the process deteriorates.

$m \setminus \lambda$	0.00001	0.00005	0.00008	0.0001	**0.0002**	0.0003	0.0004	0.0008
50000	1.68	20.27	75.44	136.39	**405.63**	369.48	287.32	144.41
	2.32	71.83	172.13	245.76	**433.18**	394.66	313	157.65
100000	1.58	11.57	50.25	108.52	**446.79**	378.87	288.13	144.41
	1.01	23.15	101.24	185.42	**459.39**	393.62	301.5	150.94
200000	1.55	9.48	37.78	87.45	**475.49**	382.08	288.28	144.41
	0.94	10.97	55.39	127.77	**480.12**	390.05	294.86	147.47
500000	1.54	8.73	32.15	73.95	**497.58**	383.32	288.31	144.41
	0.91	8.71	36.11	86.93	**498.24**	386.41	290.67	145.34
1000000	1.53	8.52	30.65	69.8	**506.17**	383.6	288.32	144.41
	0.91	8.23	32.04	75.26	**506**	384.93	289.25	144.63
2000000	1.53	8.43	29.97	67.85	**510.74**	383.73	288.32	144.41
	0.9	8.02	30.34	70.13	**510.33**	384.15	288.54	144.27
∞	1.53	8.34	29.32	65.99	**515.53**	383.84	288.32	144.41
	0.9	7.82	28.81	65.49	**515.03**	383.34	287.82	143.91

Table 6.7 Values of ARL (upper entry) and SDRL (lower entry) with Estimated (and adjusted) Control Limits, $\lambda_0 = 0.0002$

Chapter 7

Monitoring Quality Characteristics following Weibull Distribution

7.1. Weibull distribution and the t chart

Most of the studies assume that time-between events is exponentially distributed. An important assumption when exponential distribution is used is that the event occurrence rate is constant. In reliability applications, this implies that the items have no aging property. This assumption is usually violated in reality. Due to wear and tear and other usage condition, items usually have an increasing failure rate.

To be able to monitor processes for which the exponential assumption is violated, Weibull distribution is a good alternative and it is a simple generalization of the exponential distribution. This flexibility and its reasonableness have made Weibull distribution probably the most useful distribution model in reliability analysis and it has been widely used by various authors to model the failure times. There are a couple of papers where the authors have indicated the use of Weibull distribution for process monitoring in reliability (Banjevic *et al.* 2001; Sun *et al.* 2001 and Xie et al. 2002), but no detailed analysis is carried out.

Related to the use of Weibull distribution in statistical process control, Zhang *et al.* (1997) studied the economic design of X (bar) chart for monitoring systems with Weibull in-control times with the main objective being the economic performance. Ramalhoto and Morais (1999) studied the performance of a control chart for the scale parameter of the three-parameter Weibull Distribution where the location and the shape parameters are assumed to be known. Earlier, Nelson (1979) considered Weibull distribution for median

and range charge, assuming a fixed subgroup size. The use of Weibull distribution was also investigated in Johnson (1966). The cumulative distribution function of a Weibull random variable, T is given as

$$F(t) = 1 - \exp\left\{-\left(\frac{t}{\theta}\right)^{\beta}\right\},\ t \geq 0 \tag{7.1}$$

where $\theta > 0$ and $\beta > 0$ are the scale parameter and shape parameter, respectively.

Weibull distribution is a generalization of exponential distribution. Although exponential distribution has been widely used for time-between-event, Weibull distribution is more suitable as it is more flexible and is able to deal with different types of aging phenomenon. This is common, for example, when dealing with equipment failures. The main characteristics of Weibull distribution is its hazard function given by

$$h(t) = \frac{f(t)}{1 - F(t)} = \frac{\beta}{\theta}\left(\frac{t}{\theta}\right)^{\beta-1},\ t \geq 0 \tag{7.2}$$

and it can be seen that the hazard function is constant when $\beta = 1$ and increasing or decreasing according to whether $\beta > 1$ or $\beta < 1$.

7.1.1. Control limits for Weibull time-between-event chart

A process can be monitored with a control chart and the time-between events can be used. A control chart for process monitoring of time-between-event, or t chart, should have exact probability limits due to the skewness of the Weibull Distribution. Solving Equation (7.1) with respective probabilities, the control limits can be calculated as:

$$\begin{aligned} UCL &= \theta_0 \left[\ln\left(\frac{2}{\alpha}\right) \right]^{1/\beta_0} \\ CL &= \theta_0 \left[\ln(2)\right]^{1/\beta_0} \\ LCL &= \theta_0 \left[\ln\left(\frac{2}{2-\alpha}\right) \right]^{1/\beta_0} \end{aligned} \tag{7.3}$$

where α is the acceptable false alarm probability, and β_0 and θ_0 are the in-control shape and scale parameter, respectively. In the following, the false alarm probability is fixed at α = 0.0027 which is equivalent to three sigma limits for X-bar chart under normal distribution assumption. Some control limits for different values of β_0 are shown in Table 7.1. The scale parameter, θ_0, is fixed at 10. It should be noted that for the shown values of β_0, the control limits can be easily calculated for any value of the scale parameter θ_0 by multiplying the control limits, corresponding to the β_0, by a factor θ_0 / 10.

β_0	UCL	CL	LCL
0.1	1.59E+09	0.25601	2.02E-28
0.2	125960.8	1.60003	4.50E-14
0.3	5413.651	2.94726	2.73E-09
0.4	1122.323	4.00003	6.71E-07
0.5	436.6105	4.80453	1.8E-05
0.6	232.6725	5.42887	0.00017
0.7	148.4212	5.9239	0.0008
0.8	105.9397	6.32458	0.00259
0.9	81.50109	6.65487	0.00648
1	66.07651	6.93147	0.01351
1.1	55.65412	7.16631	0.02463
1.2	48.23614	7.36808	0.04063
1.3	42.73714	7.54324	0.06206
1.4	38.52547	7.69669	0.08922
1.5	35.2126	7.8322	0.1222
1.6	32.54838	7.95272	0.16093
1.7	30.36551	8.06061	0.20518
1.8	28.5484	8.15774	0.25463
1.9	27.01492	8.24563	0.30889
2	25.70535	8.32555	0.36755
2.1	24.57529	8.39852	0.43016
2.2	23.59113	8.46541	0.49629
2.3	22.727	8.52695	0.56552
2.4	21.96273	8.58375	0.63742
2.5	21.28231	8.63635	0.71162
2.6	20.67296	8.68518	0.78776
2.7	20.12432	8.73065	0.8655
2.8	19.62791	8.77308	0.94455
2.9	19.17674	8.81277	1.02462
3	18.76502	8.84997	1.10546
3.1	18.38787	8.88492	1.18685
3.2	18.04117	8.9178	1.26859
3.3	17.72144	8.94881	1.3505
3.4	17.4257	8.97809	1.43241
3.5	17.15138	9.00578	1.51419
3.6	16.89627	9.03202	1.5957
3.7	16.65844	9.05691	1.67685
3.8	16.43622	9.08055	1.75753
3.9	16.22813	9.10303	1.83765
4	16.03289	9.12444	1.91715

Table 7.1 Control Limits of a control chart based on two-parameter Weibull distribution with $\theta = 10$ and $\alpha = 0.0027$

A point plotting above the upper control limit may be due to an improvement in the reliability. If there is an assignable cause it should be maintained and the control limits should be revised. If a point falls below the lower control limit, the user should look for the assignable cause and should remove it. In either case if an assignable cause is not found, the point should be treated as a false alarm.

7.1.2. An example

An example is presented here to illustrate the charting procedure of the Weibull t chart. Some problems are also highlighted. Since there are two parameters for Weibull distribution, it is important to study how the control chart reacts when each of the parameters is changed. Table 7.2 shows the data points simulated for different parameter values. The first 50 points were simulated β = 1.3, θ = 10. The second 50 points were simulated for β = 1.3, θ = 20. While the third is for β = 2; θ = 10. These two cases are the typical and interesting ones and hence used here.

The first 50 values are assumed to come from the in-control process with parameters β_0 = 1.3, θ_0 = 10. The control limits of the Weibull t chart can be calculated by using Equation (7.3) and are found out to be, LCL = 0.062, CL = 7.54, and UCL = 42.74. Figure 7.1 depicts the scenario when the scale parameter is increased and Figure 7.2 is a t chart for the case when the shape parameter is increased.

$\beta = 1.3,\ \theta = 10$									
29.24	0.75	15.43	2.18	14.18	4.25	12.07	8.4	4.16	3.27
3.99	3.37	15.22	11.11	17.46	14.83	5.87	8.64	11.32	2.62
4.42	2.65	7.44	6.96	4.67	2.18	10.75	5.03	7.84	16.3
22.72	13.96	3.75	10.16	11.14	8.79	6.29	24.25	14.8	13.11
0.65	5.89	2.05	9.31	12.45	3.6	9.86	2.24	6.35	1.83
$\beta = 1.3,\ \theta = 20$									
48.83	28.69	39.02	7.81	0.73	0.65	21.38	19.31	9.89	13.18
7.46	21.09	15.74	22.21	6.7	8.01	11.92	3.09	14.38	1.37
27.16	46.69	2.14	41.81	29.94	5.02	4.82	21.7	28.97	4.71
14.47	2.22	14.16	23.09	7.37	11.88	47.2	0.92	1.18	4.55
16.93	43.14	16.68	3.7	27.45	59.04	14.85	5.75	50.24	31.08
$\beta = 2,\ \theta = 10$									
15.25	15.52	4.13	13.26	12.94	6.42	7.26	1.63	12.99	15.31
3.14	5.89	13.66	11.29	17.01	3.94	7.16	8.73	3.87	6.15
4.67	4.89	3.81	2.85	5.89	6.01	19.49	5.37	8.1	18.3
9.16	5.04	10.47	2.51	8.01	16.34	13.11	6.45	8.68	12.43
7.38	12.82	7.03	7.99	5.04	9.49	5.42	7.07	16.33	5.86

Table 7.2 Time between failures (read across for consecutive data points)

Figure 7.1 and Figure 7.2 are typical cases of using Weibull t chart to detect process shift. When the scale parameter is reduced, the chart behavior is similar. However, for the case when the shape parameter is increased, the chart seems to be insensitive because of the reduced variability. We do not have this problem when the shape parameter is decreased as the variability is increased and there will be a higher chance for a point to fall outside of the control limits. Here we discuss this based on the property of Weibull distribution. Note that the exponential distribution is a special case of Weibull distribution, and since the shape parameter is equal to one, no change of this parameter has been investigated previously.

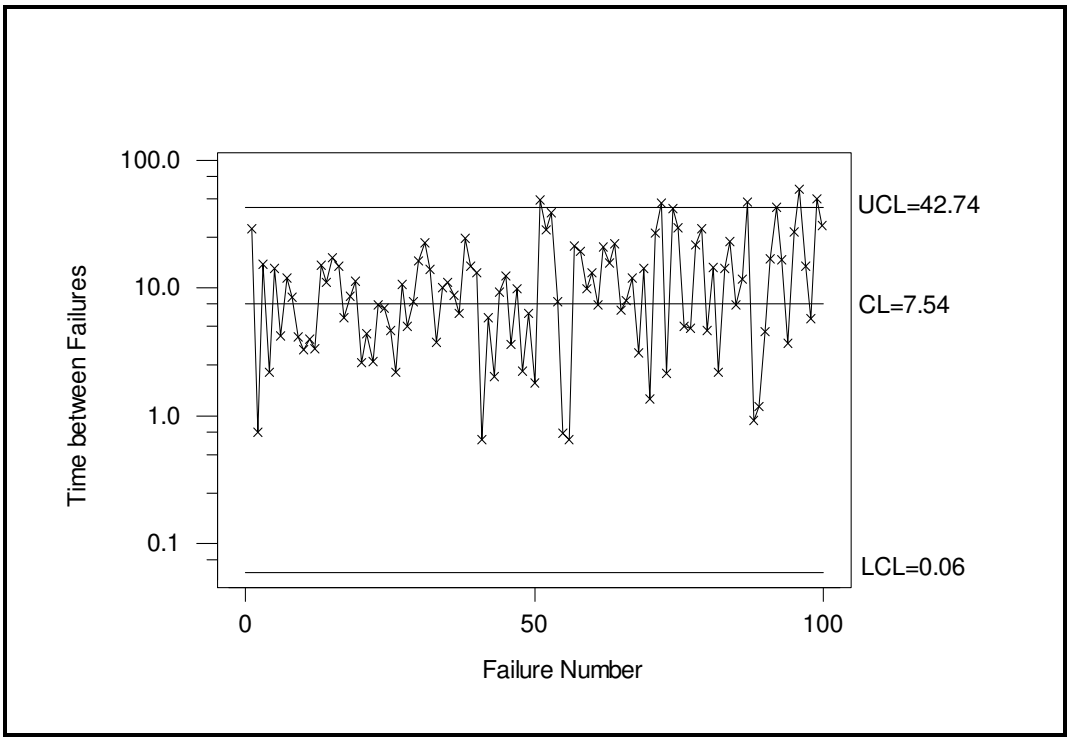

Figure 7.1 Weibull t chart for shift from $\theta = 10$ to $\theta = 20$ (with $\beta = 1.3$)

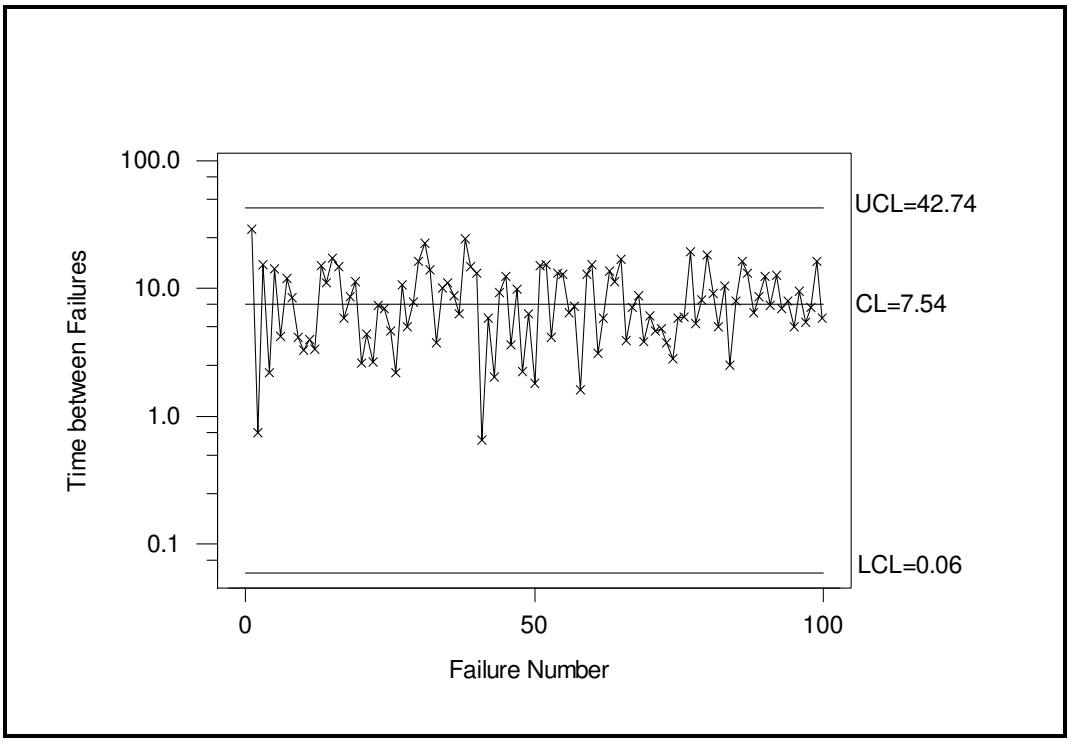

Figure 7.2 Weibull t chart for shift from $\beta = 1.3$ to $\beta = 2$

Note that for Weibull distribution, the mean and variance are given by equations (4.5) and (4.6) respectively.

It can be seen that the mean and the variance are strongly affected by the scale and shape parameter. In fact, it is decreasing when β increases. It is known that $\sigma^2 \approx \pi^2\theta^2/(6\beta^2)$ when the shape parameter is large, McEwen and Parresol (1991). When the shape parameter increases, the variance reduces significantly.

Hence it is expected that the Weibull t chart is able to detect the change in the scale parameter effectively, while it is insensitive to the increase in the shape parameter. We will investigate this in detail in the next section.

7.2. The chart properties

The Type II error, *i.e.* the probability of not detecting the shift in the following observation when the process has shifted, for the Weibull t chart can be calculated as:

$$P(Type\ II\ error) = F(UCL) - F(LCL) = \exp\left\{-\left(\frac{LCL}{\theta}\right)^{\beta}\right\} - \exp\left\{-\left(\frac{UCL}{\theta}\right)^{\beta}\right\} \quad (7.4)$$

The average run length can then be calculated as:

$$ARL = \frac{1}{1 - P(Type\ II\ error)} = \frac{1}{1 + \exp\left\{-\left(\frac{UCL}{\theta}\right)^{\beta}\right\} - \exp\left\{-\left(\frac{LCL}{\theta}\right)^{\beta}\right\}} \qquad (7.5)$$

The average run length property of for the control chart based on Weibull distribution can be studied in the same way as for other Shewhart charts. However, since there are two parameters in this case, a change in ARL may mean a change in one or two or both the parameters.

This section illustrates how the change in the parameters affect the average run length of the control chart based on Weibull distribution. As discussed before there are three ways in which the parameters can change and they are investigated in the following.

7.2.1. Case 1: Change in the scale parameter

Weibull distribution contains two parameters; a change in any of them could cause an out-of-control signal. Since the scale parameter is usually related to operating condition, the scale parameter is likely to change because of assignable causes. Figure 7.3 shows some ARL curves for a control chart based on two-parameter Weibull distribution when there is a change in only the scale parameter, with the in-control $\theta_0 = 10$.

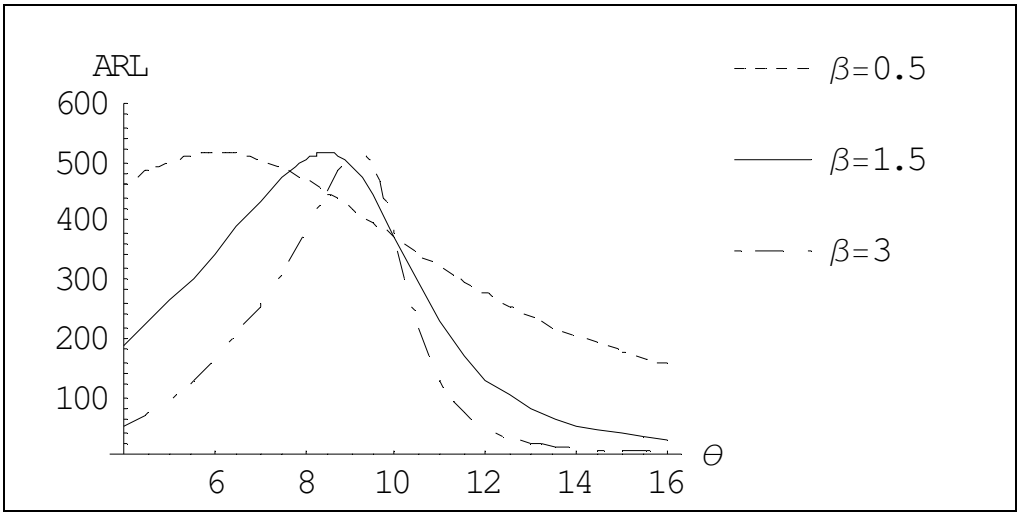

Figure 7.3 Some ARL curves with the in-control $\theta_0 = 10$

The figure shows that the ARL decreases when the scale parameter increases. However, it is interesting to note that the same is not true for a decrease in scale parameter. When the scale parameter decreases the ARL first increases and then decreases. This is due to the skewness of the Weibull distribution.

In fact, this happens also for the case of exponential chart which is a special case of the Weibull t chart. Only when the Weibull shape parameter is large, the parameter at which the maximum of the ARL will occur is close to the in-control value. As it is known, Weibull distribution can be well estimated by Normal distribution when the shape parameter is between 3-4 and when the shape parameter is larger, the variance will be very small, and hence the difference from the in-control value will be small.

7.2.2. Case 2: Change in the shape parameter

Even though the scale parameter is more likely to change but sometimes the shape parameter can also change. Figure 7.4 shows some Operation Characteristic (OC) curves when the shape parameter changes.

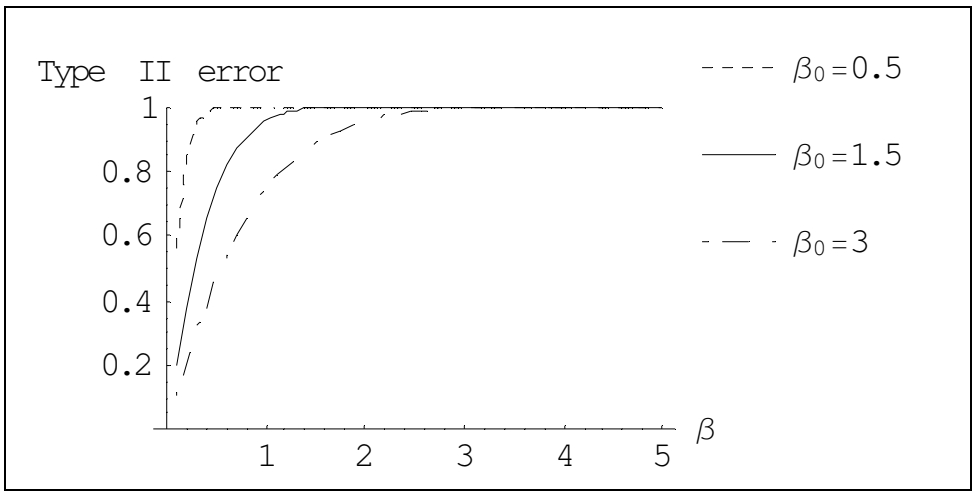

Figure 7.4 OC curves when the shape parameter increases

When the shape parameter decreases, the Type II error also decreases resulting in a decrease in the ARL and a control chart will be able to detect the decrease in the shape parameter. As the shape parameter increases, the probability of a point plotting within the control limits increases significantly and for large shifts in the process parameters, the probability approaches one. Thus the time until a point falls outside the control limits will be very long. As explained before, when the shape parameter increases, the variability is

reduced and more points will actually fall within the limits. Hence the Weibull t chart is not able to detect the increase in the shape parameter.

7.2.3. Case 3: Change in both the shape and the scale parameter

The third case, though not so common, is a change in both the parameters. Figure 7.5 shows the ARL curves when both the scale as well as the shape parameter changes.

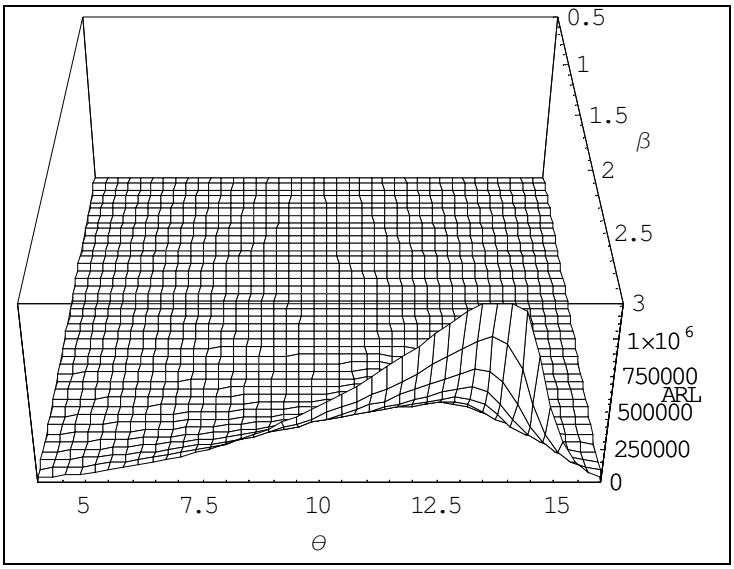

Figure 7.5 The ARL curves when both the parameters change with in-control $\theta_0 = 10$, $\beta_0 = 1.5$

The figures show that the shape parameter has the predominant effect on the ARL and it is impossible to detect increase in the shape parameter with the t chart in this case and other chart will be needed to monitor this. An increase in shape parameter increases the ARL no matter whether the scale parameter increases or decreases. This can be explained again by the fact that when the shape parameter is increased, the variability is reduced.

However, a change in the shape parameter is rare as it usually depends on intrinsic material property although it is an important aging parameter.

7.2.4. Comparison with Weibull CUSUM chart

The CUSUM charts are known to be quite sensitive to small shifts in a process. Many researchers have studied the properties and charting procedures of the time-between-events CUSUM, see Lucas (1985) and Gan (1992). If X_1, X_2,… be the inter-arrival times then the time-between-events CUSUM for detecting an increase or decrease in the inter-arrival times can be respectively defined as

$$S_i^+ = \max\{S_{i-1}^+ + (X_i - k)\}$$
$$S_i^- = \min\{S_{i-1}^- + (X_i - k)\}$$

where, k is the pre-chosen parameter. The control limits are denoted by h and the decision on the statistical control of the process is taken depending on whether $S_t^- \leq -h$ or $S_t^+ \geq h$. Most of the research on the time-between-events CUSUM assumes that the inter-arrival times follow exponential distribution. Since Weibull distribution is a generalization of the exponential and can model increasing, decreasing as well as constant failure rates, it would be interesting to see the performance of the time-between-events (Weibull) CUSUM scheme when the shape parameter changes, more specifically when there is an increase in the shape parameter.

The average run length calculation for a CUSUM scheme is comparatively more difficult than that for a Shewhart chart or, as a matter of fact, the Weibull t chart presented in this chapter. Vardeman and Ray (1985) obtained the exact expressions for the ARLs of CUSUM schemes when the inter-arrival times follow exponential distribution. Gan (1992) obtained the probability function of the run length, the ARLs, the standard deviation of the run length (SDRL) and the run length percentiles of exponential CUSUM schemes by solving the integral equations. However in this chapter we follow the Markov chain approach of Brook and Evans (1972) which gives approximate but quite accurate results. The results were obtained using 41 states and were compared with those obtained by Gan (1992) for shape parameter = 1 (exponential distribution) and no substantial difference was found. When the shape parameter increases, the mean of the Weibull distribution decreases and a lower Weibull CUSUM chart should be employed. The calculated average run lengths for the lower CUSUM scheme are shown in Table 7.3. The first row values are similar to those, except for $h = 6.506$ and $k = 0.8$, obtained by Gan (1992) for the case of exponential distribution.

It is evident from the table that the ARLs increase with an increase in shape parameter. So even the use of the CUSUM procedure does not help us detect the increase in shape parameter.

β	$h = 0, k =$ 0.002	$h = 0.737,\ k = 0.3$	$h = 1.905, k = 0.5$	$h = 4.267, k =$ 0.7	$h = 6.506, k$ = 0.8
1	500.50	500.55	500.98	500.72	481.33
1.1	931.32	940.19	850.49	692.67	561.85
1.2	1733.36	1818.88	1499.70	985.03	665.18
1.3	3226.48	3610.96	2743.74	1444.25	800.85
1.4	6006.12	7331.17	5199.43	2188.51	982.95
1.5	11180.84	15173.47	10184.46	3433.81	1232.87
1.6	20814.33	31925.55	20572.20	5585.53	1583.80
1.7	38748.47	68119.29	42749.51	9425.26	2088.45
1.8	72135.50	147082.88	91167.27	16500.83	2832.55
1.9	134290.29	320796.38	199061.53	29959.52	3958.82
2	250000.50	705674.39	444030.50	56369.46	5710.74
2.1	465411.89	1563582.50	1009754.28	109791.07	8513.89
2.2	866431.55	3485781.63	2336496.43	221078.10	13130.81
2.3	1612988.03	7811569.33	5491608.87	459579.54	20962.56
2.4	3002811.59	17583043.64	13089569.47	984821.53	34648.91
2.5	5590170.44	39726443.22	31594618.20	2172032.22	59290.46
3	125000000.07	2433113007.03	2998712632.35	165595171.05	1432836.49
3.5	2795084600.02	154851325281.86	335720509259.21	20934511413.92	72759159.68

Table 7.3 ARLs of the lower Weibull CUSUM for $\theta = 1$.

7.3. Individual chart with Weibull distribution

It is possible to directly plot the observation and use individual chart to monitor the process. However, before plotting the I chart, the Weibull data should be transformed to normal. There are different approaches to transform Weibull distribution to near normality. Yang *et al.* (2002b) discussed some transformation methods. The power transformation by Box and Cox (1964) is very suitable. A simple power transformation,

i.e. $X(\lambda) = X^{\lambda}$, where X is a Weibull random variable, can be used. Hernandez and Johnson (1980) have shown that the value of λ can be calculated as:

$$\lambda = 0.2654\beta \tag{7.6}$$

where β is the shape parameter of the Weibull distribution. The transformation method, thus, requires only an estimation of the shape parameter, which is relatively a simple task. It can be noted that for exponential distribution, $\lambda = 0.2654$ can be used as suggested in Nelson (1994). Kittlitz (1999) also proposed the double square root transformation for transforming exponentially distributed data. Some general discussion can also be found in Chou (1998).

For calculating the control limits of the I chart, though we can calculate the standard deviation of the transformed data, we do not use it for calculating the limits because the skewness and kurtosis of the transformed data departs slightly from the values 0 and 3 respectively, see Kittlitz (1999). As a result, most of the time the use of standard deviation calculated from the data will give a wider set of control limits. Alternatively the control limits of the I chart can be calculated by transforming the control limits obtained for the t chart. Thus the control limits of the I chart will be given by:

$$UCL_I = \left[\theta_0 \left[\ln\left(\frac{2}{\alpha} \right) \right]^{1/\beta_0} \right]^{0.2654\beta_0}$$

$$CL_I = \left[\theta_0 \left[\ln(2) \right]^{1/\beta_0} \right]^{0.2654\beta_0} \tag{7.7}$$

$$LCL_I = \left[\theta_0 \left[\ln\left(\frac{2}{2-\alpha} \right) \right]^{1/\beta_0} \right]^{0.2654\beta_0}$$

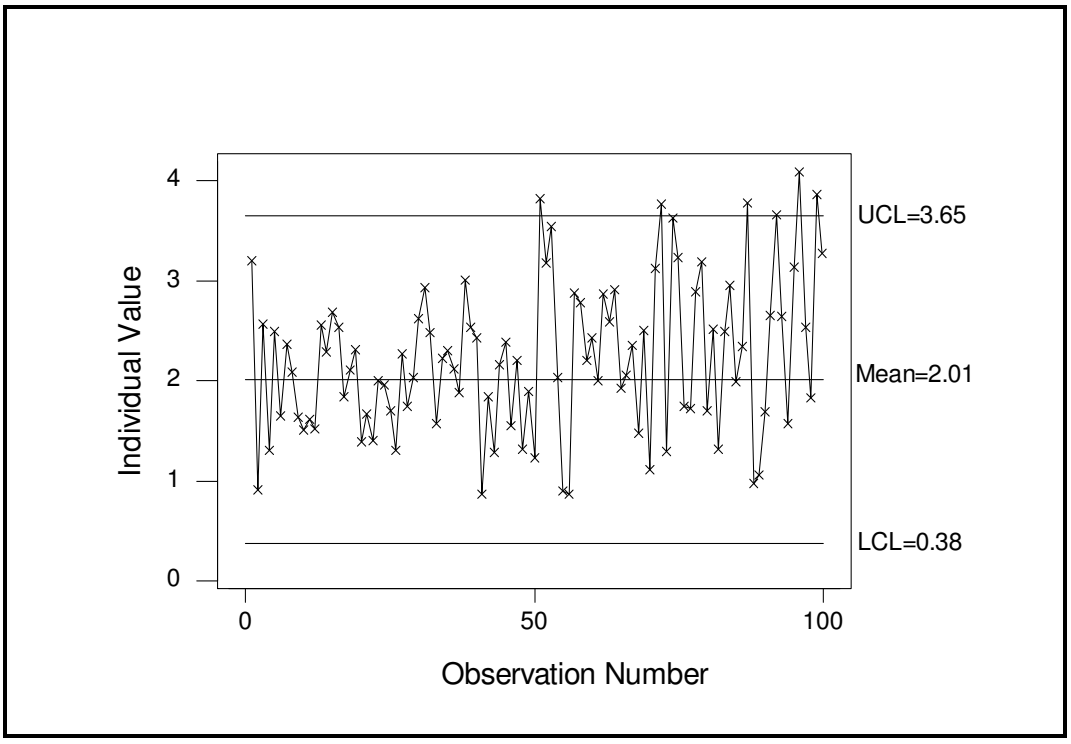

Figure 7.6 I chart for shift from $\theta = 10$ to $\theta = 20$

The individual chart and a standard EWMA chart are shown in Figures 7.6-7.7. There are quite a few points above the upper control limit, which is an indication that the process parameter has changed. Such a situation should be then followed by a search and the

causes of the improvement should be maintained and a new control chart should then be started with revised control limits.

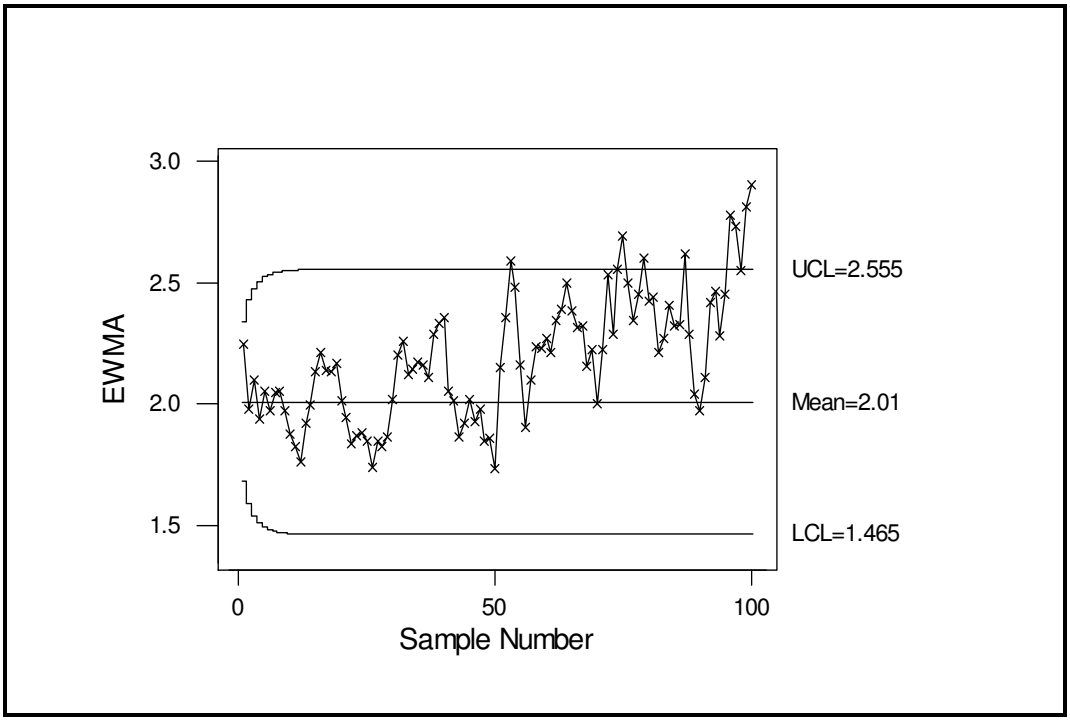

Figure 7.7 EWMA chart for shift from $\theta = 10$ to $\theta = 20$

7.4. Maximizing ARL for fixed in-control state

As mentioned before, and also evident from Figure 7.3, the maximum ARL value is reached at a value of θ different from the in-control value. In fact, by taking the derivative of ARL with respect to θ and setting it to be zero, the value of θ at which ARL will be maximum can be shown to be:

$$\theta^* = \theta_0 \left[\frac{\ln\left\{ \frac{\ln(2/\alpha)}{\ln(2/(2-\alpha))} \right\}}{\ln(2/\alpha) - \ln(2/(2-\alpha))} \right]^{1/\beta} \tag{7.8}$$

It is also possible to set the control limits so that the maximum ARL occurs at the specified in-control value of the scale parameter. This can be done by equating Equation (7.8) in place of θ_0 in Equation (7.3) to obtain the adjusted control limits as follows.

$$LCL_a = \theta_0 \left[\frac{\ln\left\{ \frac{\ln(2/\alpha)}{\ln(2/(2-\alpha))} \right\}}{\ln(2/\alpha) - \ln(2/(2-\alpha))} \right]^{1/\beta} \left[\ln\left(\frac{2}{2-\alpha} \right) \right]^{1/\beta}$$

$$CL_a = \theta_0 \left[\frac{\ln\left\{ \frac{\ln(2/\alpha)}{\ln(2/(2-\alpha))} \right\}}{\ln(2/\alpha) - \ln(2/(2-\alpha))} \right]^{1/\beta} \left[\ln(2) \right]^{1/\beta} \tag{7.9}$$

$$UCL_a = \theta_0 \left[\frac{\ln\left\{ \frac{\ln(2/\alpha)}{\ln(2/(2-\alpha))} \right\}}{\ln(2/\alpha) - \ln(2/(2-\alpha))} \right]^{1/\beta} \left[\ln\left(\frac{2}{\alpha} \right) \right]^{1/\beta}$$

When these adjusted control limits replace the old control limits in Equation (7.5), the resulting ARL will reach the maxima at the in-control θ_0. Figure 7.8 shows some ARL

curves, when only the shape parameter changes. The maximum ARL is at $\theta_0 = 10$ for all the three cases.

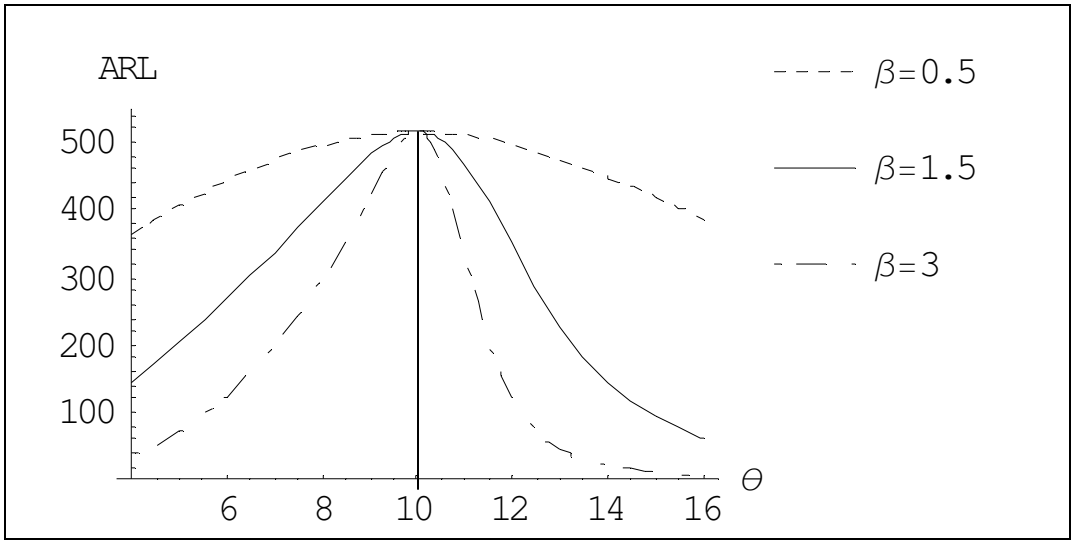

Figure 7.8 Some ARL curves with adjusted control limits and the in-control $\theta_0 = 10$

By looking at the patterns of out-of-control signal, a decision can be made on which of the parameters has changed. Basically a Weibull distribution with small shape parameter will have a "heavy" tail while one with large shape parameter is more centered around the mean.

7.5. The effect of estimated parameters on the Weibull t chart

In most of the control chart studies, it is assumed that the parameters are known or an accurate estimate is available. In reality, however, the parameters of the distribution have to be estimated and usually the sample size is small so the estimates are not accurate.

Since the control limits can be affected by the parameters, the estimation error is an important issue. Many authors have addressed this issue. An early paper is Proschan and Savage (1960) and for some recent papers, see e.g. Quesenberry (1993), Chen (1998), Braun (1999), Champ and Chou (2003), Jones (2002), Jones, and Champ (2002) and Jones *et al.* (2001). As will be seen in the following, this is a more interesting problem for the Weibull t chart.

Among the various estimation techniques the one most widely used is the Maximum Likelihood Estimators (MLE). The ML estimate of the parameters of the Weibull distribution can be obtained by solving the following two equations

$$\beta = \left[\frac{\sum_{i=1}^{n} x_i^{\beta} \ln(x_i)}{\sum_{i=1}^{n} x_i^{\beta}} - \frac{\sum_{i=1}^{n} \ln(x_i)}{n} \right]^{-1} \tag{7.10}$$

$$\theta = \left[\sum_{i=1}^{n} x_i^{\beta} / n \right]^{1/\beta} \tag{7.11}$$

The estimators are random variable and for a given set of data, the estimates could be different from the true value leading to wrong control limits. In fact, in the case of

Weibull, the MLEs are known to be biased and the bias itself could be very large for small sample. This is especially the case when the shape parameter is concerned.

A simulation study is carried out and the results are tabulated in Table 7.4. It shows the MLE of the parameters of the Weibull distribution for different sample sizes and the control limits based on the estimated parameters. The results in each row are based on 10000 random samples simulated with in-control parameters θ_0 = 10 and β_0 = 1.5. Median, due to its robustness to outliers, was used to compute the central location of the parameters and the control limits. The true control limits (for $\alpha = 0.0027$) are (from Table 7.1) 35.21 (UCL), 7.83 (CL) and 0.12 (LCL). We can also compute the relative percent error between the estimated limit and the actual limit as follows:

$$\text{Relative Error (\%)} = \frac{\text{Estimated Limit - True Limit}}{\text{True Limit}} \times 100$$

Sample Size	β	δ	Estimated Limits			Relative Error (%)		
			UCL	CL	LCL	UCL	CL	LCL
5	1.86	9.78	27.44	7.99	0.28	(-) 22.07	(+) 2.04	(+) 133.33
10	1.66	9.81	31.09	7.88	0.18	(-) 11.70	(+) 0.64	(+) 50.00
15	1.61	9.91	32.35	7.89	0.16	(-) 8.12	(+) 0.77	(+) 33.33
20	1.57	9.96	33.24	7.85	0.15	(-) 5.60	(+) 0.26	(+) 25.00
25	1.56	9.96	33.52	7.87	0.14	(-) 4.80	(+) 0.51	(+) 16.67
30	1.55	9.97	33.88	7.87	0.14	(-) 3.78	(+) 0.51	(+) 16.67

Table 7.4 The MLEs and the estimated control limits for different sample sizes (α = 0.0027, β_0 = 1.5, θ_0 = 10)

As expected, a small sample size has a drastic effect on the control limits. For a sample size of 5, in 50% of cases, the difference between the true lower control limit and the estimated one is larger than 133%. It can be seen from Equation (7.3) that a larger estimate of β results in an overestimation of the lower control limit and the centre line, and an underestimation of the upper control limit. On the other hand a larger estimate of θ will overestimate the control limits while a small θ will always underestimate them. In general, the shape parameter has a larger effect and as can be seen, this is due to the fact that it is very biased when the sample size is small.

In the above simulation study, the shape parameter was 1.5, which means increasing hazard rate. It would be interesting to study the results when the shape parameter is less than 1, *i.e.* decreasing hazard rate. Table 7.5 shows the results of the simulation for β_0 = 0.5. From Table 7.1 the true control limits are UCL = 436.61, CL = 4.8 and LCL =1.82E-05. It can be seen from Table 7.5 that the effect is more serious when the estimation problem is considered. Again, the problem is mainly due to the biased estimator.

Sample Size	β	θ	Estimated Limits			Relative Error (%)		
			UCL	CL	LCL	UCL	CL	LCL
5	0.62	9.04	206.60	5.10	2.24E-04	(-) 52.68	(+) 6.25	(+) 1126.49
10	0.55	9.52	300.42	4.90	6.07E-05	(-) 31.19	(+) 2.08	(+) 232.76
15	0.54	9.59	338.46	4.91	4.30E-05	(-) 22.48	(+) 2.29	(+) 135.82
20	0.52	9.79	367.13	4.84	3.28E-05	(-) 15.91	(+) 0.83	(+) 79.61
25	0.52	9.82	376.70	4.88	2.95E-05	(-) 13.72	(+) 1.67	(+) 61.56
30	0.52	9.87	388.95	4.87	2.76E-05	(-) 10.92	(+) 1.46	(+) 51.21

Table 7.5 The MLEs and the estimated control limits for different sample sizes (α = 0.0027, β_0 = 0.5, θ_0 = 10)

In all of the above cases it is visible that the shape parameter is overestimated. This is because the Maximum Likelihood method yields biased estimators for the Weibull parameters. Ross (1994) presented a correction formula to reduce the bias of the estimated shape parameter of the Weibull distribution. This formula when added to the ML method reduces the bias to < 3% of the shape parameter value. Ross (1994) gave a simple formula for unbiasing the shape parameter β as:

$$\beta_U = \beta \frac{n-2}{n-0.68} \tag{7.12}$$

where β_U is the corrected unbiased estimator and n is the sample size. We will show that this approach, which is simple, can be very effective in dealing with estimation error in this case.

A simulation was done using this corrected unbiased estimator. As before the results in each row are based on 10000 random samples simulated with parameters θ_0 = 10 and β_0 = 0.5. For each sample the shape parameter was first calculated by the standard ML method, and then it was unbiased by multiplying it with the correction factor. The corrected unbiased estimator was then used to calculate the scale parameter. The control limits were then calculated based on these unbiased estimators. The values shown in Table 7.6 are the median of the parameters and the estimated limits. The true control limits (for α = 0.0027) are UCL = 436.61, CL = 4.8 and LCL =1.82E-05.

Sample Size	β	θ	Estimated Limits			Relative Error (%)		
			UCL	CL	LCL	UCL	CL	LCL
5	0.43	7.41	621.89	3.07	1.61E-06	(+) 42.44	(-) 36.04	(-) 91.17
10	0.47	8.53	467.64	3.92	7.58E-06	(+) 7.11	(-) 18.33	(-) 58.44
15	0.49	9.04	449.85	4.25	1.13E-05	(+) 3.03	(-) 11.46	(-) 37.82
20	0.49	9.19	451.69	4.35	1.23E-05	(+) 3.45	(-) 9.38	(-) 32.76
25	0.49	9.46	442.24	4.48	1.36E-05	(+) 1.29	(-) 6.67	(-) 25.41
30	0.49	9.57	446.18	4.54	1.46E-05	(+) 2.19	(-) 5.42	(-) 19.94

Table 7.6 The corrected unbiased MLEs and the estimated control limits for different sample sizes ($\alpha = 0.0027$, $\beta_0 = 0.5$, $\theta_0 = 10$)

The results in Table 7.6 are completely different in nature to those displayed in Table 7.4. When the corrected unbiased estimators are used the upper control limit is overestimated while the lower control limit and the centre line are underestimated. This results in a wider control limits. This means less interruptions (false alarm) but at the same time the control chart will also become less sensitive to process shifts. However as the sample size increases the control limits approach the true limits. For a large sample size even though the limits are still slightly away from their true values (say for a sample size of 30), the overall performance will be quite satisfactory as compared to the case in Table 7.5 with biased parameters. Another interesting revelation is that when the sample size changes from 5 to 10, there is a sharp change in the estimated limits. When the sample size further increases, the estimated limits approach the true limits but the change is more gradual. To validate this finding another simulation was run by changing the value of β_0 fro 0.5 to 1.5. The results are shown in Table 7.7.

As before a sharp change was noticed in the estimated limits when the sample size changes from 5 to 10. Thus, it can be said that the corrected unbiased estimators give a better set of limits, especially for $n \geq 10$. Overall, the estimated limits are much more closer to the true limits than compared to Table 7.4.

Sample Size	β	θ	Estimated Limits			Relative Error (%)		
			UCL	CL	LCL	UCL	CL	LCL
5	1.28	8.93	39.67	6.69	5.31E-02	(+) 12.67	(-) 14.56	(-) 55.76
10	1.42	9.49	36.35	7.32	9.14E-02	(+) 3.24	(-) 6.51	(-) 23.79
15	1.45	9.63	35.53	7.46	1.02E-01	(+) 0.91	(-) 4.73	(-) 14.68
20	1.47	9.72	35.45	7.56	1.08E-01	(+) 0.68	(-) 3.45	(-) 9.69
25	1.48	9.80	35.53	7.62	1.11E-01	(+) 0.91	(-) 2.68	(-) 7.89
30	1.48	9.82	35.52	7.68	1.12E-01	(+) 0.88	(-) 1.92	(-) 6.36

Table 7.7 The corrected unbiased MLEs and the estimated control limits for different sample sizes ($\alpha = 0.0027$, $\beta_0 = 1.5$, $\theta_0 = 10$)

Chapter 8

Combined Decision Scheme for CQC Charts

8.1. The Need

Control Charts based on variable sampling intervals (VSI), where the sampling interval depend upon position of last plotted point, has been studied by many authors in detail, see Reynolds *et al*. (1988, 1990), Runger and Pignatiello (1991), Saccucci *et al*. (1992), Amin and Miller (1993), and Runger and Montgomery (1993). Similar to the idea of VSI is the variable sample size (VSS), where the size of the sample varies depending upon the plotted point, and has been studied by many authors, see Prabhu *et al*. (1993), Costa (1994), Park and Reynolds (1994), Annadi *et al*. (1995). A combination of both, where both the sample size and sampling interval are treated as variable, is the control chart with variable sample size and the sampling intervals (VSSI); see Rendtel (1990), Prabhu *et al*. (1994), Costa (1997, 1999).

The idea behind all these approaches is proper or optimum utilization of resources. Other approaches to improving the control chart's performance consist of adopting double sampling procedures; see Croasdale (1974), Daudin (1992) and Steiner (1999). Crosdale (1974) and Daudin (1992) added warning limits to the standard - X chart. In their methodology, any sample mean that falls between the warning limit and the control limit triggers the withdrawal of a second sample. In the Croasdale (1974) procedure, the in-control/out-of-control decision, after taking the second sample, is based solely on the second sample while in Daudin (1992), it is based on the combined sample. In Steiner (1999), the decision is based on the individual results extracted from each sample. Other related discussion on the use of warning limits can be found in Page (1955, 1962),

Roberts (1966), Gordon and Weindling (1975), Chiu and Cheung (1977), Rahim (1984) and Chung (1993).

Most of the work in this area has been done for control charts based on variable data. A comprehensive review of the development of Control Charts using attributes data is provided in Woodall (1997), while excellent introductions are provided in textbooks such as Duncan (1986) and Montgomery (2001).

Although the CQC charts are much more appropriate for high-quality process control, it relies purely on a single value for decision-making. As a single value is always inefficient in decision-making, it is necessary to create a new procedure either by adding an additional chart or by introducing some run rules. Another way to solve this problem is by plotting the observed quantity between every r failures. However, the user needs to wait for too long to plot a single point. Kuralmani *et al.* (2002) addressed this issue for the CCC charts by incorporating some run rules into the regular CCC control charting procedure.

8.2. The Combined scheme

The control limits of the CQC_1 chart can be calculated by Equation (2.12) and are reproduced here for ease:

$$UCL_1 = \lambda_0^{-1} \ln \frac{2}{\alpha}$$
$$CL_1 = \lambda_0^{-1} \ln 2 = 0.693\lambda_0^{-1} \quad (8.1)$$
$$LCL_1 = \lambda_0^{-1} \ln \frac{1}{1-\alpha/2}$$

where, α is an acceptable probability of false alarm, and λ_0 is the parameter of the exponential distribution. The decision rule for the CQC chart, henceforth referred to as the CQC_1 chart, proposed by Chan *et al.* (2000) is shown in Figure 8.1. The decision rule is straightforward and can be easily understood.

No doubt CQC_1 chart has many advantages compared to the traditional Shewhart chart for monitoring Poisson counts, like the c or the u charts. However, as pointed out by Xie *et al.* (2002b), one major disadvantage of the CQC_1 chart is that the decision whether the process is out of control is taken based on only one point and thus as a result, the chart may either cause many false alarms or it may be insensitive to process shift if the control limits are wide (with small value of α). To overcome this problem Xie *et al.* (2002b) suggested monitoring the time between *r* defects (events). This approach gives more credibility to the decision regarding the statistical control of the process as the decision is made on the basis of *r* points rather than a single point.

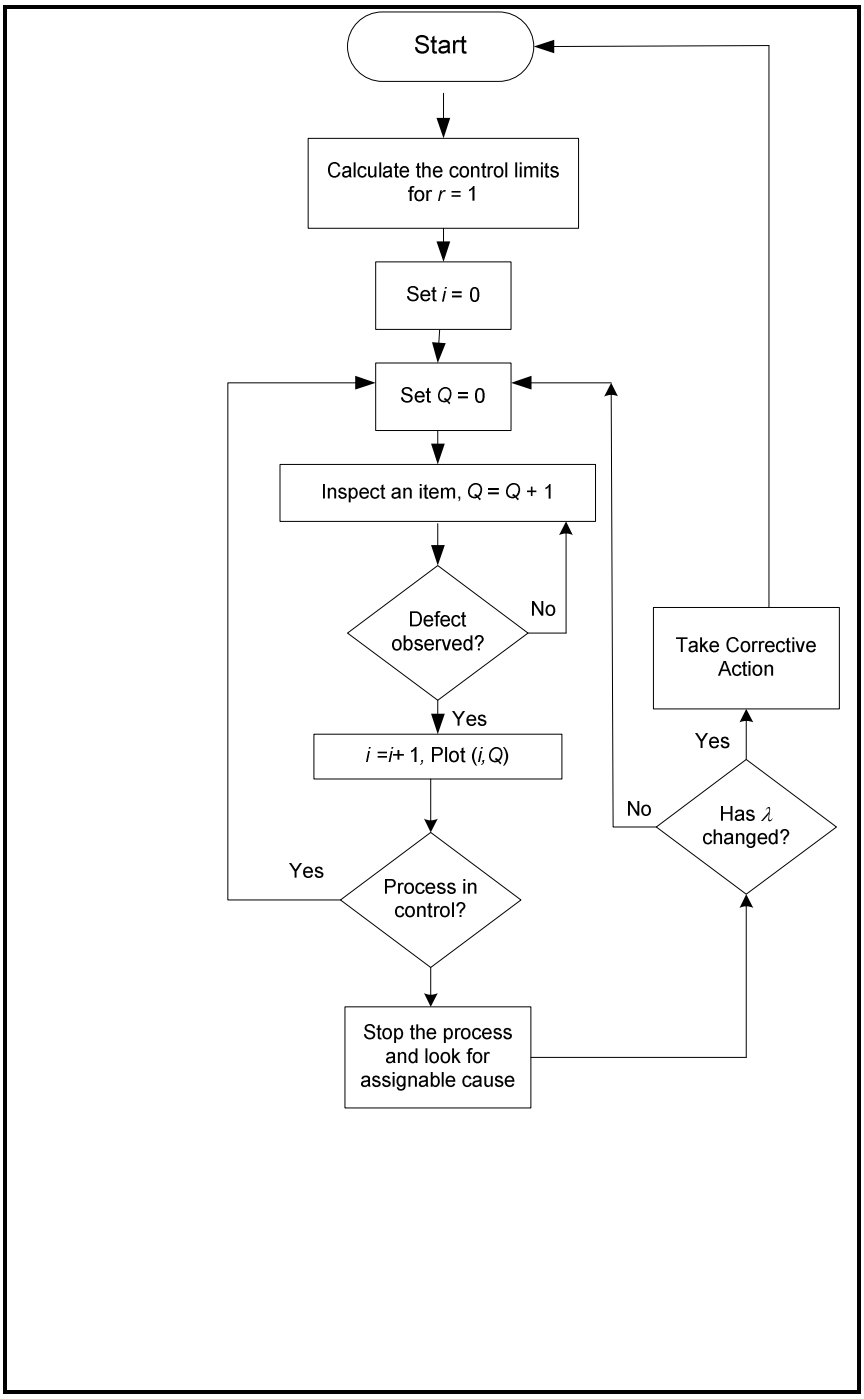

Figure 8.1 Decision Rule for CQC_1 chart

To calculate the control limits of the CQC_r chart, the concept of exact probability limits is used. If α is the accepted false alarm risk then the upper control limit, UCL_r, the center line, CL_r, and the lower control limit, LCL_r, can be calculated by using Equation (3.3) and are reproduced here for convenience:

$$\begin{aligned} F(UCL_r, r, \lambda_0) &= 1 - \sum_{k=0}^{r-1} e^{-\lambda_0 UCL_r} \frac{(\lambda_0 UCL_r)^k}{k!} = 1 - \alpha/2 \\ F(CL_r, r, \lambda_0) &= 1 - \sum_{k=0}^{r-1} e^{-\lambda_0 CL_r} \frac{(\lambda_0 CL_r)^k}{k!} = 0.5 \\ F(LCL_r, r, \lambda_0) &= 1 - \sum_{k=0}^{r-1} e^{-\lambda_0 LCL_r} \frac{(\lambda_0 LCL_r)^k}{k!} = \alpha/2 \end{aligned} \tag{8.2}$$

However, this approach too has two major disadvantages; first, the average time taken to plot a point increases with *r* and second that the average time to alarm increases as the process improves beyond a certain level. Here it must be made clear that this problem is also present for the CQC_1 chart however it is more pronounced in the case of CQC_r chart due to the effect of *r*.

The ideal condition would be to use the advantages of both these schemes, *i.e.*

- To decrease the time to plot a point, an advantage associated with the CQC_1 chart
- To take the decision regarding statistical control of the process based on one more than one point, an advantage associated with the CQC_r chart

The procedure proposed in this chapter is based on the two advantages mentioned above. A set of warning limits is established corresponding to some "critical" false alarm probability. The selection of this probability is a subjective decision and should be taken by the concerned people based on the past information about the process. The upper warning limit is named as UCL_c and the lower warning limit as LCL_c (where *c* stands for "critical"). These warning limits can be calculated just like the control limits of CQC_1 chart as:

$$LCL_c = \lambda_0^{-1} \ln \frac{1}{1-\alpha_c/2}, \quad \text{and} \quad UCL_c = \lambda_0^{-1} \ln \frac{2}{\alpha_c} \tag{8.3}$$

where α_c is the specified critical false alarm probability

The individual time (or quantity) to failure (or defect) is plotted on the control charts. If the point plots above or below the UCL or the LCL, respectively, of the CQC_1 chart (henceforth referred to as the UCL_1 and the LCL_1 respectively), the process is deemed out of control. If the point, Q_1, plots between LCL_c and LCL_1 or the UCL_c and the UCL_1, no decision regarding the statistical control of the process is made, however since the plotted point lies in the warning zone and hence provide a strong evidence regarding possible shift in the process, the user switches over from the CQC_1 charting procedure to CQC_r charting procedure. Once the r^{th} event occurs, the sum of observed quantity, Q_r, and the initial observation Q_1 is plotted on the chart. If this sum lies above the UCL_{1+r} or below the LCL_{1+r}, the process is declared out of control else the process is declared in

control and the user goes back to the normal plotting procedure for the CQC_1 chart. Figure 8.2 shows the decision rule for this combined procedure.

The procedure can be thought of as "switch-over" procedure where the user switches, from the one plotting method to another. The advantage of this combined plotting method is that we consider more points only when there is strong evidence that the process might have shifted. Thus we do not compromise on the waiting time (to plot a point) and at the same time we get a better performance as compared to the CQC_1 chart.

Since the user plots the sum of initial (1) and last r observations, the charting procedure is given the name of CQC_{1+r} chart.

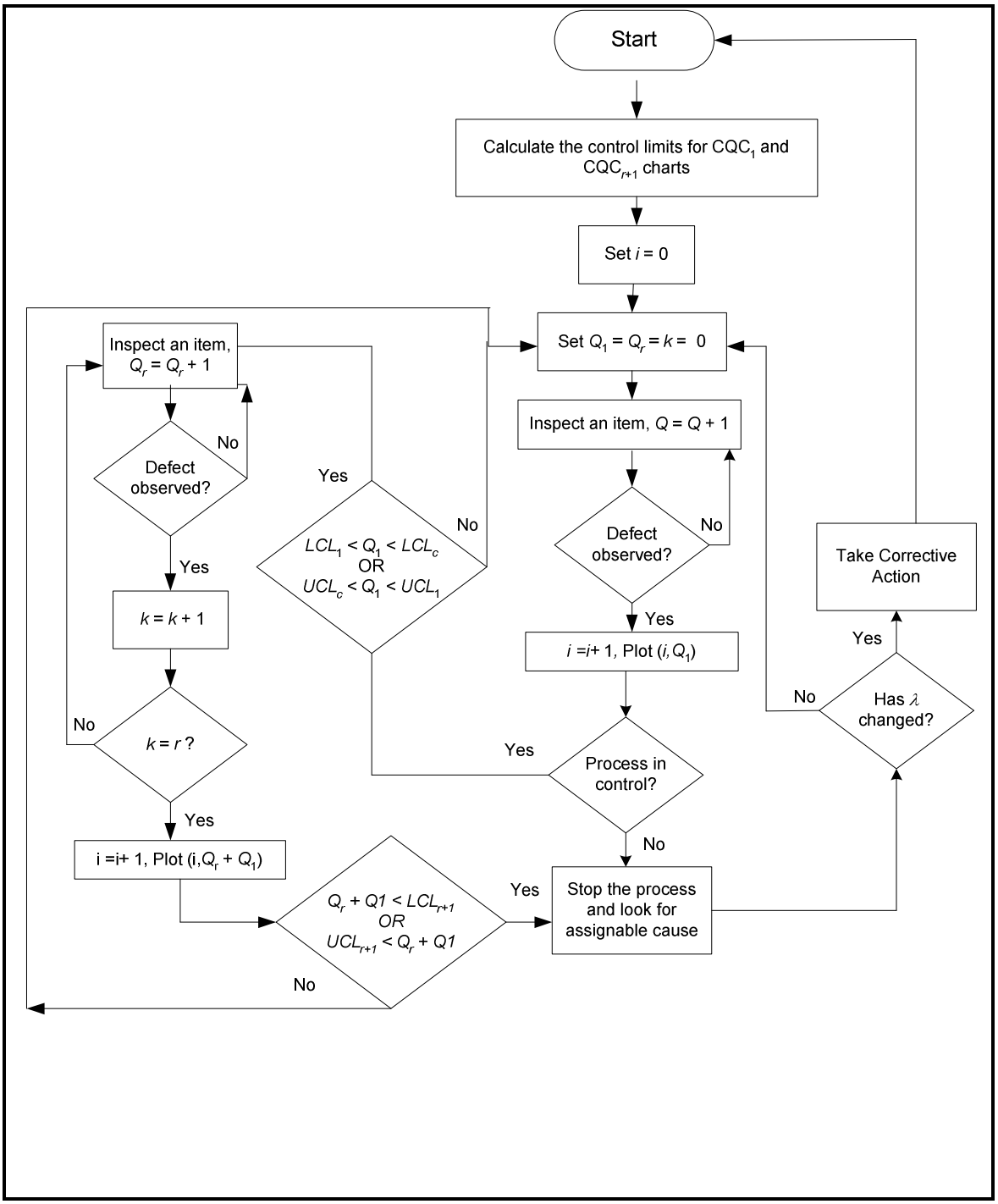

Figure 8.2 Decision Rule for the combined procedure

8.3. Average Run Length of the combined scheme

Average run length of a control chart is defined as the number of points plotted on the control chart before the chart raises an out of control alarm. The ARL of any chart can be represented by the formula

$$ARL = \frac{1}{\text{probability of a point to fall outside the limit}} \tag{8.4}$$

To calculate this probability for the combined scheme we need to consider four scenarios:

Case 1: The plotted point falls outside UCL_1 and LCL_1, with probability p_1

The probability p_1 can be calculated as:

$$p_1 = 1 + e^{-\lambda UCL_1} - e^{\lambda LCL_1} \tag{8.5}$$

Case 2: The plotted point, a, falls between UCL_c and UCL_1. The sum of a and next quantity, b falls beyond UCL_{1+r} with probability p_2

The quantity b is actually the sum of r exponential random variables and thus follows Gamma distribution with parameters r and λ. Therefore, the probability, p_2, can be calculated as:

$$p_2 = \int_{UCL_c}^{UCL_1} \int_{UCL_r - a}^{\infty} f(a,b)\, db\, da \tag{8.6}$$

Assuming independence between initial and next r observations, the joint probability function of observations a and b can be found as

$$f(a,b) = \lambda e^{-\lambda a} \times \frac{\lambda^r b^{r-1}}{(r-1)!} \exp\{-\lambda b\} \tag{8.7}$$

where, λ is the out of control parameter.

Substituting the above equation in Equation (8.6) we can obtain the probability p_2

Case 3: The plotted point, a, falls between LCL_1 and LCL_c. The sum of a and next quantity, b falls below LCL_{1+r} with probability p_3 and it can be calculated as:

$$p_3 = \int_{LCL_1}^{LCL_c} \int_{0}^{LCLr - a} f(a,b)\, db\, da \tag{8.8}$$

Case 4: The plotted point, a, falls between LCL_1 and LCL_c. The sum of a and next quantity, b falls beyond UCL_{1+r}. This probability, p_4, can be calculated as:

$$p_4 = \int_{LCL_1}^{LCL_c} \int_{UCL_r - a}^{\infty} f(a,b)\, db\, da \tag{8.9}$$

So, the overall probability, p, for a point to indicate an out of control situation is:

$$p = p_1 + p_2 + p_3 + p_4$$

As an illustration for $r = 1$, *i.e.* for CQC_{1+1} chart, the four probability components can be calculated as:

$$p_1 = 1 - \left(1 - \frac{\alpha}{2}\right)^{\lambda/\lambda_0} + \left(\frac{\alpha}{2}\right)^{\lambda/\lambda_0}$$

$$p_2 = e^{-\lambda UCL_2} \frac{\lambda}{\lambda_0} \ln\left(\frac{\alpha_c}{\alpha}\right)$$

$$p_3 = \left(1 - \frac{\alpha}{2}\right)^{\lambda/\lambda_0} - \left(1 - \frac{\alpha_c}{2}\right)^{\lambda/\lambda_0} - e^{-\lambda LCL_2} \frac{\lambda}{\lambda_0} \ln\left(\frac{1-\alpha/2}{1-\alpha_c/2}\right)$$

$$p_4 = e^{-\lambda UCL_2} \frac{\lambda}{\lambda_0} \ln\left(\frac{1-\alpha/2}{1-\alpha_c/2}\right)$$

where, λ and λ_0 are the out of control and in control parameter respectively. Substituting this sum in Equation (8.4) we can compute the ARL for the combined scheme. Tables 1-4 show the ARL values of CQC_{1+r} chart for different values of r. The parameters used in the ARL computation are as follows:

- The false alarm probability for calculating the limits of the CQC_1 and the CQC_{1+r} chart in the combined procedure was assumed to be, $\alpha = 0.0027$.
- The critical false alarm probability was assumed to be, $\alpha_c = 0.01$

- The in-control parameter (λ_0) for all the charts is assumed to be 1
- The false alarm probability for the "matched" CQC_1 chart were selected to give the same in-control ARL as the CQC_{1+r} chart. For example for in Table 8.1 the false alarm probability for the CQC_1 chart was taken as 0.003056 while those in Tables 8.2, 8.3 and 8.4 were taken as 0.002917, 0.002868 and 0.00284 respectively.

λ	ARL		Reduction in the out of control ARL (%)	λ	ARL		Reduction in the out of control ARL (%)
	CQC_{1+1}	CQC_1			CQC_{1+1}	CQC_1	
0.01	1.05	1.07	1.87	1.1	403.79	403.28	-0.13
0.05	1.31	1.38	5.07	1.2	440.62	444.22	0.81
0.1	1.75	1.91	8.38	1.3	443.79	453.64	2.17
0.15	2.36	2.64	10.61	1.4	428.14	443.89	3.55
0.2	3.21	3.65	12.05	1.5	404.9	425.37	4.81
0.25	4.4	5.05	12.87	1.6	379.98	404.05	5.96
0.3	6.04	6.97	13.34	1.7	355.95	382.77	7.01
0.35	8.34	9.62	13.31	1.8	333.71	362.68	7.99
0.4	11.54	13.27	13.04	1.9	313.46	344.15	8.92
0.45	15.99	18.27	12.48	2	295.11	327.22	9.81
0.5	22.16	25.09	11.68	2.1	278.48	311.78	10.68
0.55	30.67	34.36	10.74	2.2	263.39	297.69	11.52
0.6	42.32	46.82	9.61	2.3	249.65	284.8	12.34
0.65	58.1	63.4	8.36	2.4	237.09	272.96	13.14
0.7	79.1	85.05	7	2.5	225.59	262.07	13.92
0.75	106.4	112.68	5.57	2.6	215.01	252.01	14.68
0.8	140.8	146.82	4.13	2.7	205.26	242.7	15.43
0.85	182.1	187.26	2.76	2.8	196.25	234.05	16.15
0.9	229.1	232.69	1.55	2.9	187.89	226	16.86
0.95	278.8	280.52	0.6	3	180.12	218.48	17.56
1	327.2	327.22	0				

Table 8.1 The ARL values for CQC_{1+1} and CQC_1 charts

λ	ARL		Reduction in the out of control ARL (%)	λ	ARL		Reduction in the out of control ARL (%)
	CQC_{1+2}	CQC_1			CQC_{1+2}	CQC_1	
0.01	1.05	1.07	1.23	1.1	428.74	423.08	-1.34
0.05	1.31	1.39	5.84	1.2	471.78	466.13	-1.21
0.1	1.72	1.92	10.66	1.3	477.21	475.84	-0.29
0.15	2.28	2.66	14.31	1.4	461.14	465.42	0.92
0.2	3.06	3.69	16.9	1.5	436.12	445.84	2.18
0.25	4.16	5.11	18.57	1.6	408.87	423.39	3.43
0.3	5.69	7.07	19.47	1.7	382.33	401.03	4.66
0.35	7.85	9.78	19.75	1.8	357.6	379.95	5.88
0.4	10.88	13.52	19.5	1.9	334.95	360.52	7.09
0.45	15.14	18.66	18.83	2	314.31	342.77	8.3
0.5	21.12	25.69	17.81	2.1	295.54	326.6	9.51
0.55	29.45	35.27	16.48	2.2	278.42	311.83	10.71
0.6	41	48.18	14.91	2.3	262.78	298.32	11.91
0.65	56.81	65.41	13.14	2.4	248.46	285.92	13.1
0.7	78.12	87.97	11.2	2.5	235.29	274.51	14.29
0.75	106.17	116.85	9.14	2.6	223.17	263.98	15.46
0.8	141.9	152.63	7.03	2.7	211.97	254.22	16.62
0.85	185.48	195.13	4.95	2.8	201.6	245.16	17.77
0.9	235.69	242.98	3	2.9	191.98	236.72	18.9
0.95	289.59	293.45	1.32	3	183.05	228.85	20.01
1	342.77	342.77	0				

Table 8.2 The ARL values for CQC_{1+2} and CQC_1 charts

As can be see from the tables, the combined scheme gives a better ARL performance than the current design. It can also be seen that for small process deterioration the ARL of both the charts increase and later decrease as the magnitude of shift becomes large. Moreover, the CQC_1 chart gives a better performance than the CQC_{1+r} charts for small process deteriorations.

λ	ARL		Reduction in the out of control ARL (%)	λ	ARL		Reduction in the out of control ARL (%)
	CQC_{1+3}	CQC_1			CQC_{1+3}	CQC_1	
0.01	1.05	1.07	1.87	1.1	437.05	430.65	-1.49
0.05	1.3	1.39	6.47	1.2	481.06	474.51	-1.38
0.1	1.7	1.92	11.46	1.3	486.32	484.33	-0.41
0.15	2.24	2.67	16.1	1.4	469.38	473.65	0.9
0.2	2.99	3.7	19.19	1.5	443.12	453.67	2.33
0.25	4.02	5.13	21.64	1.6	414.43	430.78	3.8
0.3	5.47	7.11	23.07	1.7	386.38	408.01	5.3
0.35	7.52	9.84	23.58	1.8	360.1	386.54	6.84
0.4	10.43	13.61	23.37	1.9	335.91	366.77	8.41
0.45	14.54	18.8	22.66	2	313.79	348.72	10.02
0.5	20.37	25.92	21.41	2.1	293.57	332.26	11.64
0.55	28.57	35.61	19.77	2.2	275.09	317.23	13.28
0.6	40.03	48.7	17.8	2.3	258.16	303.49	14.94
0.65	55.86	66.16	15.57	2.4	242.63	290.88	16.59
0.7	77.35	89.08	13.17	2.5	228.34	279.27	18.24
0.75	105.82	118.43	10.65	2.6	215.18	268.55	19.87
0.8	142.29	154.84	8.11	2.7	203.04	258.62	21.49
0.85	186.94	198.12	5.64	2.8	191.82	249.4	23.09
0.9	238.53	246.9	3.39	2.9	181.43	240.82	24.66
0.95	293.99	298.39	1.47	3	171.81	232.81	26.2
1	348.72	348.72	0				

Table 8.3 The ARL values for CQC_{1+3} and CQC_1 charts

λ	ARL		Reduction in the out of control ARL (%)	λ	ARL		Reduction in the out of control ARL (%)
	CQC_{1+4}	CQC_1			CQC_{1+4}	CQC_1	
0.01	1.05	1.07	1.87	1.1	441.24	434.95	-1.45
0.05	1.3	1.39	6.47	1.2	485.14	479.28	-1.22
0.1	1.7	1.93	11.92	1.3	489.73	489.16	-0.12
0.15	2.23	2.67	16.48	1.4	471.77	478.32	1.37
0.2	2.94	3.71	20.75	1.5	444.26	458.11	3.02
0.25	3.93	5.14	23.54	1.6	414.17	434.99	4.79
0.3	5.32	7.13	25.39	1.7	384.64	411.97	6.63
0.35	7.28	9.88	26.32	1.8	356.85	390.3	8.57
0.4	10.07	13.67	26.34	1.9	331.17	370.33	10.57
0.45	14.05	18.89	25.62	2	307.59	352.1	12.64
0.5	19.74	26.05	24.22	2.1	286	335.47	14.75
0.55	27.8	35.8	22.35	2.2	266.23	320.3	16.88
0.6	39.17	48.99	20.04	2.3	248.12	306.43	19.03
0.65	54.99	66.59	17.42	2.4	231.52	293.69	21.17
0.7	76.61	89.7	14.59	2.5	216.3	281.97	23.29
0.75	105.39	119.32	11.67	2.6	202.32	271.15	25.38
0.8	142.39	156.09	8.78	2.7	189.49	261.12	27.43
0.85	187.79	199.82	6.02	2.8	177.69	251.82	29.44
0.9	240.26	249.13	3.56	2.9	166.84	243.15	31.38
0.95	296.6	301.19	1.52	3	156.85	235.06	33.27
1	352.09	352.1	0				

Table 8.4 The ARL values for CQC_{1+4} and CQC_1 charts

The increase in ARL for small process deterioration is because of the skewness of the underlying distribution and is a general problem associated with the control charts based on run length distribution as discussed in 5.1. However, from the Figure 5.1 it is obvious that the effect is less prominent for large *r*. So, it can be argued that the better performance of the CQC_1 chart is not due to the skewness. The reason behind this slightly better performance is the fact that the ARL for the two charts were computed for different

false alarm probability. For the CQC_1 chart in Table 8.1, we had assumed a false alarm probability of 0.003056. When the process deteriorates, the Type II error of CQC_1 chart first increases from its in-control value of 0.996944 and then decreases with further deterioration. The Type II error for the CQC_{1+r} chart also increases as the process deteriorates but the increase is more as compared to the CQC_1 chart. As a result of this the CQC_1 chart performs better than the CQC_{1+r} chart for small process deteriorations. This can also be seen from Figures 8.3-8.6 which plot the Type II errors for the two charts for different values of r for small increase in λ.

The problem of increment in ARL for small process deteriorations can be corrected by placing the optimal limits on the control chart as shown in Chapter 5. Kuralmani *et al.* (2002) too obtained the optimal limits for their proposed combined decision scheme for CCC charts.

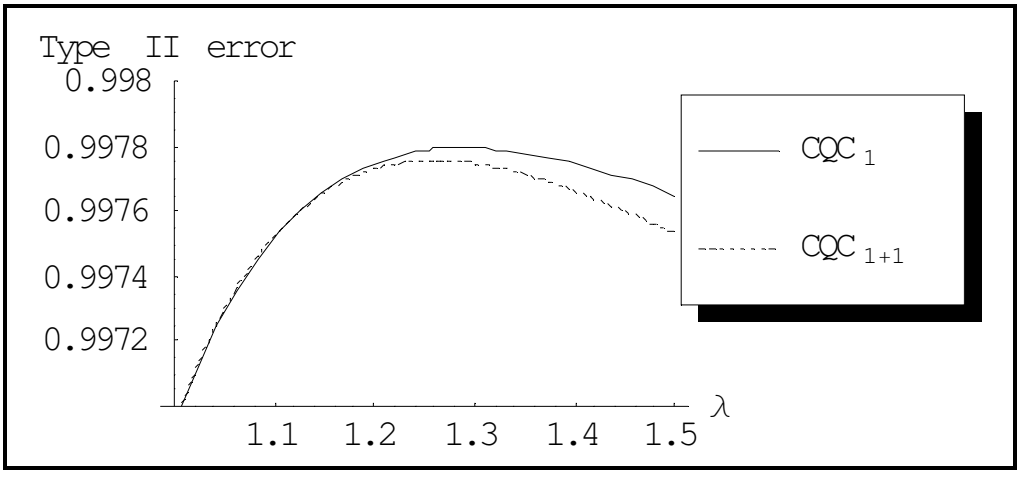

Figure 8.3 OC Curves of CQC_{1+1} and CQC_1 charts for small process deteriorations

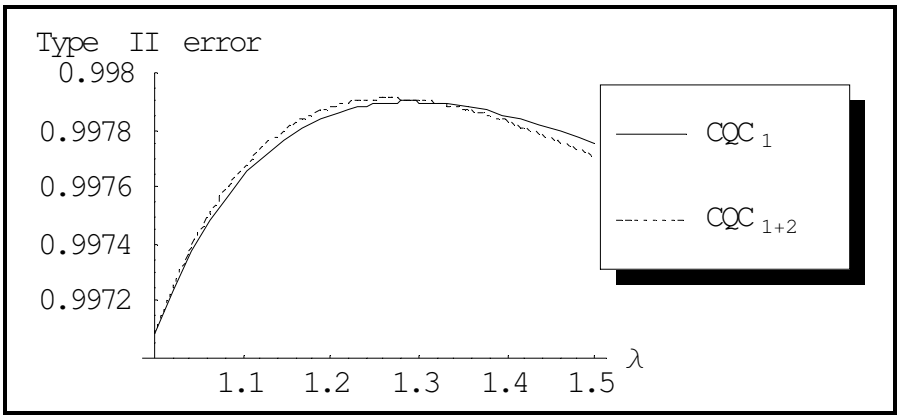

Figure 8.4 OC Curves of CQC_{1+2} and CQC_1 charts for small process deteriorations

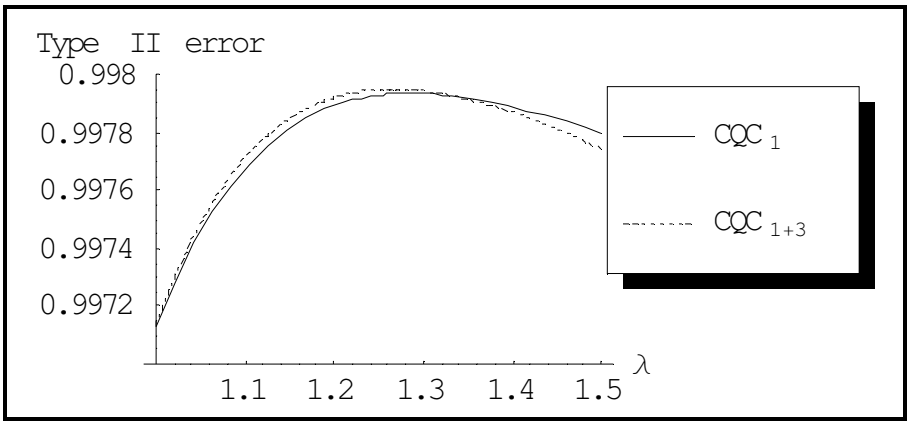

Figure 8.5 OC Curves of CQC_{1+3} and CQC_1 charts for small process deteriorations

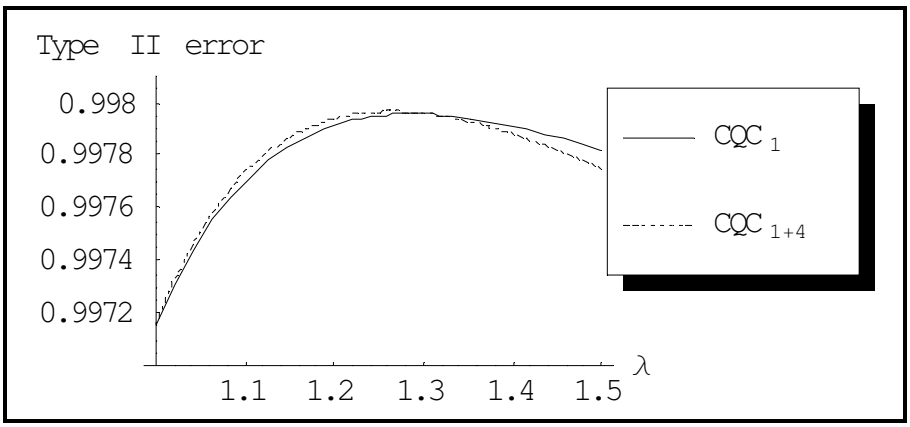

Figure 8.6 OC Curves of CQC_{1+4} and CQC_1 charts for small process deteriorations

8.4. Average Time to Signal of the combined scheme

As discussed before the disadvantage of the CQC_r charts is that the average time to plot a point is r times that for the CQC_1 chart, thus it would be interesting to study the performance of the combined in terms of average time to signal (ATS). A simulation study was carried out in which 100000 points were simulated for the CQC_{1+1} and CQC_{1+2} schemes and their ATS was noted. The performance of the combined decision scheme is compared with the current CQC_2 and CQC_3 chart.

Table 8.5 compares the performance of CQC_{1+1} chart with that of the CQC_2 chart. The false alarm probability for the CQC_2 chart was assumed to be 0.003056, so that both the charts have the same in-control ARL, as shown in Table 8.1. This results in a higher in control ATS for the CQC_2 chart. However there can be certain situations where the time to signal may actually be more important than number of false alarm. Thus we have also compared the performance of the CQC_{1+1} chart with the CQC_2 chart having same in control average time to signal though with a higher false alarm probability (0.006112).

For process improvements, not only the CQC_{1+1} performs much better than the matched CQC_2 chart having same in control false alarm probability, but also performs better than the CQC_2 chart (having same in control average time to signal) for large process improvement ($\lambda \leq 0.3$) .

λ	CQC_{1+1}	CQC_2 (α = 0.003056)	CQC_2 (α = 0.006112)	λ	CQC_{1+1}	CQC_2 (α = 0.003056)	CQC_2 (α = 0.006112)
0.01	106.3	200.73	200.61	1.1	370.1	717.16	351.31
0.05	27.81	43.11	42.61	1.2	393.35	667.64	327.9
0.1	18.87	25.6	24.71	1.3	310.65	571.17	283.04
0.15	16.96	21.44	20.1	1.4	285.56	474.15	236.77
0.2	17.39	20.96	19.01	1.5	284.25	391.91	196.73
0.25	18.92	22.41	19.65	1.6	245.79	325.75	164.1
0.3	21.24	25.44	21.53	1.7	201.7	273.12	137.95
0.35	25.16	30.14	24.6	1.8	167.34	231.12	116.97
0.4	31.17	36.87	29	1.9	156.59	197.31	100.04
0.45	37.88	46.22	35.01	2	152.6	169.81	86.24
0.5	46.25	59.07	43.07	2.1	135.65	147.25	74.9
0.55	58.79	76.64	53.75	2.2	121.62	128.55	65.49
0.6	72.83	100.55	67.78	2.3	118.89	112.92	57.62
0.65	89.08	132.87	86.01	2.4	102.74	99.75	50.98
0.7	112.16	176.06	109.36	2.5	99.41	88.58	45.34
0.75	143.92	232.63	138.56	2.6	91.28	79.04	40.52
0.8	181.49	304.22	173.75	2.7	79.1	70.84	36.38
0.85	205.75	390.07	213.88	2.8	78.38	63.76	32.79
0.9	269.29	484.89	256.11	2.9	64.7	57.6	29.67
0.95	285.15	577.83	295.73	3	61.03	52.22	26.94
1	332.95	654.45	327.23				

Table 8.5 The ATS of CQC_{1+1} and CQC_2 charts

For process deterioration the CQC_{1+1} outperforms CQC_2 ($\alpha = 0.003056$) chart except for large deterioration ($\lambda \geq 2.3$). The other CQC_2 ($\alpha = 0.006112$) chart gives the best performance though at the expense of a higher false alarm probability, *i.e.* one interruption per 164 plotted points.

λ	CQC_{1+2}	CQC_3 (α = 0.002917)	CQC_3 (α = 0.005834)	λ	CQC_{1+2}	CQC_3 (α = 0.002917)	CQC_3 (α = 0.005834)
0.01	108.04	200.74	300.04	1.1	389.93	752.34	353.79
0.05	28.65	43.14	60.75	1.2	449.19	700.24	307.42
0.1	19.65	25.66	32.27	1.3	401.13	598.72	246.31
0.15	17.77	21.54	24.11	1.4	339.54	496.79	192.92
0.2	17.87	21.09	21.21	1.5	279.97	410.5	151.48
0.25	19.25	22.61	20.68	1.6	228.63	341.13	120.27
0.3	21.54	25.73	21.64	1.7	231.46	285.98	96.75
0.35	25.22	30.56	23.88	1.8	206.38	241.97	78.85
0.4	30.21	37.47	27.45	1.9	196.3	206.55	65.03
0.45	36.36	47.09	32.6	2	169.05	177.75	54.22
0.5	44.75	60.34	39.74	2.1	128.36	154.12	45.66
0.55	56.32	78.49	49.48	2.2	134.16	134.53	38.8
0.6	72.31	103.25	62.63	2.3	117.27	118.16	33.24
0.65	87.88	136.8	80.26	2.4	109.65	104.38	28.7
0.7	118.15	181.78	103.6	2.5	96.9	92.68	24.94
0.75	146.39	240.85	133.88	2.6	82.06	82.69	21.82
0.8	179.4	315.87	171.8	2.7	80.77	74.11	19.2
0.85	217.68	406.11	216.6	2.8	68.03	66.69	16.99
0.9	286.67	506.12	264.82	2.9	67.8	60.24	15.1
0.95	278.5	604.41	309.71	3	67.3	54.62	13.49
1	343.53	685.64	342.82				

Table 8.6 The ATS of CQC_{1+2} and CQC_3 charts

Table 8.6 shows the ATS values of CQC_{1+2} and CQC_3 charts. The findings remain same as before with CQC_{1+2} chart performing better than the CQC_3 (α = 0.002917) chart except for $\lambda \geq 2.4$. The other CQC_3 (α = 0.005834) chart performs better than the combined scheme in detecting process deterioration and are also more sensitive to small process deteriorations ($\lambda \leq 0.35$) though again at the expense of a higher false alarm probability (one interruption per 171 plotted points).

8.5. An example to illustrate the charting procedure

Table 8.7 shows a set of simulated data. The first 50 point were simulated from exponential distribution with the assumed in control parameter of $\lambda = 1$ and the last 25 points were simulated using an out of control parameter of $\lambda = 0.5$.

The control limits of CQC_1 and CQC_2 chart were calculated for a false alarm probability of 0.0027 and were found to be, $LCL_1 = 0.00135$, $UCL_1 = 6.61$, $LCL_2 = 0.053$, and $UCL_2 = 8.9$. The critical control limits were calculated using $\alpha_c = 0.01$ and were found out to be $LCL_c = 0.005$, and $UCL_c = 5.3$.

Figure 8.7 shows the CQC_{1+1} control chart. Observation number 19 falls below the lower critical limit and the LCL_1. As a result of this the next observation that should be plotted on the control chart would be the sum of observation 19 and 20. Since the sum lies above LCL_2 so the process is deemed in control and the point is referred to as false alarm and the user returns to the normal (CQC_1) charting procedure. Here, it is noteworthy to point out that since we know the parameters of the distribution hence we can straightaway make decisions regarding the statistical control of the process. However, while monitoring an actual process, the same is not true and any decision regarding the control of the process must be only taken before a search for assignable cause has been carried out.

0.06763	2.62971	0.23131	0.05702	0.94536	1.19876
2.84374	0.78621	1.55125	0.81133	0.50925	1.7095
5.19695	0.01452	0.23274	0.26251	1.25752	2.2016
0.00242	0.053706	0.03238	2.42276	1.22476	1.40963
3.39545	4.09971	0.69249	1.20512	0.43853	0.33546
0.81617	0.1695	0.83702	1.30658	0.17296	0.41078
0.84988	1.2547	3.01973	0.11204	1.94414	1.74562
2.97139	0.09142	1.74312	2.45504	0.27786	0.40286
1.95582	2.66957	2.71678	1.99529	1.40049	2.07538
0.40925	1.29001	5.5146	10.4798	0.05315	0.2981
0.90513	0.45038	0.156	0.06605	1.41496	0.94376
0.26997	5.80523	8.09719	1.23991	4.30271	1.90137
3.46928	1.51564	0.30338			

Table 8.7 Simulated data set to (Read across for consecutive data point)

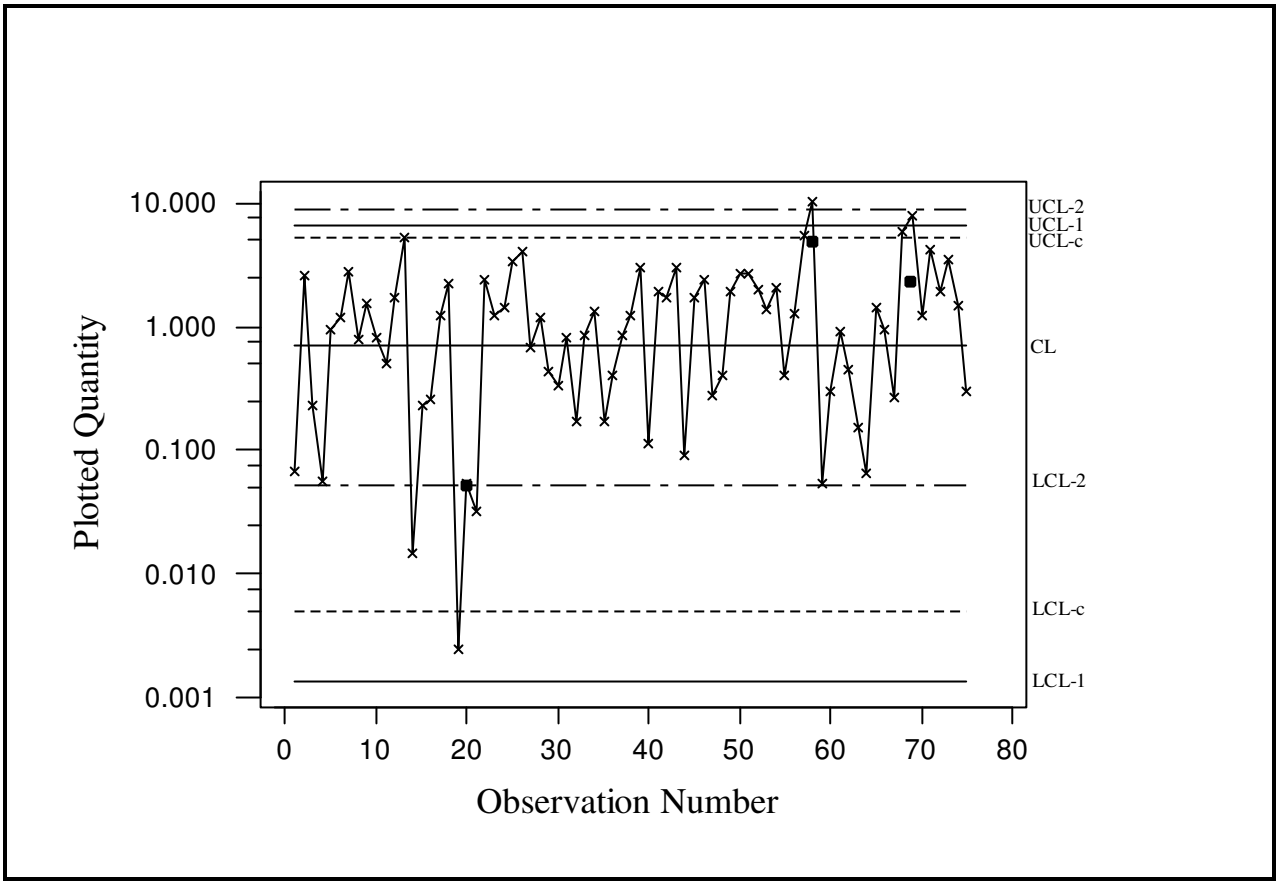

Figure 8.7 The CQC_{1+1} chart

The chart finally raises an alarm at observation 59, which is actually the sum of observation 58 and 59. Observation 58 falls between UCL_c and UCL_1 and the sum of observation 58 and 59 plots beyond UCL_2 thus indicating a possible shift in the process. The black circle represents plot of the actual value of the observation.

Chapter 9

Conclusion and Recommendation

The Shewhart type control charts such as the p chart or the c chart have proven their usefulness over time but are ineffective when the fraction nonconforming level reaches a low value. An alternative process monitoring technique that can be useful in such a case are the control charts based on the cumulative count of conforming (CCC) items or cumulative quantity (CQC) produced between two nonconforming items or between two nonconformities respectively. These two types of charts have been shown to be very useful, especially for high quality processes, those with very low defect or defective levels.

For this type of process, even for fairly large sample size, the number of nonconforming items can be very small or even zero for most of samples. When a p chart or c chart is used for monitoring such a process, first, there will be a large number of false alarms and second, process improvement cannot be detected because the lower control limit is usually negative and thus taken as zero. In this dissertation, some applications and extensions based on cumulative quantity are proposed and studied.

Until now statistical control charts have been mostly used to monitor production processes. Although reliability monitoring, especially for complex equipment or fleet of systems, is an important subject, little study has been carried out on the applications of traditional control chart for defects such as the c chart or u chart. In fact, they might not be suitable unless the number of failures per monitoring interval is large. If the time interval itself is long, such as months or quarters, deteriorating systems will not be

detected quickly. In this dissertation we studied the use of control charting technique to monitor the failure of components.

Chapter 2 reviews some of the recent work in control charting techniques that are suitable or can be suitably applied for high quality processes. Apart from the other monitoring techniques, the cumulative count of conforming control (CCC) charting and cumulative quantity control (CQC) charting are explained and their applications and extensions are reviewed.

In Chapter 3 a procedure based on the monitoring of quantity to observe r defects is proposed and is given the name CQC_r chart. It is an extension of the CQC chart. This procedure is useful and more sensitive compared to the CQC chart although the user needs to wait until r defects to make a decision. Statistical properties of this procedure are investigated. Also notable is the fact that unlike the traditional c chart and u chart, where the lower limit is commonly set to zero, the CQC_r chart is able to detect process improvement as well as deterioration. The use of the CQC_r control charting technique is extended to monitor the failure of components and an example is given to illustrate the charting procedure.

The procedure can also be extended to general nonrepairable system when non-homogeneous Poisson process has to be used as well. For this type of processes, a time-dependent intensity function is needed and the data can be transformed to another time-scale so that the process becomes Poisson process. On the other hand, for the non-

homogeneous Poisson process, what is usually more important is to predict the trend rather than monitoring the failure process itself. The CQC_r charting method is compared with the c chart on the basis of their Average item run length performance. It is found that CQC_r chart not only detects the process improvement but also out performs the c chart in detecting large process deteriorations.

As seen in Chapters 2 and 3, the traditional attribute control charts like c and u charts do not provide satisfactory results, which is mostly due to the violation of the normal approximation to the Poisson distribution. The CUSUM charts and the CQC_r charts are free from the sample size constraint and are thus superior to the c and the u chart. In Chapter 4 the performance of the time-between-events CUSUM chart has been compared to that of the CQC chart and the CQC_r charts.

The results in chapter 4 suggest that if the focus is on small process deterioration then the user can select a CUSUM chart while if the concern is on large deteriorations then a CUSUM or a CQC_r chart (with large r) can be selected. In case of process improvements even though, based on the ARL performance, the CQC_r charts give a superior performance for moderate and large shifts, still it is recommended that a CUSUM chart be used as the ARL performance of the CQC_r charts can be quite misleading. Again if the concern is on large process improvements the CQC chart can be used. It is found that when the underlying distribution changes to Weibull both the CUSUM and the CQC_r charts turn out to be incapable of detecting the increase in shape parameter. The performance of the CQC_r charts is also studied when the underlying distribution changes

from exponential to lognormal and it is found that when either of the parameters of the lognormal distribution decreases the CQC_r takes longer time to detect the shift.

The control charts based on run length, like the CCC and the CQC chart have an undesirable property of reacting late to small process deterioration, which may lead to misinterpretation that the process is well in control, or even improved. This drawback can be removed by adjusting the control limits by multiplying them with an adjustment factor so that a minimum false alarm probability and maximum average run length is reached at the process average. However, it makes the chart take more time to react to process improvements as the limits are widened due to the adjustment.

In the CQC chart; the average time to alarm increases in the beginning when the process deteriorates. This simply means that by the time the deterioration will be detected, many "bad" items would have been already produced. So the control limits should be adjusted to attain maximum average run length so that the process deterioration can be identified and at the same time the false alarms can be reduced. In Chapter 5 a simple procedure is proposed which results in maximum ARL at the process average and the issue of adjusting the false alarm probability is discussed to make the chart more sensitive to process shifts. With the current CCC chart practice the ARL is maximized at an out of control value of the proportion nonconforming which can be significantly above the in control value. With the proposed design the ARL is maximized at the in control value, improving the out of control performance.

Most of the research on the CCC chart has been based on the assumption of an error free inspection, and this assumption is rarely met in reality. In this chapter the problem of inspection errors is discussed for the case of control charts based on cumulative count of conforming (CCC) items. For high yield processes, the inspection error will have significant impact on chart performance. Furthermore, the error of classifying a nonconforming item as a conforming one is the critical type of error as the other error (classifying a conforming item as nonconforming) can be easily rectified by further checking the item. Hence we have focused on the first type of inspection error here. As an application example optimizing procedure is applied to CCC charts in presence of inspection errors.

In Chapter 6, the effect of estimated control limits on the performance of CQC chart is studied. All the previous chapters have shown that the CQC chart is particularly useful in the high quality manufacturing environment when the count of defects is of interest. However, the performance of CQC chart is subject to the estimating accuracy of the exponential parameter, since the true value of the parameter is generally unknown. Furthermore, due to the low defect level of processes, it is difficult to obtain an accurate estimate of the parameter when the size of preliminary sample is not large. When there is no process shift, the estimated false alarm rates are commonly larger than the theoretical value, and the effect can be quite significant even if the sample size is large. However, when there is a process shift, the alarm rates are usually underestimated mildly. On the other hand, the average run length is underestimated when the exponential parameter is unknown.

As stated before the main problem in implementing any chart is the estimation of parameter. Even if one is confident of the accuracy of parameter still caution should be maintained while interpreting an out of control point. For a control chart, the larger the sample size, the better the performance. Too small preliminary sample size will result in inaccurate estimation of the parameter and control limits, and finally wrong decisions could be made. On the other hand, a larger sample size means the consumption of more resources. Hence, it is important to choose a reasonable sample size when constructing the control chart. Apart from this, to encounter the undesirable property of CQC chart, it will be worthwhile to adjust the control limits. The results in this chapter can be used selecting a suitable sample size for the CQC control chart when some criteria are preferred, for example, certain in-control average run length.

Chapter 7 proposes a control chart based on Weibull distribution and is given the name Weibull t chart. The control charts have been successfully used for the monitoring of manufacturing processes. As shown in Chapter 3, they can be also used to monitor the equipment performance, especially in terms of failures or breakdowns. A common assumption used when discussing time-between-events chart is that the underlying distribution is exponential, but this is not always true. In such cases it becomes essential to look for other alternatives and Weibull distribution has shown to be a very flexible option. Control chart based on the monitoring of time-between-events for a more general case of Weibull characteristics is investigated in this chapter. The Weibull t chart for

time-between-events can detect the shift from the nominal scale parameter effectively. However, the study of the chart properties shows that the ARL is also heavily influenced by the shape parameter and especially by an increase in the shape parameter. When the shape parameter increases, the variability is reduced, and hence the process will act more in-control. Furthermore, an accurate estimate of the shape parameter is very important (when the exponential time-between-event is used, the shape parameter is assumed to be one) and it can affect chart performance significantly. When MLE is used, the Weibull shape parameter is known to be biased. However, a simple adjustment can be adopted.

In Chapter 8 a combined charting procedure is proposed for the CQC chart and is the given the name CQC_{1+r} chart. It is seen that combined decision has a better average run length performance than the current design of the CQC chart and is more sensitive than the CQC_1 chart in detecting process changes.

The major portion of this dissertation is dedicated to the study of the CQC_r charts. This study has attempted to look at the various problems associated with chart, and has tried to remove them or propose an alternative solution. However, not all issues have been addressed. For example it would be interesting the study the behavior of the chart in presence of inspection errors. This gives way to another important issue that requires further research, the estimation of inspection errors. In this dissertation, we have assumed that they are known.

Usually the probability of inspection error has to be estimated and this can usually be done based on the information from the inspection in similar processes. It would also be interesting to study effect on ARL when a random shift model is used rather than the current practice of assuming a fixed shift model. This dissertation has not addressed the issue of economic design of the chart and few things that can be studied in the future are obtaining the optimum r and designing the other chart parameters from an economic design perspective. Another important issue is to unbias the behavior of ARL that is the getting the same reduction in ARL on both sides of the process average like in the case of Shewhart chart. Furthermore, the performance of CQC chart is quite satisfactory under the assumption that the data collected is independent. It will be interesting to study the effect of data correlation on its performance.

DECLARATION

This is for the information that I changed my name from PRIYA RANJAN to PRIYA RANJAN SHARMA on October 7th, 2003.

Under my previous name of PRIYA RANJAN, I have co-authored four publications, the details of which are as follows:

B. He, M. Xie, T.N. Goh, and P. Ranjan (2003). "On the estimation error in zero-inflated Poisson model for process control," *International Journal of Reliability, Quality and Safety Engineering*, 10 (2), pp. 159-169.

Ranjan, P., Xie, M., and Goh, T. N. (2003). Optimal Control Limits for *CCC* Chart in the Presence of Inspection Errors. *Quality and Reliability Engineering International*, 19 (2), pp. 149-160.

Ranjan, P., Xie, M., and Goh, T. N. (2003). "On some control chart procedures for monitoring the inter-arrival times", *Proceedings of Ninth ISSAT International Conference on Reliability and Quality in Design*, August 7-9, Honolulu, Hawaii, pp. 60-64.

Xie, M., Goh, T. N. and Ranjan, P. (2002). Some effective control chart procedures for reliability monitoring. *Reliability Engineering and Systems Safety*, 77 (2), pp. 143-150.

BIBLIOGRAPHY

Acosta-Meija, C. A. (1999). Improved p charts to monitor process quality. *IIE Transactions*, 31, pp. 509-516.

Amin, R. W. and Miller, R. W. (1993). A robustness study of - *X* charts with variable sampling intervals. *Journal of Quality Technology,* 25, pp. 36-44.

Annadi, H. P., Keats, J. B., Runger, G. C. and Montgomery, D. C. (1995). An adaptive sample size CUSUM control chart. *International Journal of Production Research,* 33, pp. 1605-1616.

Aparisi, F. and Haro, C. L. (2001). Hotelling's T^2 control chart with variable sampling intervals. *International Journal of Production Research*, 39 (14), pp. 3127-3140.

Banjevic, D., Jardine, A. K. S., Makis, V., and Ennis, M. (2001). A Control-limit Policy and Software for Condition-based Maintenance Optimisation. *INFOR*, 39 (1), pp. 32-50.

Berthouex, P.M., Hunter, W.G. and Pallesen, L. (1978). Monitoring Sewage treatment plants: some quality control aspects. *Journal of Quality Technology*, 10, pp. 139-149.

Bhat, U.N. and Lal, R. (1990). A sequential inspection plan for Markov dependent production processes. *IIE Transactions*, 22, pp. 56-64.

Bhat, U.N., Lal, R. and Karunaratne, M. (1990). Attribute control charts for Markov dependent production processes. *IIE Transactions*, 22, pp. 181-188.

Bischak, D. P. and Silver, E. A. (2001). Estimating the rate at which a process goes out of control in a statistical process control context, *International Journal of Production Research*, 39 (13), pp. 2957-2971.

Bohning, D. (1998). Zero-inflated Poisson models and C.A.MAN: a tutorial collection of evidence. *Biometrical Journal*, 40(7), pp. 833-843.

Bohning, D., Dietz, E., Schlattmann, P., Mendonca, L., and Kirchner, U. (1999). The zero-inflated Poisson model and the decayed, missing and filled teeth index in dental epidemiology. *Journal of the Royal Statistical Society Series A- Statistics in Society*, 162(2), pp. 195-209.

Borror, C. M., Montogomery, D. C., Runger, G. C. (1999). Robustness of the EWMA control chart to non-normality. *Journal of Quality Technology*, 31 (3), pp. 309-316.

Bourke, P.D. (1991). Detecting a shift in fraction non-conforming using run-length control charts with 100% inspection. *Journal of Quality Technology*, 23, pp. 225-238.

Bourke, P. (2001a). Sample size and the binomial CUSUM control chart: the case of 100% inspection, *Metrika*, 53, pp. 51-70.

Bourke, P.D. (2001b). The geometric CUSUM chart with sampling inspection for monitoring fraction defective, *Journal of Applied Statistics*, 28 (8), pp. 951-972.

Box, G.E.P. and Cox, D.R. (1964). An Analysis of Transformations. *Journal of the Royal Statistical Society - Series B*, 26, pp. 211-252.

Braun, W. J. (1999). Run length distributions for estimated attribute charts, *Metrika*, 50 (2), pp. 121-129.

Broadbent, S. R. (1958). The inspection of a Markov Process. *Journal of the Royal Statistical Society. Series B (Methodological)*, 20 (1), pp. 111-119.

Brook, D. and Evans, D. A. (1972). An approach to the probability distribution of cusum run length. *Biometrika*, 59, pp. 539-549.

Burke, R. J., Davis, R. D., Kaminsky, F. C. and Roberts, A. E. P. (1995). The effects of inspection errors on the true fraction nonconforming: An industrial experiment. *Quality Engineering*, 7, pp. 543-550.

Calvin, T. W. (1983). Quality Control Techniques for 'zero-defects'. *IEEE Transactions on Components, Hybrid and Manufacturing Technology* CHMT-6, pp. 323-328.

Case, K. (1980). The *p* control chart under inspection errors. *Journal of Quality Technology*, 12, pp. 1-9.

Cassady, C. R., Bowden, R. O., Liew, L., and Pohl, E. A. (2000). Combining Preventive Maintenance and Statistical Process Control: a Preliminary Investigation. *IIE Transactions*, 32, pp. 471-478.

Champ, C. W., Chou, S.P. (2003). Comparison of standard and individual limits phase I Shewhart (X)over-bar, R, and S charts. *Quality and Reliability Engineering International*, 19 (2), pp. 161-170.

Chan, L.Y., Xie, M. and Goh, T.N. (1997). Two-stage control charts for high yield processes. *International Journal of Reliability, Quality and Safety Engineering*, 4, pp. 149-165.

Chan, L. Y., Lin, D. K. J., Xie, M. and Goh, T. N. (2002). Cumulative probability control charts for geometric and exponential process characteristics. *International Journal of Production Research*, 40 (1), pp. 133-150.

Chan, L. Y., Xie, M. and Goh, T. N. (2000). Cumulative quantity control charts for monitoring production processes. *International Journal of Production Research*, 38 (2), pp. 397-408.

Chang, T. C., and Gan, F. F. (1999). Charting techniques for monitoring a random shock process, *Quality and Reliability Engineering International*, 15, pp. 295-301.

Chen, G. (1997). The mean and standard deviation of the run length distribution of X (over bar) charts when control limits are estimated. *Statsitica Sinica*, 7, pp. 789-798.

Chen, G. (1998). The run length distribution of R, s, and s^2 control charts when s is estimated. *Canadian Journal of Statistics*, 26, pp. 311-322.

Cheng, P. C. H. and Dawson, C. D. (1998). A study of statistical process control: practice, problems, and training needs. *Total Quality Management*, 9, pp. 3-20.

Cheng, S. L. and Chung, K. J. (1994). Inspection error effects on economic selection of target values for a production process. *European Journal of Operational Research*, 79, pp. 311-324.

Chiu, W. K. and Cheung, K. C. (1977). An economic study of X-over-bar charts with warning limits. *Journal of Quality Technology*, 9, pp. 166–171.

Chou, Y. M., Polansky, A. M., and Mason, R. L. (1998). Transforming Non-normal Data to Normality in Statistical Process Control. *Journal of Quality Technology*, 30, pp. 133-141.

Chung, Kun-Jen (1993). An economic study of X-over-bar charts with warning limits. *Computers & Industrial Engineering,* 24 (1), pp. 1-7.

Costa, A. F. B. (1994). *X* Charts with variable sample size. *Journal of Quality Technology,* 26, pp. 155-163.

Costa, A. F. B. (1997). *X* charts with variable sample sizes and sampling intervals. *Journal of Quality Technology,* 29, pp. 197-204.

Costa, A. F. B. (1999). *X* and *R* Charts with variable sample size and sampling intervals. *Journal of Quality Technology,* 31, pp. 387-397.

Crosdale, R. (1974). Control charts for a double-sampling scheme based on average production run length. *International Journal of Production Research,* 12, pp. 585-592.

Crowder, S. V. (1987). A Simple Method for Studying Run-Length Distributions of Exponentially Weighted Moving Average Charts. *Technometrics*, 29, pp. 123-129.

Crowder, S. V. (1989). Design of Exponentially Weighted Moving Average Schemes. *Journal of Quality Technology*, 21, pp. 155-162.

Daudin, J. J. (1992). Double sampling - *X* Charts. *Journal of Quality Technology,* 24, pp. 78-87.

Duncan, A. J. (1986). *Quality Control and Industrial Statistics*. Irwin, Homewood.

Ewan, W. D. (1963). When and how to use Cu-sum charts. *Technometrics*, 5, pp. 213-119.

Fellener, W. H. (1990). Average run lengths for cumulative sum schemes. *Applied Statistics*, 39, pp. 402-412.

Gan, F. F. (1991). An optimal design of CUSUM quality control charts. *Journal of Quality Technology*, 23, pp. 279-286.

Gan, F. F. (1992). Exact Run Length Distributions for One-sided Exponential CUSUM Schemes. *Statistica Sinica*, 2, pp. 297-312.

Gan, F. F. (1993). An optimal design of CUSUM control charts for binomial counts. *Journal of Applied Statistics*, 20, pp. 445-458.

Gan, F. F. (1994). Design of Optimal Exponential CUSUM Control Charts. *Journal of Quality Technology*, 26, pp. 109-124.

Gardiner, J. S. (1987). A Note on the average run length of cumulative sum control charts for count data. *Quality and Reliability Engineering International*, 3, pp. 53-55.

Glushkovsky, E. A. (1994). On-line G-control chart for attribute data. *Quality and Reliability Engineering International,* 10, pp. 217-227.

Goh, T. N. (1987a). A charting technique for control of low-nonconformity production. *International Journal of Quality & Reliability Management*, 4 (1), pp. 53-62.

Goh, T. N., (1987b). A control chart for very high yield processes. *Quality Assurance*, 13 (1), 18-22.

Goh, T. N. (1991). Statistical monitoring and control of a low defect process. *Quality and Reliability Engineering International,* 7, pp. 479-483.

Goh, T. N. (1993). Some practical issues in the assessment of nonconforming rates in a manufacturing process. *International Journal of Production Economics,* 33, pp. 81-88.

Goh, T. N. and Xie. M. (1994). A new approach to quality in near-zero defect Environment. *Total Quality Management,* 12, pp. 241-250.

Goh, T. N. and Xie. M. (1995). Statistical process control for low nonconformity processes. *International Journal of Reliability, Quality and safety Engineering,* 2, pp. 15-22.

Gordon, G. R. and Weindling, J. I. (1975). A cost method for economic design of warning limit control chart schemes. *AIIE Transactions*, 7, pp. 319–329.

Grant, E.L. and Leavenworth, R.S. (1998). *Statistical Quality Control.* McGraw-Hill, New York.

Greenberg, B.S. and Stokes, S.L. (1995). Repetitive testing in the presence of inspection errors. *Technometrics,* 37, pp. 102-111.

Hawkins, D. M. (1981). A CUSUM for a scale parameter. *Journal of Quality Technology,* 13, pp. 102-110.

Hawkins, D. M. (1992). A fast accurate approximation of average run lengths of CUSUM control charts. *Journal of Quality Technology*, 24, pp. 37-42.

Haworth, D. A. (1996). Regression Control Charts to Manage Software Maintenance. *Journal of Software Maintenance: Research and Practice*, 8, pp. 35-48.

He, B. and Goh, T. N. (2002). Defect data modeling with extended Poisson distributions. *The 2002 International Conference on Industrial Engineering - Theory, Applications and Practice*, October 2002, Pusan, Korea.

He, B., Xie, M., Goh, T. N. and Ranjan, P. (2002). On the estimation error in zero-inflated Poisson model for process control. *The 2002 International Conference on Industrial Engineering - Theory, Applications and Practice*, October 2002, Pusan, Korea.

Hernandez, F. and Johnson, R. A. (1980). The Large-Sample Behavior of Transformations to Normality. *Journal of the American Statistical Association* 75, pp. 855-861.

Hillier, F. S. (1969). $\overline{X}$ and R chart control limits based on a small number of subgroups. *Journal of Quality Technology*, 1, pp.17-26.

Huang, Q., Johnson, N. L. and Kotz, S. (1989). Modified Dorfman-Sterett screening (group testing) procedures and the effects of faulty inspection *Communications in Statistics: Theory and Methods*, 13, pp. 1203-1213.

Johnson, N. L. (1961). A simple theoretical approach to cumulative sum procedures. *Journal of American Statistical Association*, 56, pp. 835-840.

Johnson, N. L. (1966). Cumulative Sum Control Charts and the Weibull Distribution. *Technometrics*, 8, pp. 481-491.

Johnson, N. L., Kotz, S. and Wu, X. (1991). *Inspection Errors for Attributes in Quality Control*. Chapman & Hall, London.

Jones, L. A. (2002). The Statistical Design of EWMA Control Charts with Estimated Parameters. *Journal of Quality Technology*, 34, pp. 277-288.

Jones, L. A. and Champ, C. W. (2002). Phase I Control Charts for Times Between Events. *Quality and Reliability Engineering International*, 18 (6), pp. 479-488.

Jones, L. A, Champ, C. W., Rigdon, S. E. (2001) The performance of exponentially weighted moving average charts with estimated parameters, *Technometrics*, 43 (2), pp. 156-167.

Kaminsky, F. C., Benneyan, J. C., Davis, R. D. and Burke, R. J. (1992). Statistical control charts based on a geometric distribution, *Journal of Quality Technology*, 24 (2), pp. 63-69.

Katter, J. G., Tu, J. F., Monacelli, L. E., and Gartner, M. (1998). Predictive Cathode Maintenance of an Industrial Laser Using Statistical Process Control Charting. *Journal of Laser Applications*, 10, pp. 161-169.

Kittlitz R. G., Jr. (1999). Transforming the Exponential for SPC Applications. *Journal of Quality Technology*, 31, pp. 301-308.

Kopnov, V. A. and Kanajev, E. I. (1994). Optimal Control Limit for Degradation Process of a Unit Modeled as a Markov chain. *Reliability Engineering and System Safety*, 43, pp. 29-35.

Kuralmani, V., Xie, M., Goh, T. N., and Gan, F. F. (2002). A conditional decision procedure for high yield processes, *IIE Transactions*, 34, pp. 1021-1030.

Lai, C. D., Govindaraju, K. and Xie, M. (1998). Effects of correlation on fraction nonconforming statistical process control procedures, *Journal of Applied Statistics*, 25 (4), pp. 535-543.

Lai, C. D., Xie, M. and Govindaraju, K. (2000). Study of a Markov model for a high-quality dependent process, *Journal of Applied Statistics*, 27, pp. 461-473.

Lambert, D. (1992). Zero-inflated Poisson regression with application to defects in manufacturing. *Technometrics*, 34, pp. pp. 1-14.

Lawson, J. R. and Hathway, J. (1990). Monitoring attribute data for low-defect products and processes. *Proceedings of the 4th International SAMPE Electronics Conference*, June 12-14, pp. 589-599.

Lindsay, B. G. (1985). Errors in inspection: Integer parameter maximum likelihood in a finite population. *Journal of American Statistical Association*, 80, pp. 827-855.

Lorden, G. and Eisenberger, I. (1973). Detection of failure rate increases. *Technometrics*, 15, pp. 167-175.

Lorenzen, T. J., and Vance, L. C. (1986). The Economic Design of Control Charts: A Unified Approach. *Technometrics*, 28, pp. 3-10.

Lu, X. S., Xie, M. and Goh, T. N. (1998). A CCC-2 charting procedure for monitoring automated manufacturing processes with serial correlation. *International Manufacturing Conference '98*, Singapore, pp. 306-311.

Lu, X. S., Xie, M. and Goh, T. N. (2000). An Investigation of the effects of Inspection errors on the run length control charts, *Communication in Statistics: Simulation and computation*, 29 (1), pp. 315-335.

Lu, X. S., Xie, M., Goh, T. N., Chan, L. Y. (1999). A quality monitoring and decision-making scheme for automated production processes. *International Journal of Quality and Reliability Management*, 16 (2), pp. 148-157.

Lucas, J. M. (1976). The design and use of cumulative sum quality control schemes. *Journal of Quality Technology*, 8, pp. 124-132.

Lucas, J. M. (1982). Combined Shewhart-CUSUM quality control schemes. *Journal of Quality Technology*, 24, pp. 87-90.

Lucas, J. M. (1985). Counted data CUSUMs, *Technometrics*, 27 (2), pp. 129-144.

Lucas, J.M., (1989). Control scheme for low count levels, *Journal of Quality Technology*, 21 (3), pp. 199-201.

Lucas, J. M. and Saccucci, M. S. (1990). Exponentially Weighted Moving Average Control Schemes: Properties and Enhancements. *Technometrics*, 32, pp. 1-12.

McCool, J. I., and Joyner-Motley. T. (1998). Control Charts applicable when the fraction nonconforming is small. *Journal of Quality Technology*, 30, pp. 240-247.

McEwen, R. P. and Parresol, B. R. (1991). Moment Expressions and Summary Statistics for the Complete and Truncated Weibull Distribution. *Communications in Statistics – Series A: Theory and Methods*, 20, pp. 1361-1372.

Montgomery, D. C. and Friedmann, J. J. (1989). Statistical process control in a computer-integrated manufacturing environment. *Statistical process control in Automated Manufacturing*, edited by Keats, T. B. and Hubele, N. F., Marcel Dekker, Series in Quality and Reliability, New York.

Montgomery, D. C. (2001). *Introduction to Statistical Quality Control*. John Wiley & Sons Inc., New York.

Montgomery, D. C. and Runger, G. C. (1999). *Applied Statistics and Probability for Engineers*. John Wiley & Sons Inc., New York.

Moustakides, G. V. (1986). Optimal stopping times for detecting changes in distributions, *The Annals of Statistics*, 14, pp. 1379-1387.

Nelson, L. S. (1994). A control chart for parts-per-million nonconforming items. *Journal of Quality Technology*, 26 (3), pp. 239-240.

Nelson, P. R. (1979). Control Charts for Weibull Processes with Standards Given. *IEEE Transactions on Reliability*, 28, pp. 283-288.

Ohta, H., Kusukawa, E. and Rahim, A. (2001). A CCC-r chart for high-yield processes. *Quality and Reliability Engineering International*, 17 (6), pp. 439-446.

Page, E. S. (1954). Continuous inspection schemes. *Biometrika*, 24, pp. 199-205.

Page, E. S. (1955). Control charts with warning limits. *Biometrika*, 42, pp. 243–257.

Page, E. S. (1961). Cumulative sum control charts. *Technometrics*, 3, pp. 1-9.

Page, E. S. (1962). A modified control chart with warning lines. *Biometrika* 49, pp. 171–176.

Park, C. and Reynolds, M. R. (1994). Economic design of a variable sample size - *X* chart. *Communication in Statistics: Simulation and Computation,* 23, pp. 467-483.

Perry, M. B., Spoerre, J. K. and Velasco, T. (2001). Control chart pattern recognition using back propagation artificial neural networks, *International Journal of Production Research*, 39 (15), pp. 3399-3418.

Pesotchinsky, L. (1987). Plans for very low fraction nonconforming. *Journal of Quality Technology*, 19, pp. 191-196.

Prabhu, S. S., Runger, G. C. and Keats, J. B. (1993). An adaptive sample size - *X* chart. *International Journal of Production Research*, 31, pp. 2895-2909.

Prabhu, S. S., Montgomery, D. C. and Runger, G. C. (1994). A combined adaptive sample size and sampling interval - *X* control scheme. *Journal of Quality Technology,* 26, pp. 164-176.

Proschan, F. and Savage, I. R. (1960). Starting a control chart, *Industrial Quality Control*, 17 (3), pp. 12-13.

Quesenberry, C. P (1993). The Effect of Sample Size on Estimated Limits for *X* (over bar) and *X* Control Charts. *Journal of Quality Technology*, 25, pp. 237-247.

Quesenberry, C. P. (1995). Geometric *Q* charts for high quality processes. *Journal of Quality Technology*, 27, pp. 304-313.

Quesenberry, C. P. (1997). *SPC Methods for Quality Improvement.* John Wiley & Sons, Toronto.

Radaelli, G. (1998). Planning Time-between-events Shewhart Control Charts. *Total Quality Management*, 9, pp. 133-140.

Rahim, M. A. (1984). Economically optimal determination of the parameters of X-over-bar charts with warning limits when quality characteristics are non-normally distributed. *Engn. Opt.*, 7, pp. 289–301.

Ramalhoto, M. F. and Morais, M. (1999). Shewhart Control Charts for the Scale Parameter of a Weibull Control Variable with Fixed and Variable Sampling Intervals. *Journal of Applied Statistics*, 26, pp. 129-160.

Ranjan, P., Xie, M., and Goh, T. N. (2003). Optimal Control Limits for *CCC* Chart in the Presence of Inspection Errors. *Quality and Reliability Engineering International*, 19 (2), pp. 149-160.

Ranjan, P., Xie, M., and Goh, T. N. (2003). "On some control chart procedures for monitoring the inter-arrival times", *Proceedings of Ninth ISSAT International Conference on Reliability and Quality in Design*, August 7-9, Honolulu, Hawaii, pp. 60-64.

Rendtel, U. (1990). CUSUM-schemes with variable sampling intervals and sample sizes. *Statistical Papers*, 31, pp. 103-118.

Reynolds, M. R. Jr. (1975). Approximations to the average run length in cumulative sum control charts. *Technometrics*, 17, pp. 65-71.

Reynolds, M. R., Jr., Amin, R. W. and Arnold, J. C. (1990). Cusum charts with variable sampling intervals. *Technometrics,* 32, pp. 371-384.

Reynolds, M. R., Jr., Amin, R. W., Arnold, J. C. and Nachlas, J. A. (1988). *X* charts with variable sampling intervals. *Technometrics*, 30, pp. 181-192.

Reynolds, M. R., Jr. & Stoumbos, Z. G. (1998) The SPRT chart for monitoring a proportion. *IIE Transactions on Quality and Reliability*, 30, pp. 545- 561.

Reynolds, M. R., Jr. & Stoumbos, Z. G. (1999) A CUSUM chart for monitoring a proportion when inspecting continuously. *Journal of Quality Technology*, 31, pp. 87-108.

Roberts, S. W. (1966). A comparison of some control chart procedures. *Technometrics*, 8, pp. 411–430.

Ross, R. (1994). Formulas to Describe the Bias and Standard Deviation of the ML-Estimated Weibull Shape Parameter. *IEEE Transactions on Dielectrics and Electrical Insulation*, 1, pp. 247-253.

Rowlands, H. (1992). Control charts for low defect rate in the electronic manufacturing industry. *Journal of Systems Engineering*, 2, pp. 143-150.

Runger, G. C. and Montgomery, D. C. (1993). Adaptive sampling enhancements for Shewhart control charts. *IIE Transactions,* 25, pp. 41-51.

Runger, G. C. and Pignatiello, J. J., Jr. (1991). Adaptive sampling for process control. *Journal of Quality Technology,* 23, pp. 135-155.

Ryan, T. P. (1989). *Statistical Methods for Quality Improvement*. John Wiley & Sons Inc., New York.

Ryan, T. P. and Schwertman, N. C. (1997). Optimal control limits for attribute control charts. *Journal of Quality Technology*, 29, pp. 86-98.

Saccucci, M. S., Amin, R. W. and Lucas, J. M. (1992). Exponentially weighted moving average control schemes with variable sampling intervals. *Communication in Statistics: Simulation and Computation*, 21, pp. 627-657.

Sharma, P. R., Xie, M., and Goh, T. N. "Monitoring inter-arrival times with Statistical control charts," *Accepted for publication as a chapter in the book titled Reliability Modeling, Analysis and Optimization*.

Shewart, W. A. (1926). Quality control charts. Bell Sys. Tech. J., October, pp. 593-603.

Shewart, W. A. (1931). *Economic control of Quality of Manufactured product.* Van Nostrand, New York.

Steiner, S. H. (1999). Confirmation sample control charts. *International Journal of Production Research*, 37, pp. 737-748.

Suich, R. (1988). The *c* control chart under inspection errors, *Journal of Quality Technology*, 20, pp. 263-266.

Sun, F. B., Yang, J., del Rosario, R. and Murphy, R. (2001). A Conditional-reliability Control-chart for the Post-production Extended Reliability-test. *Proceedings: Annual Reliability and Maintainability Symposium*, pp. 64-69.

Tang, X. Y., Xie., M., and Goh, T. N. (2000). A note on economical-statistical design of cumulative count of conforming control chart. *Economic Quality Control*, 15, pp. 3-14.

Vardeman, S. and Ray. D. (1985). Average run lengths for CUSUM schemes when observations are exponentially distributed. *Technometrics*, 27, pp. 145-150.

Wetherill, G. B. and Brown, D. W. (1991). *Statistical process Control-Theory and Practice*. Chapman & Hall, London.

Winterbottom, A. (1993) Simple adjustments to improve control limits on attribute charts. *Quality and Reliability Engineering International*, 9, pp. 105-109.

Woodall, W. H. (1983). The distribution of run length of one-sided CUSUM scheme for continuous random variables. *Technometrics*, 25, pp. 295-301.

Woodall, W. H. and Ncube, M. M. (1985). Multivariate CUSUM quality control procedures. *Technometrics*, 27, pp. 285-292.

Woodall, W. H. and Adams, B.M. (1993). The Statistical design of CUSUM Charts. *Quality Engineering*, 5, pp. 559-570.

Woodall, W. H. (1997). Control charts based on attribute data: Bibliography and Review, *Journal of Quality Technology*, 29 (2), pp. 172-183.

Woodall, W. H. and Montgomery, D. C. (1999). Research issues and ideas in statistical process control, *Journal of Quality Technology*, 31 (4), pp. 376-386.

Wu, Z. and Spedding, T. A. (1999). Evaluation of ATS for CRL control chart, *Process Quality Control*, 11, pp. 183-191.

Wu, Z., Yeo, S. H., and Fan, H. T. (2000). A comparative study of the CRL-type control charts. *Quality and Reliability Engineering International*, 16, pp. 269-279.

Wu, Z., Zhang, X. L., and Yeo, S. H. (2001). Design of the sum-of-conforming-run-length control charts. *European Journal of Operation Research*, 132, pp. 187-196.

Xie, M. and Goh, T. N. (1992). Some procedures for decision making in controlling high yield processes. *Quality and Reliability Engineering International*, 8, pp. 355-360.

Xie, M. and Goh, T. N. (1993a). Improvement detection by control charts for high yield processes. *International Journal of Quality and Reliability Management*, 10 (7), pp. 23-29.

Xie, M. and Goh, T. N. (1993b), SPC of A Near Zero-defect Process Subject to Random Shock. *Quality and Reliability Engineering International*, 9, pp. 89-93.

Xie, M. and Goh, T.N. (1997). The use of probability limits for process control based on geometric distribution. *International Journal of Quality & Reliability Management*, 14 (1), pp. 64-73.

Xie, M., Goh, T. N. and Kuralmani, V. (2000a). On optimal setting of control limits for Geometric chart. *International Journal of Reliability, Quality and Safety Engineering*, 7 (1), pp. 17-25.

Xie, M., Goh, T. N. and Kuralmani, V. (2002a). *Statistical Models and Control Charts for High Quality Processes*, Kluwer Academic Publishers, Boston.

Xie, M., Goh, T. N., and Lu, X. S. (1998a). A comparative study of CCC and CUSUM charts. *Quality and Reliability Engineering International*, 14, pp. 339-345.

Xie, M., Goh, T. N. and Lu, X. S. (1998b). Computer aided statistical monitoring of automated manufacturing processes. *Computers and Industrial Engineering*, 35, pp. 189-912.

Xie, M., Goh, T. N. and Ranjan, P. (2002b). Some effective control chart procedures for reliability monitoring. *Reliability Engineering and Systems Safety*, 77 (2), pp. 143-150.

Xie, M., Goh, T. N. and Tang, X. Y. (2000b). Data Transformation for geometrically distributed quality characteristics. *Quality and Reliability Engineering International*, 16, pp. 9-15.

Xie, M., Goh, T. N. and Tang, X. Y. (2001a). A study of economic design of cumulative count of conforming control chart. *International Journal of Production Economics*, 72, pp. 89-97.

Xie, M., Goh, T. N. and Xie, W. (1997). A study of economic design of control charts for cumulative count of conforming items. *Communications in Statistics – B: Computation and Simulation*, 26, pp. 1009-1027.

Xie, M., He, B., and Goh, T. N. (2001b). Zero-inflated Poisson model for statistical process control. *Computational Statistics and Data Analysis*, 38, pp. 191-201.

Xie, M., Lu, X. S., Goh, T. N and Chan, L. Y. (1999). A quality monitoring and decision making scheme for automated manufacturing processes. *International journal of Quality and Reliability Management*, 16 (2), pp. 148-157.

Xie, W., Xie, M. and Goh, T. N. (1995a). A Shewhart like control charting technique for high yield processes. *Quality and Reliability Engineering International*, 11, pp. 189-96.

Xie, W., Xie, M. and Goh, T. N. (1995b). Control charts for processes subject to random shocks. *Quality and Reliability Engineering International*, 11, pp. 355-60.

Yang, Miin-Shen and YANG, Jenn-Hwai (2002). A fuzzy-soft learning vector quantization for control chart pattern recognition, *International journal of Production Research*, 40 (12), pp. 2721-2731.

Yang, Z. H., Xie, M., Kuralmani, V. and Tsui, K. L. (2002a). On the Performance of Geometric Charts with Estimated Control Limits, *Journal of Quality Technology*, 34 (4), pp. 448-458.

Yang, Z., See, S.P., and Xie, M. (2002b). An Investigation of Transformation-based Prediction Interval for the Weibull Median Life. *Metrika*, 56, pp. 19-29.

Zhang, G. Q. and Berardi, V. (1997). Economic Statistical Design of X over bar Control Charts for Systems with Weibull In-control Times. *Computers & Industrial Engineering*, 32, pp. 575-58.

Zimmer, L. S., Montgomery, D. C. and Runger, G. C. (2000). Guidelines for the application of adaptive control charting schemes. *International Journal of Production Research*, 38 (9), pp. 1977-1992.